MATERIAL SELECTION AND TESTING FOR A RADIATION THERAPY CATHETER

A Thesis

presented to

the Faculty of California Polytechnic State University,

San Luis Obispo

In Partial Fulfillment

of the Requirements for the Degree

Master of Science in Biomedical Engineering

by

Philip James Wadlow

August 2016

COMMITTEE MEMBERSHIP

TITLE:	Material Selection and Testing for a Radiation Therapy Catheter
AUTHOR:	Philip James Wadlow
DATE SUBMITTED:	August 2016
COMMITTEE CHAIR:	Kristen O'Halloran Cardinal, Ph.D. Associate Professor of Biomedical Engineering
COMMITTEE MEMBER:	Lily Laiho, Ph.D. Associate Professor of Biomedical Engineering
COMMITTEE MEMBER:	Michael Whitt, Ph.D. Lecturer in Biomedical Engineering

ABSTRACT

Material Selection and Testing for a Radiation Therapy Catheter

Philip James Wadlow

Three different polymers (a high-density polymer and two other polymers) were tested for use as an x-ray catheter in a radiation therapy application. This report describes the testing of these three materials to determine which material is the best option for a long use catheter. Tests included tensile, simulated clinical life, and other tests. Some testing was performed using nitrogen and an industrial coolant. Testing revealed significant non-circularities for some catheters. With increasing pressure, the circularity of these catheters increased. The tensile tests were performed on samples with varying doses of radiation. Tensile testing showed significant decreases in ultimate tensile strength with increasing radiation dose for both polyurethanes. Other testing was performed on the two polyurethanes to determine their compatibility with the industrial coolant. The test showed good compatibility with the coolant. Simulated clinical life tests were performed on a test fixture and with software to run the radiation source automatically for several hours at a time. Overall, one material was found to have very low ductility, made lower with increasing radiation. The material with the higher ductility was chosen as the better catheter material despite some disadvantages when compared to the stiffer polymer. This report describes necessary tests for thin polymer geometries used in applications where resistance to radiation, mechanical integrity, and coolant compatibility are the main considerations.

ACKNOWLEDGMENTS

SPECIAL THANKS TO:

Rob Neimeyer, Linda Kelley, Aaron Castillo, and Frank Perez at Xoft for all their assistance and guidance throughout the project.

Dr. Kristen O'Halloran Cardinal for providing excellent advising through the project

Dr. Michael Whitt and Dr. Lily Laiho for their presence on the thesis defense committee

Xoft, Inc. for providing me with the necessary resources to complete the project

TABLE OF CONTENTS

Page

LIST OF TABLES

LIST OF FIGURES

1.0 BACKGROUND

The medical device industry has revolutionized the way that diseases are treated, and one of the most prominent examples is clinical treatment of various cancers. Radiation therapy is one of the older techniques for treating cancer, but due to advances in radiation therapy technology, this type of cancer treatment is even more relevant than it was 15 years ago. One technology that has allowed radiation therapy to remain one of the most common treatments for cancer is the development of targeted radiation therapy. The Xoft Axxent® eBx™ is currently one of the leading technologies is the field of targeted radiation therapy, but to remain at the forefront of treatment options for cancer, constant improvements to the system are necessary. The materials used within the Axxent system play a large role in determining the longevity and effectiveness of the entire system; and, as a result, materials selection is a very important part of the design process. In this report, the selection and testing process of a new material for a component of the Axxent system is documented.

Currently, the Xoft Axxent eBx system is cleared by the FDA for treating any "condition in or on the body where radiation therapy is indicated" [1]. The system is currently used for early stage breast cancer, non-melanoma skin cancer (NMSC), vaginal, and uterine cancers (including uterine corpus and cervical cancers). While the system can be used to treat all of these cancers, in this background section, the focus of the clinical results will be on early stage breast cancer and NMSC, as these three conditions (technically NMSC encompasses two conditions) constitute the majority of the clinical treatments performed using the Xoft system. The gynecological cancers that the system is used to treat will only be briefly mentioned in the subsequent sections.

1.1 The Impact of Cancer

In general, cancer is an overproliferation of abnormal cells. This can be caused by the inactivation or suppression of tumor suppressing signals, or by hyperactive growth or division signals. Cancer is the second leading cause of death in the United States (behind only heart disease) [2]; and, while the mortality due to cancer is immense, the impact of cancer on society is much greater even than the number of deaths due to cancer suggest. The morbidity due to cancer is significant because many cancers require consistent treatment courses ranging from weeks to years. The impact that these prolonged treatment courses have on society is almost immeasurable, but two of the most significant impacts are the increased financial burden due to cost of treatment and the decreased quality of life for the patients. The Xoft Axxent eBx system seeks to treat cancer effectively and reduce the burden that lengthy treatment courses impose.

1.1.1 Breast Cancer Impact. In 2016, it is estimated that breast cancer will be the most diagnosed type of cancer, with 249,260 cases diagnosed (246,660 in women) [2]. It has also been estimated that between 2005 and 2011, 61.1% of all female breast cancer cases were diagnosed at localized (early) stages [3]. The stage at which breast cancer is diagnosed is critical in determining what treatment course will be followed, and the Xoft Axxent system is only cleared for treating early stage breast cancer.

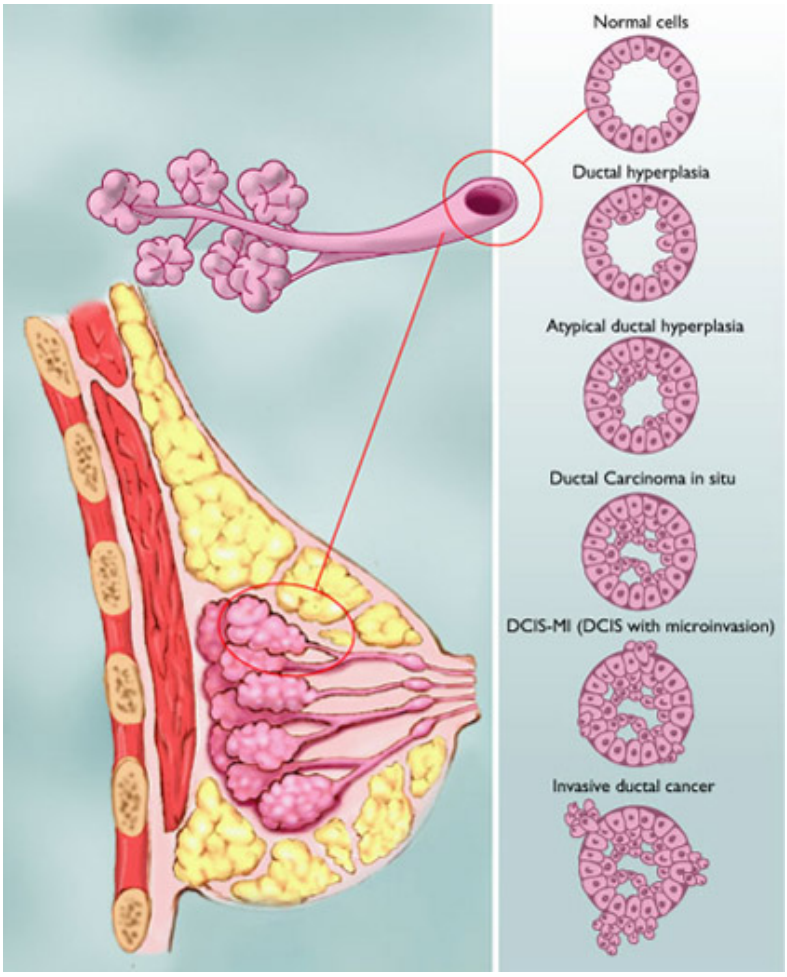

Figure 1. Breast cancer can progress from hyperplasia to invasive carcinoma [4].

Based on the previously mentioned statistics, it is likely that over 150,000 cases of early stage female breast cancer cases will be diagnosed in 2016 alone. As the numbers show, there is a significant need for a fast, minimally invasive, and effective treatment for early stage breast cancer. As this report will later discuss, the Xoft Axxent eBx system meets these requirements and can provide an excellent treatment option for patients with early stage breast cancer.

1.1.2 Non-Melanoma Skin Cancer Impact. Non-melanoma skin cancer has the potential, and has previously proved, to be the largest market for the Xoft therapy system. The minimal impacts to the patient, fast setup time, and apparent efficacy (as discussed in section 1.2.2.6)

have made the Axxent system a popular choice when treating NMSC. NMSC specifically includes basal cell carcinoma (BSC), squamous cell carcinoma (SCC), Merkel cell carcinoma, Kaposi sarcoma, cutaneous lymphoma, and other tumors that originate in hair follicles or skin glands [5]. While there are several varieties of NMSC, the vast majority of NMSC cases are comprised of BSC (approximately 80% of NMSC cases) and SCC (approximately 20% of NMSC cases) [5]. From this point in the report, NMSC will refer only to BSC and SCC. A diagram of the cells that NMSC originates from is shown in Figure 2.

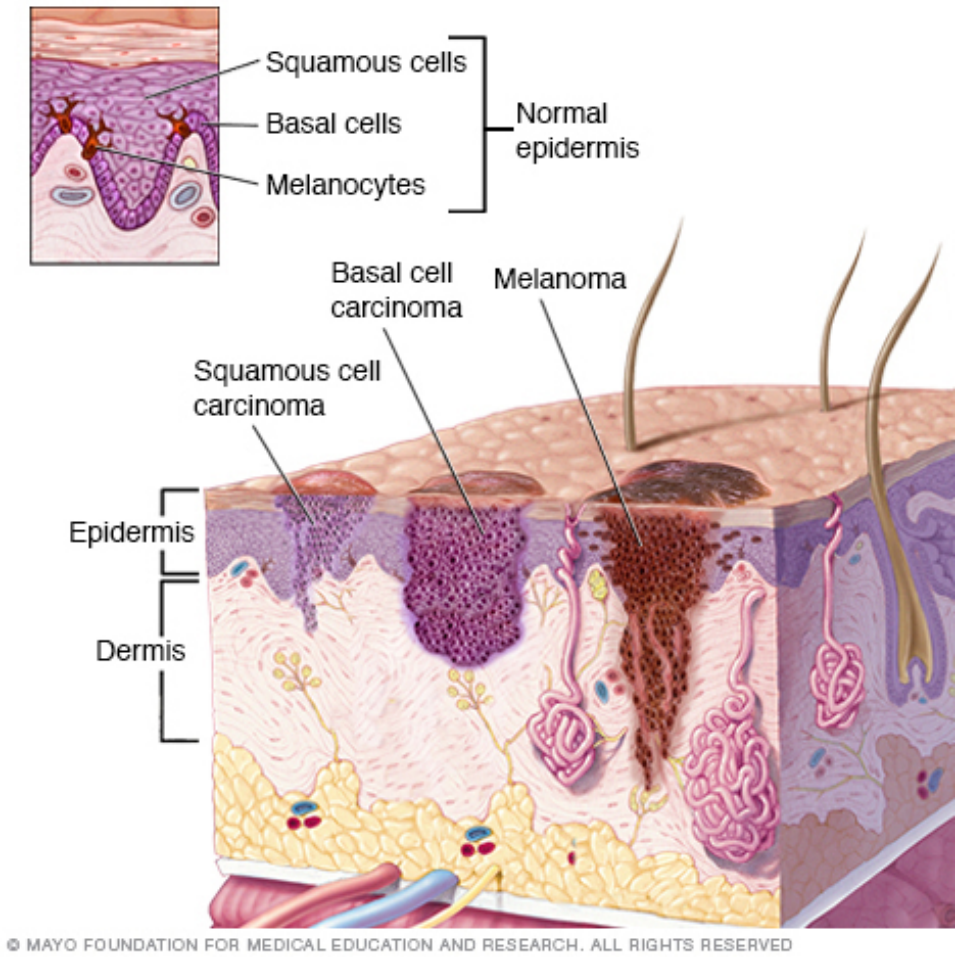

Figure 2. Squamous cell and basal cell carcinoma are the two major types of NMSC [6].

A study performed in 2006 estimated that in 2006, over 2 million patients were treated for some form of NMSC in the U.S. alone [7]. Even with a better understanding of risk factors for skin cancer, the same study suggests that the incidence rates of skin cancer could be increasing [7], meaning that the current incidence rate for NMSC could be higher than estimated in 2006. Despite the fact that NMSCs are not as invasive as melanoma, if they are left untreated, they can spread to other organs [5]. This possibility to metastasize necessitates treatment for BSC and SCC; as a result, non-melanoma skin cancer represents a massive opportunity for a fast and effective therapy, like the Axxent system, to improve treatment options for patients.

1.1.3 Uterine Cancer Impact. Finally, the impact of uterine cancers, while significantly less than breast and NMSC, is still large enough to require a streamlined and effective treatment option. It is estimated that in 2016 12,990 cervical cancer and 60,050 uterine corpus cancer cases will be diagnosed [2]. These numbers show that there is an opportunity to provide a minimally invasive and effective treatment option to a significant number of patients.

1.2 Cancer Therapies

As the previous section detailed, the impact of cancer in the United States alone is enormous, but one positive result of this has been the advances in medical knowledge and treatment. Cancer therapies have been have technically been available since ancient times, but more sophisticated treatments have only truly been developing since the mid-19th century [8]. The options for treating breast, NMSC, vaginal, and uterine cancer are numerous, with some of the more common treatments being surgery, chemotherapy, and radiation therapy. Currently, there are new and exciting targeted therapies being developed for treating these cancers, including

therapies (like chimeric antigen receptor therapy or CART [9]) that modify the cells of the immune system to target cancer cells specifically.

1.2.1 Surgical and Chemotherapeutic Treatments. Surgery to treat cancer has been performed since ancient times, but significant advances in surgery to treat cancer were not made until the 19th century [8]. Currently, surgery is still a widely used method to treat cancer, but there are now several minimally invasive surgical techniques including laparoscopic, thorascopic, and endoscopic surgery that are commonly used to remove cancerous tissue [8]. Chemotherapy is another commonly used therapy for the cancers that the Xoft system is cleared to treat. Chemotherapy encompasses a number of different treatments, ranging from broad spectrum chemotherapy to targeted drugs that inhibit oncogenes. The biological basis for chemotherapy (the ability of some chemicals to kill cancer cells) was discovered during World War II while scientists were trying to develop new chemical warfare agents and develop methods to protect soldiers from these new chemicals [8]. Chemotherapy was first used to treat metastatic cancer in 1956, and since then, chemotherapy has been used to induce remission in or even cure many types of cancer [8]. Currently, research related to this therapy is focused on targeted chemotherapeutic agents to more effectively treat cancer and reduce the many side effects of traditional broad-spectrum chemotherapy [8].

1.2.2 Radiation Therapy. Radiation therapy, specifically x-ray radiation, is the treatment principle that the Xoft system operates on. Radiation therapy was originally developed based on the discovery of x-rays by Wilhelm Conrad Roentgen in 1896; this scientific discovery was first used as a therapy approximately 3 years later [8]. Similarly to surgery and chemotherapy, there

are a number of different types of ionizing radiation therapy available to patients today, including gamma ray, x-ray, electron, proton, radioactive isotope, neutron, and carbon ion radiation [10]. It is important that the radiation be ionizing radiation, and the reason for this will be discussed in section 1.2.2.2. While the scientific principles behind radiation therapy are complex, this complexity has allowed and will continue to allow treatments to be developed for specific type of cancer. For example, proton therapy is often used specifically for treatment of cancers near the brain or spinal cord because proton beams cause very little harm to tissues in the proton path but are effective in destroying cancer cells at the end of the proton path [8,10]. There are two broad classes of radiation therapy that will be discussed in this report to highlight the features of the Xoft Axxent system: external beam radiation and brachytherapy. A diagram showing the distinctions between the various types of radiation therapy is given in Figure 3.

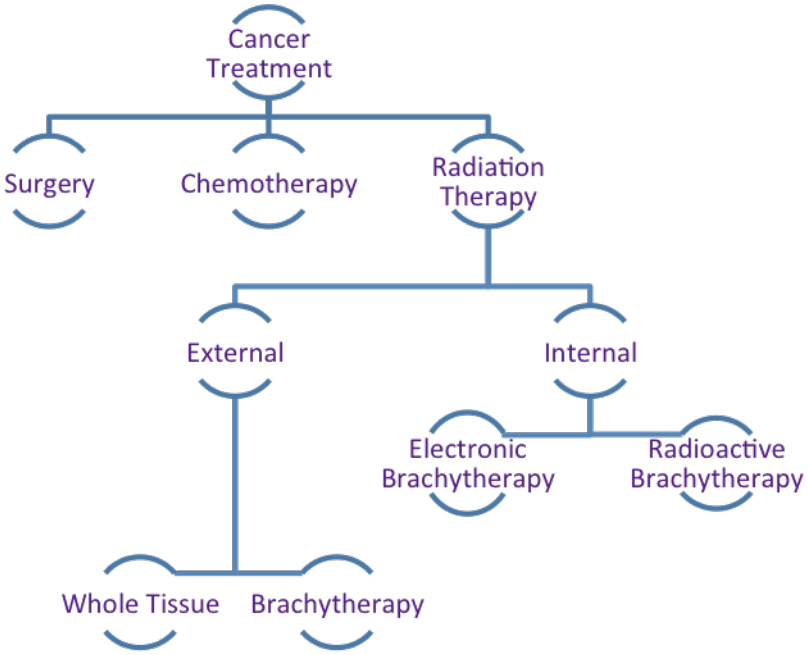

Figure 3. Many types of radiation therapy exist, and brachytherapy may fall under the category of external or internal radiation therapy depending on the specific application.

In the majority of cases, brachytherapy can be considered internal radiation, however when treating NMSC, there is an overlap between external radiation and brachytherapy. Due to the overlapping and confusing nomenclature for some radiation therapy treatments, this report will clearly define the type of radiation therapy referred to in each section.

1.2.2.1 Physics of Ionizing Radiation Therapy. To fully understand the differences between different types of radiation therapy, a brief discussion of the physics behind the different types of treatments is relevant. When discussing radiation therapies, as the previous section

mentioned, there are many different types of ionizing radiation that can be used. These specific types of ionizing radiation fall under one of the following categories: alpha, beta, gamma, x-ray, neutron, or proton radiation [8,10]. Alpha radiation is the emission of alpha particles (consisting of 2 protons and 2 neutrons) from the nucleus of an atom undergoing radioactive decay [11]. This type of radiation is only given off by certain radioactive isotopes of elements, like polonium-210 [11]. In general, in terms of penetration distance, because alpha particles have strong interactions with other particles in matter, this type of radiation is the least penetrating radiation [11]. A diagram of alpha radiation emission is shown in Figure 4.

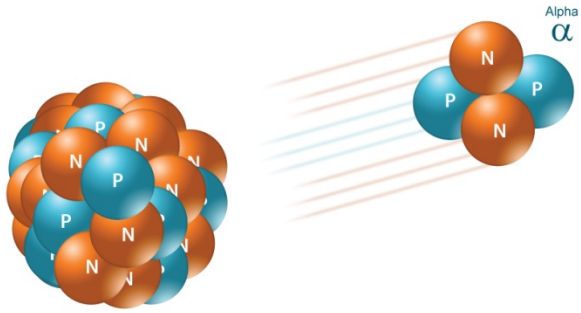

Figure 4. Alpha particles consist of 2 protons and 2 neutrons. This type of radiation significantly interacts with surrounding matter and has the weakest penetration strength [11].

Beta radiation is similar to alpha radiation, but instead of alpha particles being emitted from the nucleus of an atom, beta particles are emitted [11]. Beta particles are comprised of either electrons or positrons (particles with the mass and equal but opposite charge as an electron) [11]. Beta radiation has the ability to penetrate slightly further than alpha radiation, but its penetration

strength is still relatively weak [11]. A diagram of beta particle emission radiation is shown in Figure 5.

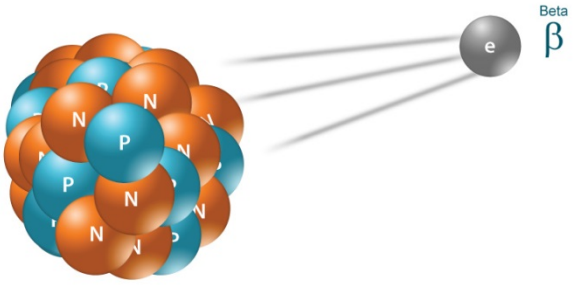

Figure 5. Beta particles are electrons or positrons emitted from the nucleus of an atom [11].

Gamma radiation is different from the previous two types of radiation because gamma radiation consists of photons of energy (wavelengths) emitted from the nucleus of an atom instead of particles [11]. Gamma radiation can travel significantly further than alpha or beta radiation because of its wave (as opposed to particle) nature [11]. X-ray radiation is very similar to gamma radiation, with the main difference being that x-ray radiation waves are emitted from the electron cloud instead of the nucleus of the atom [11]. X-ray radiation is the type of ionizing radiation produced by the Xoft Axxent system. X-rays are slightly lower energy than gamma radiation, but x-rays have similar penetration strength to gamma radiation waves [11]. A diagram depicting x-ray emission is shown in Figure 6. This diagram would look nearly identical for gamma radiation, with the sole difference being a shorter wavelength (higher energy) emission.

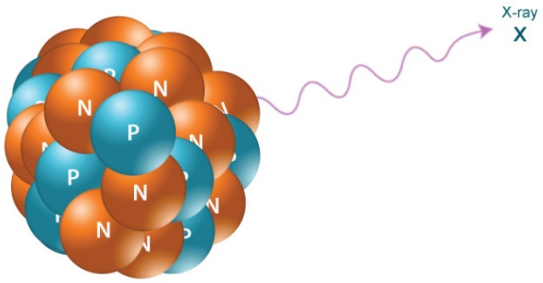

Figure 6. X-rays are photons (energy) generated from the electron cloud of an atom [11].

Neutron radiation is another type of particle radiation, but instead of alpha or beta particles being emitted, free neutrons are emitted [11]. This type of radiation can travel the furthest in air, and can only be stopped by hydrogen-rich materials [11]. While neutron radiation is not considered direct ionizing radiation, it can indirectly ionize atoms or molecules, making it a viable treatment option [11]. Proton radiation emission is similar in principle to neutron radiation because protons are particles contained within the nucleus of an atom, but the nature of proton radiation is much different due to the charged nature of protons [12,13]. Protons will interact with matter in a similar manner to alpha and beta particles, but proton radiation will travel further than alpha or beta radiation [13]. A diagram of typical penetration strengths for all radiation types except proton beam is shown in Figure 7.

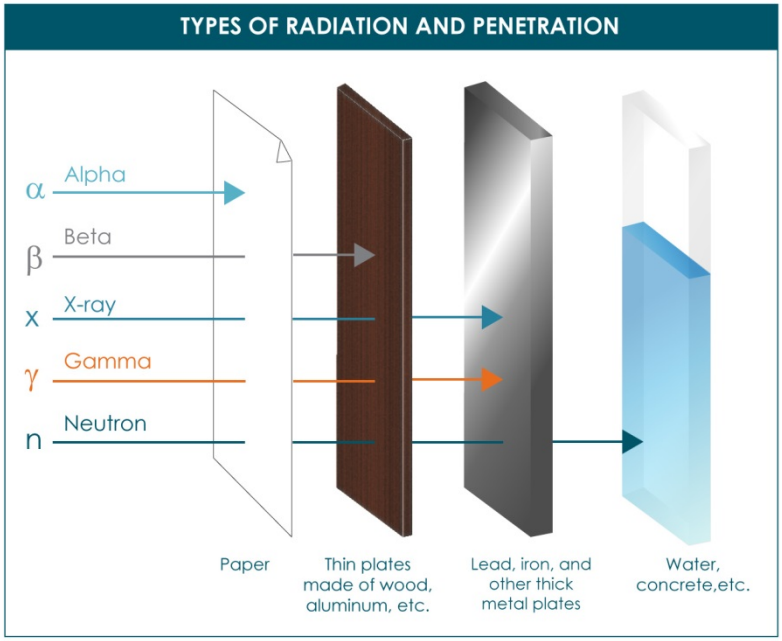

Figure 7. Depending on the type of radiation, the penetration strength will vary. This strength is important when planning out a treatment course for a patient [11].

1.2.2.2 Effects of Radiation Therapy on Cancer Cells. Radiation can affect cells in two main ways; the cell itself can be damaged by the radiation, or the DNA of the cell can be damaged [10]. In either case, the mechanism behind the radiation induced damage is ionization of essential atoms or molecules in the cells [10]. When the radiation (either particles or photons) interact with these atoms or molecules, the result is a change to the number of electrons in the electron cloud [10]. This process is termed ionization. By ionizing atoms and molecules that are the basic "building blocks" of crucial proteins, the ability of the protein to function normally is either severely hindered or completely removed. On the cellular level, this can result in immediate or delayed cell death [10]. Radiation therapy for cancer is often effective because the cells that are most affected by radiation are the actively dividing cells, and metastatic cancer cells are constantly dividing [10]. Unlike immunomodulation therapies, like CART, there is no way for the cancer cells to be specifically targeted by the radiation, so it is important to limit the

radiation exposure of healthy tissue to a minimum. The level of healthy tissue exposure is one of the main differences between external beam radiation and brachytherapy.

1.2.2.3 External Beam Radiation. External beam radiation consists of many different specific types of radiation, but does not involve any radioactive materials. In this report, external beam radiation will refer to radiation given using large machines that are often not transported from one room to another (let alone from one treatment center to another). Some external beam radiation can be targeted radiation; however, in most cases external beam radiation can have a significant effect on normal tissue around the cancer, even when directed at the cancerous tissue [10]. External beam radiation is typically photon radiation, but in some cases, such as proton beam, it can be particle radiation. The cancers that the Xoft system is cleared to treat are commonly treated with external beam radiation; and at the moment, external beam radiation is the more widely used treatment when compared to brachytherapy for these cancers [13-18]. For breast cancer specifically, external beam radiation is more common than brachytherapy [13], but sometimes a combination of external radiation and brachytherapy is used [14]. While external beam radiation is more common than brachytherapy for breast cancer, the growing use of brachytherapy in early stage breast cancer will be discussed in the next section. For the gynecological cancers that the Xoft system is used to treat, a combination of external beam radiation and brachytherapy is usually used [15-17].

Finally, for NMSC, there are many different treatments that are commonly used, depending on the location of the cancer and the specific patient, but external beam radiation is one of the therapeutic options [18]. When external beam radiation is chosen to treat NMSC, electron beam

radiation is often the best method because it does not penetrate much deeper than the skin [18]. It is important to note, that while almost all radiation therapies for NMSC are technically external beam radiation because the cancer is usually on the skin, in this report, brachytherapy will be considered a separate treatment than external beam radiation to clarify the differences in the two processes. With all of these cancers, the effects of external beam radiation have been well documented, which makes it a good option for treatment in many cases. External beam radiation is also good choice when the cancer has metastasized significantly. Despite some of these advantages, there are disadvantages to external beam radiation, which the next section will discuss. Brachytherapy has the potential, and in some cases has been shown, to significantly improve upon some of these disadvantages.

1.2.2.4 Brachytherapy. Brachytherapy is a newer type of radiation therapy than external beam radiation. While many organizations will use the terms "brachytherapy" and "internal radiation" synonymously, there is a difference between the two. Technically, brachytherapy only means that the source of radiation is brought close to the cancer, and this does not limit brachytherapy to internally placed sources. In the following paragraphs, the distinction between types of brachytherapy will be made clear.

In traditional brachytherapy, radioactive sources (like pellets or wires) are implanted (temporarily or permanently) near the tumor or placed inside a device like a catheter, cylinder, or balloon that is then inserted near the tumor [10,19]. A diagram of LDR radioactive brachytherapy for prostate cancer is shown in Figure 8; the procedure is relatively similar for the treatment of breast and gynecological cancers.

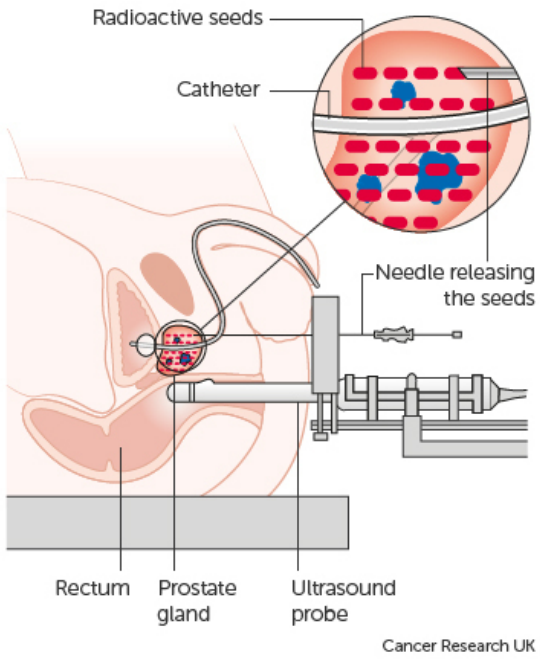

Figure 8. In traditional brachytherapy, radioactive seeds or wires are inserted either temporarily or permanently (depending on the dose rate) to treat the cancer [19].

Depending on the radiation dose rate, the treatment is termed high-dose rate (HDR) or low-dose rate (LDR). Permanent implantation of a radioactive seed is performed with very low-dose rate radiation sources [10]. HDR brachytherapy can be administered in treatment times on the order of minutes, while LDR seeds can be left in place for up to 1 week [10]. As section 1.2.2.1 discussed, this type of radiation is alpha radiation because it originates from radioactive isotopes. This type of radiation has some advantages when compared to external beam radiation including more localized treatment and possibly higher doses to the tumor. By placing the source close to the cancerous tissue, radiation to healthy tissue is minimized. This is an advantage because, as section 1.2.2.2 explained, the radiation can kill healthy tissue as well as cancerous tissue. By minimizing the exposure of healthy tissue, the side effects can be reduced, thereby improving not only the quality of life, but also the safety of the treatment. This localization allows for a higher

dose to be administered because there is less concern about healthy tissue receiving doses of radiation. There are disadvantages to this type of brachytherapy, including safety concerns related to the handling of the radioactive materials and inability to treat highly metastasized cancers.

In x-ray, or electronic brachytherapy (EBT), which will be used synonymously in this report, high voltage creates the radiation source. In the Xoft system (an HDR x-ray system), a cathode wire inside a tube (shown in Figure 9) charged with 50,000 volts is spaced a distance from an anode at 0 volts. Due to this large potential difference, electrons flow from the cathode to the anode, and hit the anode at a velocity large enough to interact with the inner shell tungsten electrons. To prevent scattering of the electrons before they hit the anode, the tube is held at a very high vacuum.

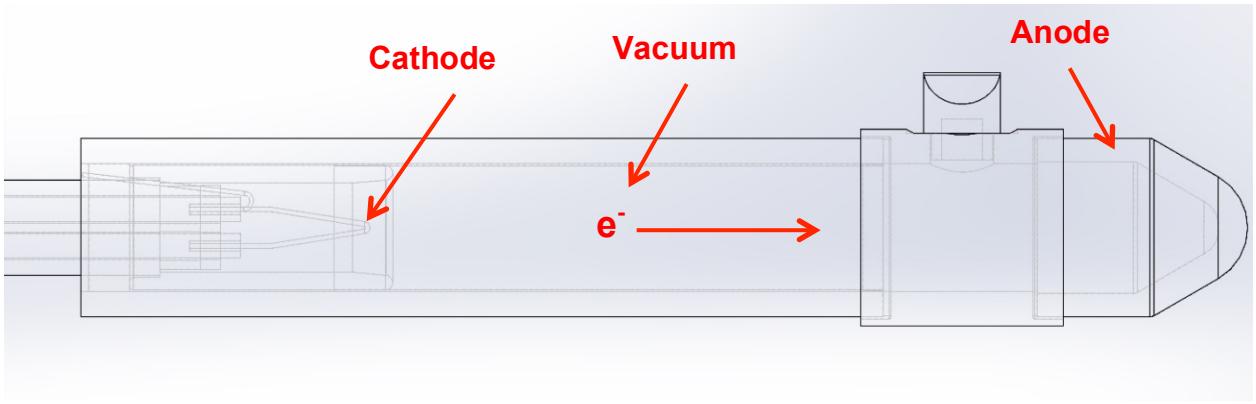

Figure 9. The x-ray radiation in the Xoft Axxent system is created by the potential difference between the cathode and the anode. The tube is at a high vacuum to prevent electron scattering.

When the electrons from the cathode interact with the anode electrons, the inner shell electrons are dislodged, and outer shell electrons drop down to the lower energy state vacated by the dislodged electrons. When the outer shell electrons drop down to a lower energy state, according

to conservation of energy, energy must be released in some form. In this case, the energy is released in the form of photons that create the HDR x-ray radiation source. A diagram of the electron energy state change is shown in Figure 10.

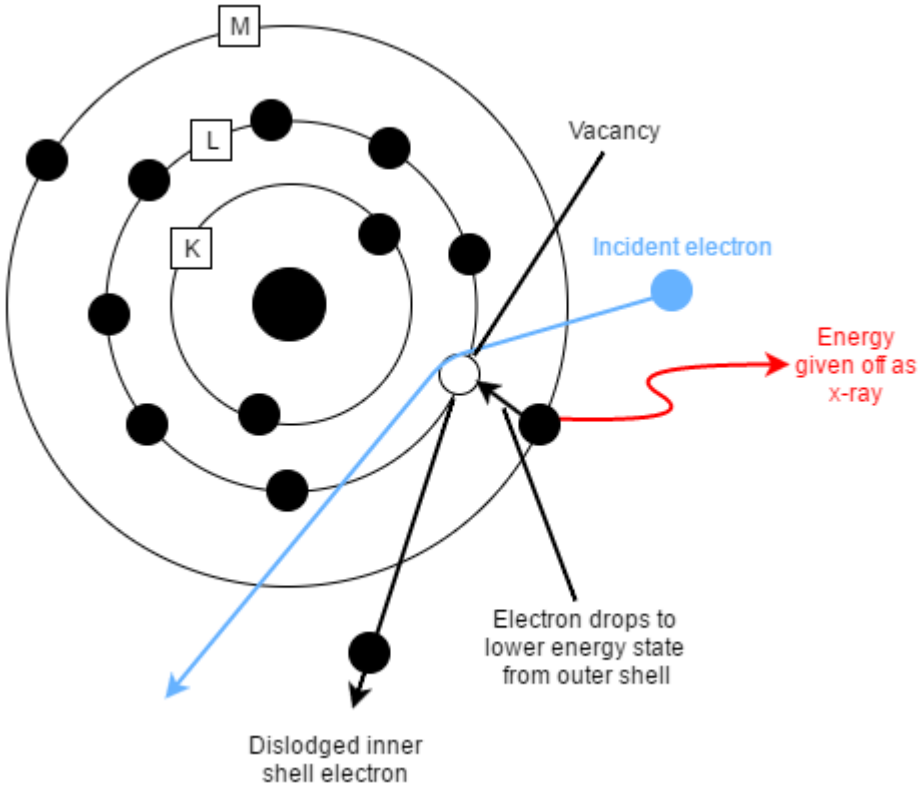

Figure 10. Incident electrons from the anode dislodge inner shell electrons, allowing outer shell electrons to drop to a reduced energy state. The energy is given off in the form of photons, creating x-rays.

In x-ray brachytherapy, the radiation source (the tip of the anode) is brought close to the cancerous tissue at some point during the course of treatment (during or after surgery if surgery is necessary). As opposed to LDR traditional brachytherapy, the source of radiation is never implanted in the patient's body. Because the source is an HDR source that can be brought very close to the diseased tissue, treatments are typically under 20 minutes. There are a few disadvantages to EBT including the inability to treat highly metastasized cancers and a lack of

data to understand long-term side effects and long-term efficacy. The advantages of EBT when compared to external beam radiation and traditional brachytherapy are significant and will be discussed in section 1.2.2.5.

One type of procedure that EBT is becoming popular for is Intraoperative Radiation Therapy (IORT). As the name suggests, in this procedure the radiation is administered to the patient during the surgery to remove cancerous tissue. IORT is not limited to EBT (traditional brachytherapy can be used); but, as the next section will discuss, the advantages of EBT as compared to traditional will likely make EBT a better choice for IORT in the future. The advancement of radiation therapy has made IORT a viable treatment option because the tissue immediately surrounding the tumor can be targeted with much smaller doses reaching nearby healthy tissue. Ideally IORT could be used for most cases where the cancer has not metastasized; this would provide the advantage of shorter treatment times, higher doses of radiation delivered to the cancerous tissue, and lower doses delivered to healthy tissue. All of these factors would likely lead to faster and more effective cancer treatments, but there is some uncertainty about the effectiveness of IORT. One of the main areas that IORT has been used for is to treat early stage breast cancer patients; and as a result, most of the data currently used to evaluate the efficacy of the procedure is from breast cancer studies.

To date, the IORT studies have been somewhat inconclusive [20-22]. Two large studies, TARGIT-A and ELIOT, have shown similar survival rates between groups receiving IORT and traditional whole-breast irradiation [21,22]. The studies found that there was a higher rate of recurrence in the same breast, but there were significantly fewer side effects in the group that

received IORT [21,22]. In the context of this report, the TARGIT-A study is more relevant because the radiation therapy device used in this study (Intrabeam, Carl Zeiss Meditec) more closely resembles the Xoft, Axxent device. In the TARGIT-A study, at approximately 5 years post-treatment, the number of breast cancer related deaths were not significantly different between the IORT and whole-breast radiation, but there were significantly fewer deaths due to other causes (specifically cardiovascular and other cancers) in the IORT group [21]. This 5 year data suggests that there is the possibility for IORT to provide advantages not only in terms of treatment time and access, but also in terms of reducing deaths due to complications from radiation therapy. Early data from IORT studies performed using the Xoft Axxent system has been positive with low recurrence rates, low rates of low-grade adverse events and good or excellent cosmetic results [23-25]. Specific results from studies performed with the Xoft Axxent device will be discussed in the next section

1.2.2.5 Advantages of EBT. There are several advantages of EBT when compared to whole breast radiation and traditional radioactive brachytherapy including advantages in terms of side effects, treatment length, cosmetic results, and even cure rates in some NMSC cases. In general, when compared to external radiation, many of the advantages of EBT are the same as the advantages of radioactive isotope brachytherapy (higher dose to cancerous tissue, shorter treatment course); however, there are some additional advantages of EBT when compared to radioactive isotope treatment.

The first advantage, fewer side effects, is probably the most clinically relevant advantage of EBT. In a retrospective analysis of EBT using the Xoft Axxent system after surgery for treatment

of early stage breast cancer funded by Xoft, Inc., there were fewer side effects found in patients who received EBT than patients who received comparable treatments with external radiation or radioactive isotope brachytherapy (Iridium-192 HDR brachytherapy) [14]. The metrics used to analyze the doses to healthy tissue were the volume percentages of ipsilateral breast tissue that received 50% of the prescribed dose (Breast V50), lung tissue that received 30% of the prescribed dose (Lung V30), and heart tissue that received 5% of the prescribed dose Heart V5) [14]. For example, if half of the patient's total lung tissue received a dose equal to 30% of the prescribed treatment dose, the Lung V30 would be 50%; a lower percentage indicates a more targeted treatment with less healthy tissue exposed to radiation. The maximum dose to the skin and ribs was also reported. In this study, it was found that the Breast V50, Lung V30, and Heart V5 doses were significantly lower in patients treated with the Xoft Axxent EBT system as opposed to the patients treated with the iridium-192 brachytherapy [14].

Previous literature has already suggested that external radiation poses a significant risk to healthy tissue due to the relatively large amounts of radiation that can be received by the heart, and a correlation between a left ventricular dose over specific thresholds (depending on the treatment type) and diminished myocardial perfusion has been established in a previous study [14]. In this study, no patients treated with EBT were above this threshold, but 1 patient out of 12 iridium-192 treated patients was above the threshold [14]. Despite the small sample size, the numbers indicate that there is consistently less radiation to healthy tissue when patients are treated with EBT as opposed to radioactive isotope brachytherapy or external radiation therapy. More research is still necessary to show a large-scale, long-term benefit of EBT, but the current information seems very promising for EBT as an advantageous therapy.

When compared with radioactive isotope brachytherapy EBT is also advantageous in that it requires no special handling or shielding while treatment is not in progress. With radioactive materials, constant shielding is necessary because there is no way to turn the radiation off as there is with EBT. Without the need for constant shielding or special handling, EBT is a treatment that can be provided in more settings than isotope radiation; this makes EBT a more accessible treatment to patients. It has also been found in studies that in treatment of early stage breast cancer, EBT has similar low to medium grade toxicity (skin rash, infection, fibrosis, etc.) and similar short-term outcomes to a typical radioactive isotope brachytherapy procedure [14,26].

When compared to external radiation therapy, the Xoft Axxent EBT has a shorter treatment course than external radiation (approximately 5 days for Axxent, compared to 6-7 weeks for external) [13,14]. The shorter treatment times are a result of the higher dose rate of the Axxent system. At first glance, this may seem like a convenience, but the shorter treatment time makes EBT a more viable option for patients who do not live near to a clinic and do not have the resources to travel back and forth to the clinic for nearly two months. Importantly, the Xoft Axxent system has shown low recurrences at 5 years post-treatment [25].

Compared to external beam radiation for early stage breast cancer and surgery for NMSC, EBT has also shown better cosmetic results [27,28], which is important when considering quality of life for the patient after treatment. In terms of treating NMSC, it has been found that EBT can even result in better cure rates than surgery alone [27].

1.2.2.6 Clinical Studies Using Xoft Axxent EBT. There have been several clinical studies performed using the Xoft Axxent EBT (trade name Xoft Axxent eBx) system to treat early stage breast cancer and NMSC, but for the sake of brevity, only the results for a few of these studies will be presented in this section.

A study was published in 2011 detailing the treatment for 44 ductal carcinoma or ductal carcinoma in situ patients with the Xoft Axxent. The study found that there were low rates of low-grade adverse events (with the exception of approximately 43% of patients experiencing low grade erythema) [26]. The rates of adverse events were less than or comparable to patients treated with iridium brachytherapy [26]. Of the 43 patients that reported through 6 months and the 36 patients that reported through 1 year, no tumor recurrences were found [29]. Another study reported the treatment of 11 patients for early stage breast cancer using the Xoft Axxent eBx system. In this study, the cosmesis was rated by physicians as either good (9%) or excellent (91%) and as excellent by all patients [24]. As Table 1 shows, there were no adverse events, and no severe mammographic findings. In addition, all patients were followed for 1 year, and no recurrences at 1 year were reported. [24].

Table 1. 11 early stage breast cancer patients were treated with the Xoft Axxent eBx system [24].

	Minimal	Moderate	Marked
Adverse events			
Pain	0	0	0
Fibrosis	0	0	0
Erythema	0	0	0
Mammographic findings			
Breast edema	11 (100%)	0	0
Skin thickening	9 (82%)	2 (18%)	0
Architectural distortion	5 (45%)	6 (55%)	0

The last observation was carried forward for one patient with 6-month data only

In addition to these two studies, up to 5 year data was presented at the American Society for Radiation Oncology (ASTRO) in October of 2015 that detailed 136 breast cancer lesion treatments [25]. The data showed few low-grade adverse events and a low recurrence rate [25].

A study examining the treatments of 122 patients with 171 NMSC lesions was published in 2013 and showed no recurrences at an average follow-up time of 10 month [30]. Cosmetic outcomes were also evaluated at 1 year post-treatment in 42 lesions and were found to be either excellent (39 patients) or good (3 patients) [30]. Figure 7 shows a woman treated for basal cell carcinoma with the Xoft Axxent eBx system pre- and post-treatment. Similar images showing cosmetic results are in Appendix A.

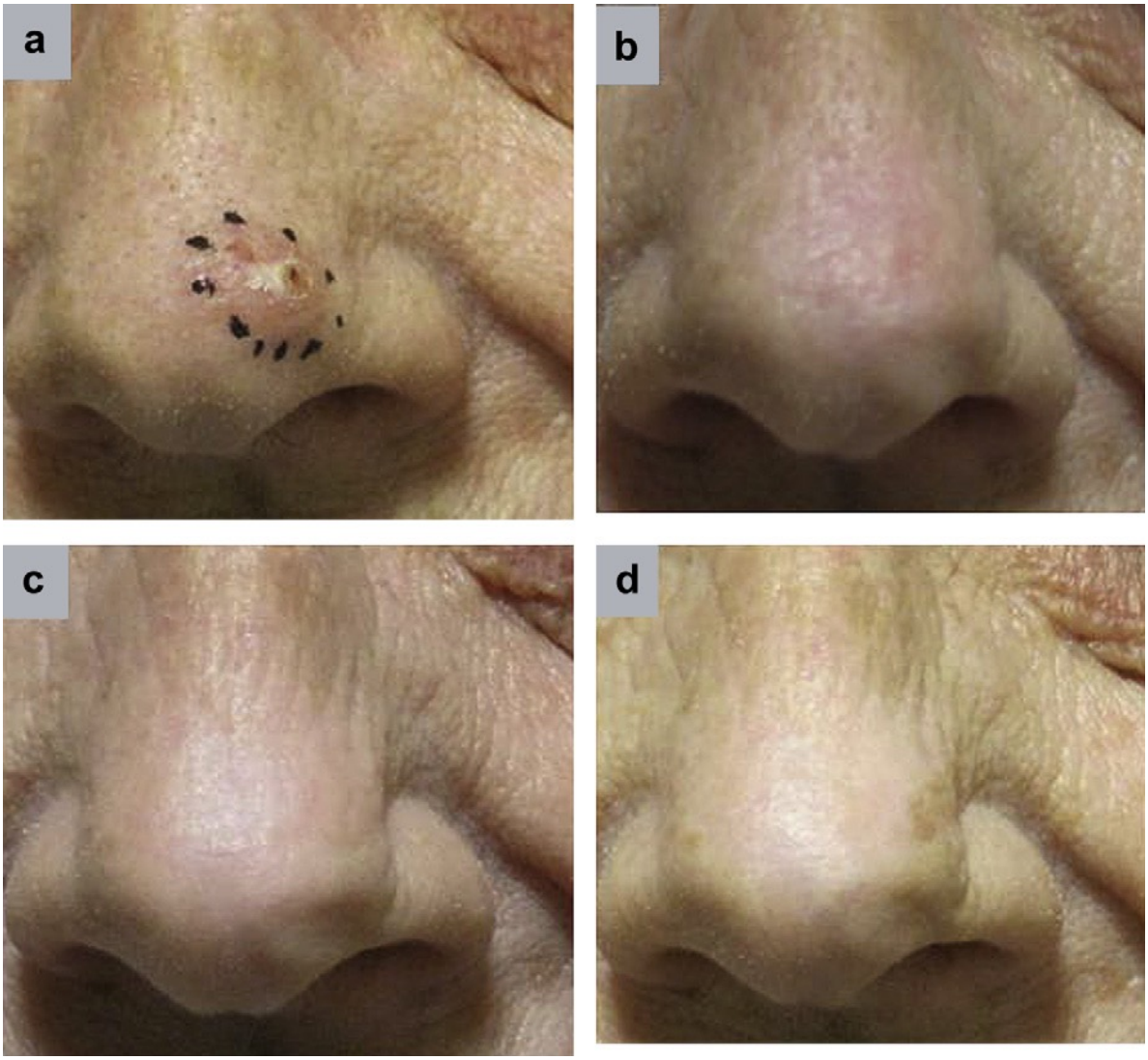

Figure 11. A 73 year old woman pre-treatment (a) and 4 (b), 16 (c), and 23 (d) months post treatment. The resulting cosmesis at 23 months is excellent [30].

The adverse events reported from this study are shown in Table 2. As the table shows, there were very few adverse events at 1 year, and there were no serious-grade adverse events.

Table 2. Adverse events at 1 year post-treatment for NMSC using the Xoft Axxent eBx System were recorded for 46 lesions [30].

Adverse event	AEs 1-year post-Tx ($N = 46$ lesions) (%)
Hypopigmentation	5 (10.90)
Rash dermatitis	3 (6.5)
Alopecia	1 (2.2)
Dry desquamation	1 (2.2)

AE = adverse events; Tx = treatment.

Finally, data for 565 lesions treated using the Xoft Axxent eBx system at Aegis Oncology has been presented. This data shows only 4 recurrences and only 7 cases of prolonged skin healing [31]. The mean follow-up time for this data was 9.2 months, and cosmesis was evaluated as generally excellent [31].

As these studies show, electronic brachytherapy is an excellent treatment option with many advantages for early stage breast cancer and non-melanoma skin cancer. Despite the promising data, long-term results will need to continue to be monitored and analyzed to gain a better understanding of the effectiveness of this therapy and any of its long term systemic side effects. It is also important to note that each cancer case is unique, with many factors that determine the best treatment course, and patients must consult with their oncologist before determining the best therapy for their unique situation. Despite any limitations presented, electronic brachytherapy has made a significant positive impact in the radiation therapy arena, and the Xoft system has been shown to be effective as one of the leaders in electronic brachytherapy. Improvements and further work to improve the system as described in this report will continue to keep the Axxent eBx system at the forefront of radiation therapies.

1.3 Xoft Axxent System

The Xoft Axxent eBx system is an HDR x-ray brachytherapy system; at the highest level the system consists of an x-ray source, a method to cool the source, a catheter to allow cooling of the source, and a controller to turn the source on and off. In this section the components of the Xoft system relevant to this report will be described, and the relevance of each component to this report will be explained.

1.3.1 X-ray Source and Cable. The x-ray source is truly the functional unit of the whole system, with all the other components supporting the function of the source. The source has already been described in section 1.2.2.4, so an in-depth description will not be provided in this section. A diagram of the source is shown in Figure 12.

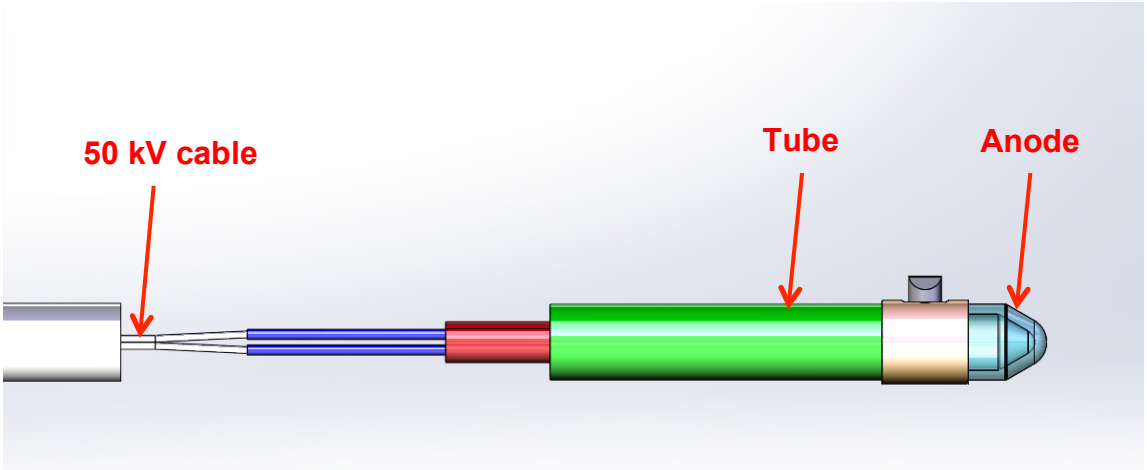

Figure 12. The x-ray source is comprised of a cathode (hidden), anode, and a tube under high vacuum. The source is connected to a cable that provides the 50kV potential.

As Figure 12 shows, the source is connected to a cable that provides the current to create the flow of electrons down the tube from the cathode to the anode. Production sources are wrapped with a polymer that extends from before the cable-source connection up to the beginning of the

anode to cover the connection between the cable and the source. The assembly of the cable and source without this final polymer wrap is shown in Figure 13.

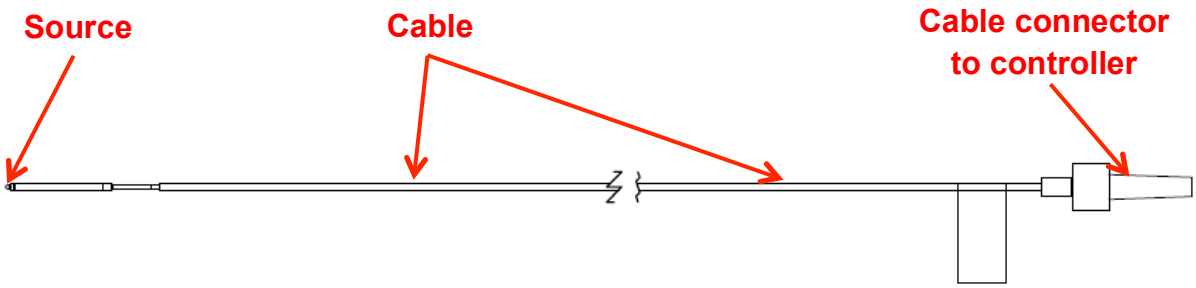

Figure 13. The assembly of the cable and source is connected to the controller at the cable connector. The cable provides the power to create the x-rays.

The cable-source assembly is relevant to this report because, as it is producing x-rays, additional energy due to electron interactions with the anode is given off as heat. As a result, without cooling in some form, the anode will overheat. This necessitates a coolant, which will be discussed in the next section.

1.3.2 Coolant, Pump, and Cooling Tubing Set.

There are currently 2 types of coolants used in the Xoft System to cool the source: water and a perfluorinated polyether (trade name Galden HT-135). Water was the original coolant used in the system. Galden HT135 was chosen as the next coolant, and both coolants are currently in production. The systems that utilize Galden are termed Extended Source Life systems (ESL). These systems are designed to run longer than sources that utilize water as a coolant. The properties of Galden can be found in Appendix B, but one of the most important properties is its chemical inertness [32]. The coolant

(either water or Galden) is stored in a bag connected to the tubing that it flows through as shown in Figure 14. In this report, the only coolant considered will be Galden HT135.

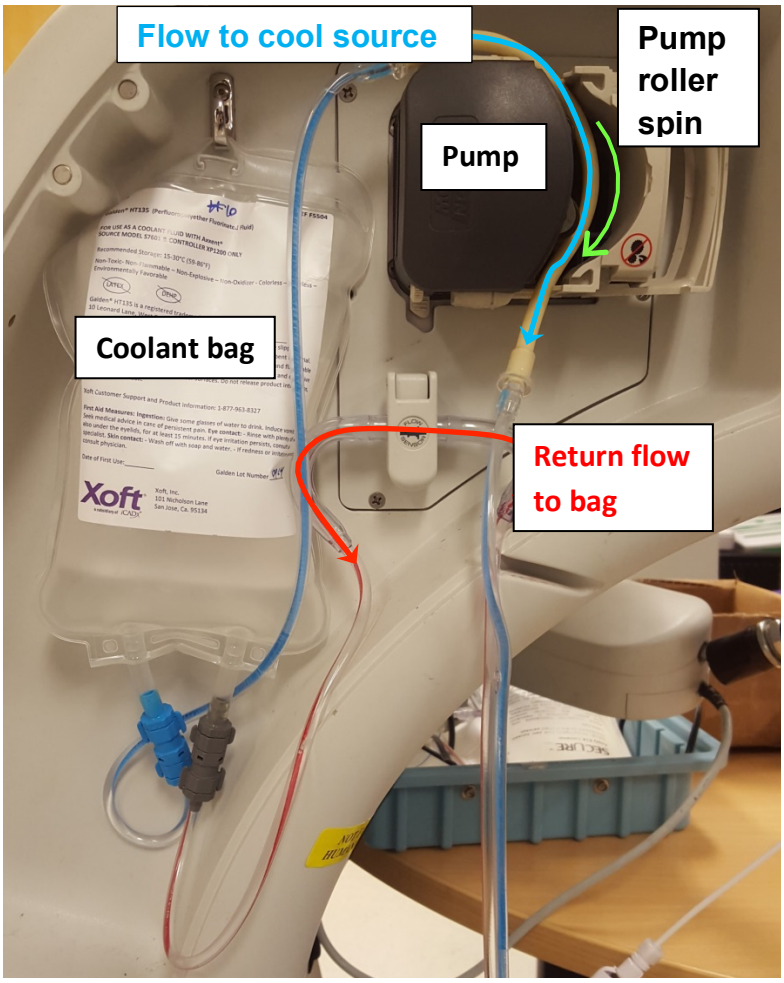

Figure 14: The coolant is stored in a bag and pumped through the cooling tubing set using a 4-roller, peristaltic pump.

The set of tubes that the Galden flows through is termed the cooling tubing set, and it is mostly made from Tygon tubing. The section of the tubing set that is placed in the pump is made from another polymer. A diagram of a component of the cooling set is shown in Figure 15.

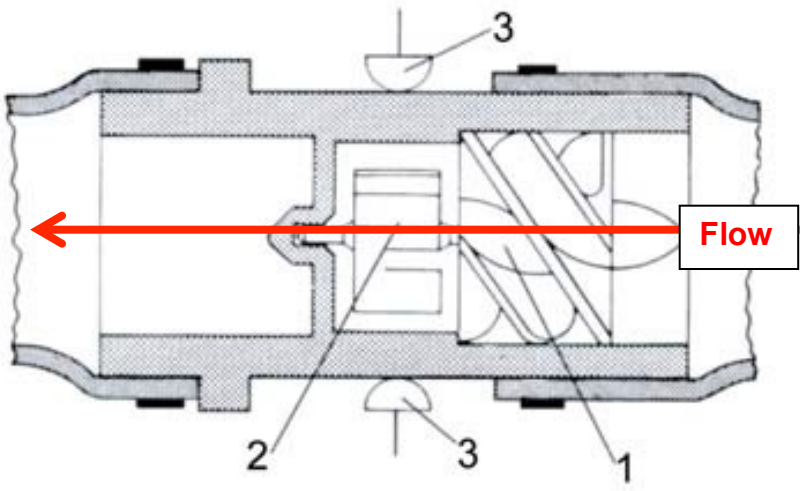

Figure 15. A diagram of a cooling tubing set component [33].

A picture of the coolant bag, entire cooling tubing set, and a catheterized source and cable is shown in Figure 16. A large portion of the cable, including the controller connector, has been cut off for the cable in this figure. The catheter will be discussed in its own section because it is the main component that this report focuses on.

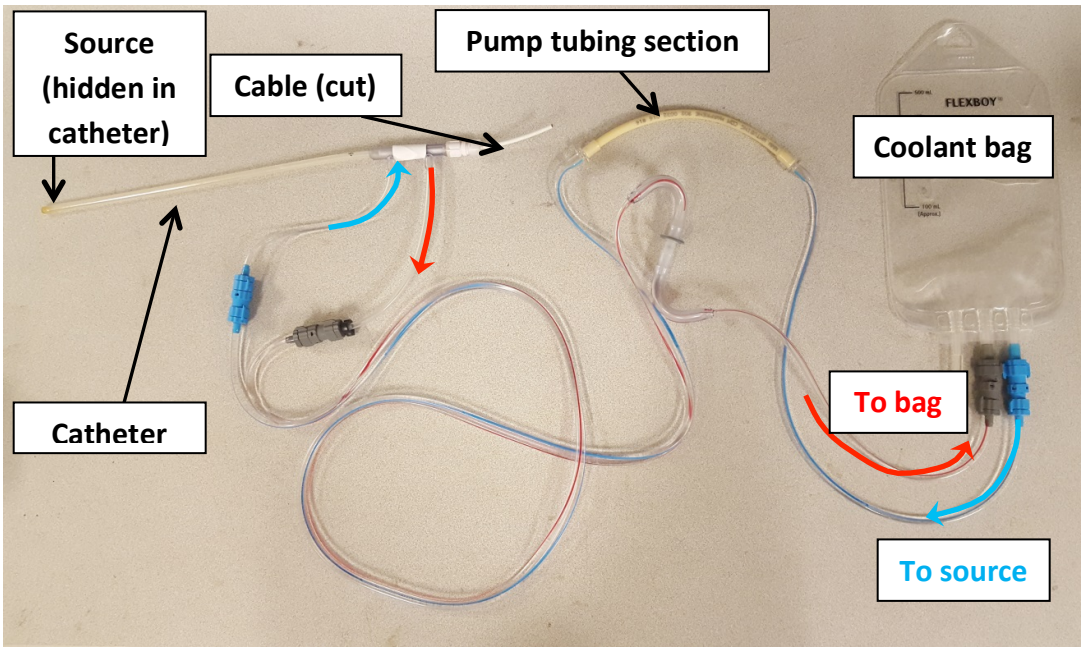

Figure 16. The cooling tubing set, coolant bag, and catheter make up the system that cools the source.

The pump tubing section of the cooling tubing set is placed into the pump (as shown in Figure 14). The pump is a 4-roller peristaltic pump capable of producing relatively continuous flow rates [34]. Images of the pump open and closed with tubing inside are shown in Figures 17 and 18.

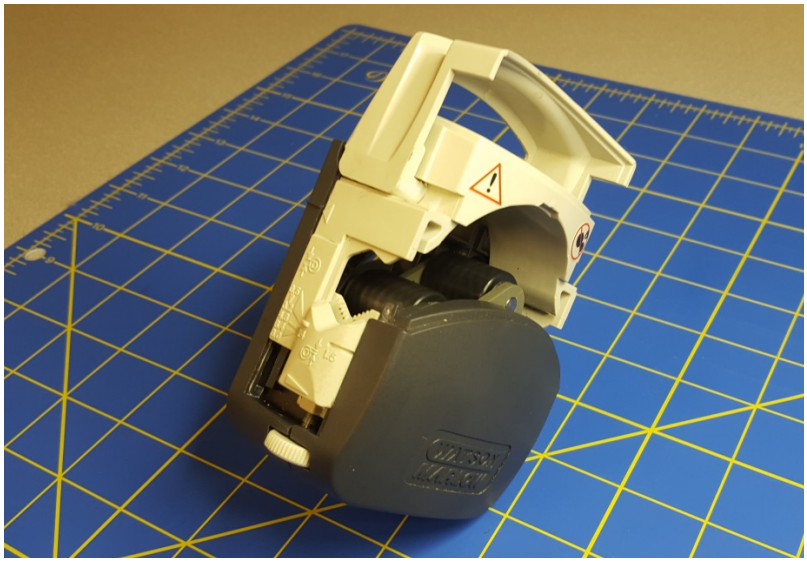

Figure 17. The pump has 4 rollers that spin to propel fluid through the cooling tubing set.

Figure 18. The pump closes on the pump tubing section to prevent movement of the tube.

One important parameter that the pump influences is the flow rate (and thus, pressure) seen by the cooling tubing set and the catheter. The revolutions per minute of the pump have been found to be an important factor in ensuring that the source receives a flow rate capable of effectively cooling the anode.

1.3.3 Catheter. The most important part of the system with respect to this report is the catheter that the source and part of the cable are inserted into. The purpose of the catheter is mostly to direct the flow of coolant past the tip of the anode and back to the bag, where it is pumped out to cool the anode again. The catheter performs other functions, including providing protection for the source from impact, and providing a marked region to indicate to radiation oncologists how far they are moving the source during procedures that require movement. A solid model of the catheter is shown in Figure 19.

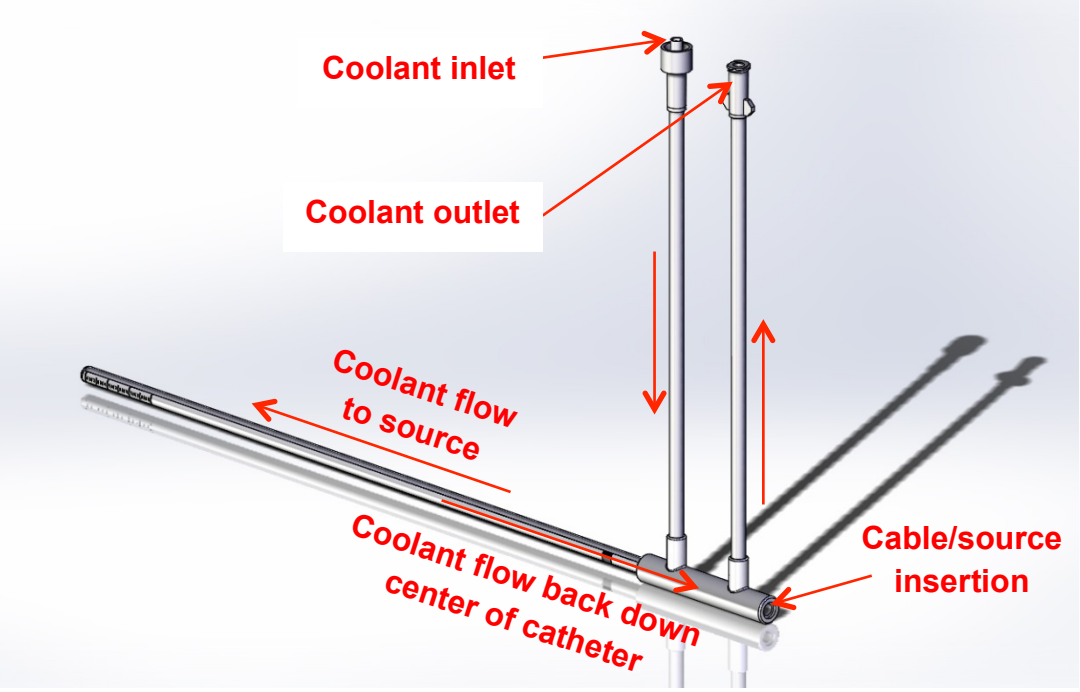

Figure 19. The catheter that the source and cable are inserted into allows coolant to flow. The coolant flows down to the source, flows over the source tip, and back down the catheter.

As the figure shows, the coolant flows down the catheter towards the source to cool the anode.

1.3.4 Controller. The controller is the largest portion of the Xoft Axxent system, and it contains the electronic components necessary to create the 50 kV potential (the controller plugs into a typical wall outlet) as well as the necessary hardware and software to interface with the radiation oncologist. An image of a typical controller is shown in Figure 20.

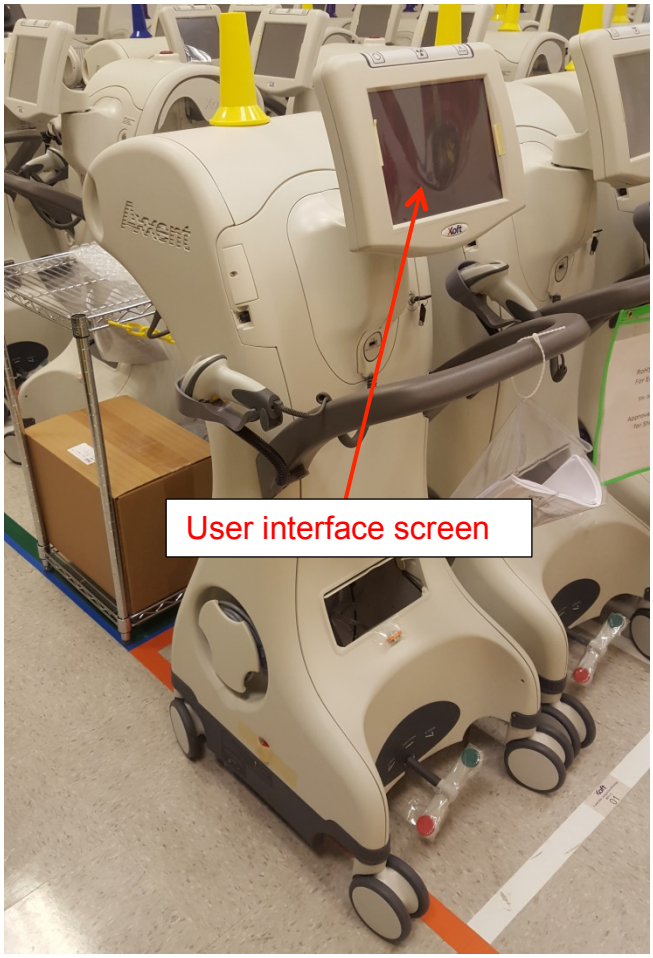

Figure 20. The controller contains the user interface for the radiation oncologist.

All of the components previously described fit in or onto the controller in some way. As Figure 14 in section 1.3.2 shows, the controller has a cutout to house the pump and the coolant bag. Within this cutout is the flow sensor and part of the cooling tubing set. The tubes carrying fluid away from and to the controller run between this cutout section and the catheter, source, and cable assembly. On the side of the controller that the source, cable, and catheter assembly extends from, there is a calibration chamber used before each treatment called the well chamber; this component is shown in Figure 21.

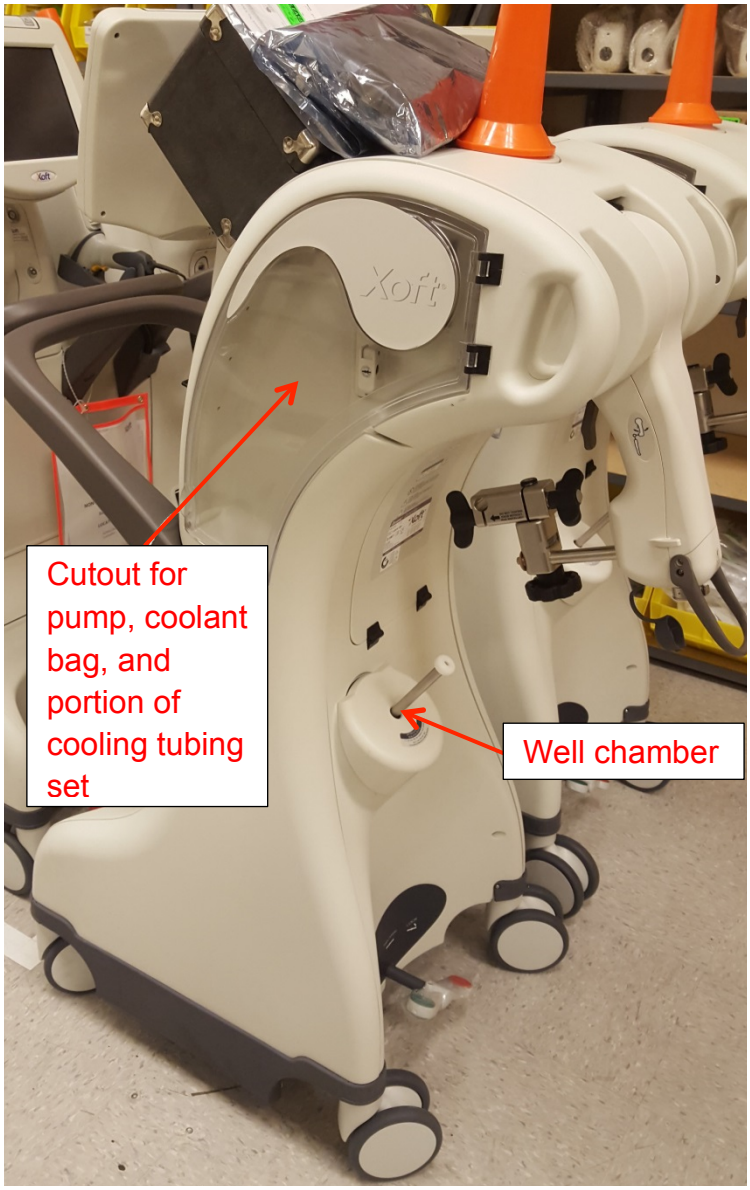

Figure 21. The controller has cutouts for the cooling components and a calibration chamber.

In Figure 22, an overview of the controller with the components integrated is shown. It is important to note that the appearance of the controller in Figure 22 is not accurate for a production controller in Figure 22 and the pressure gauge that the cooling tubing set is connected to is not present in production controllers. Despite the differences, all of the components previously described are present.

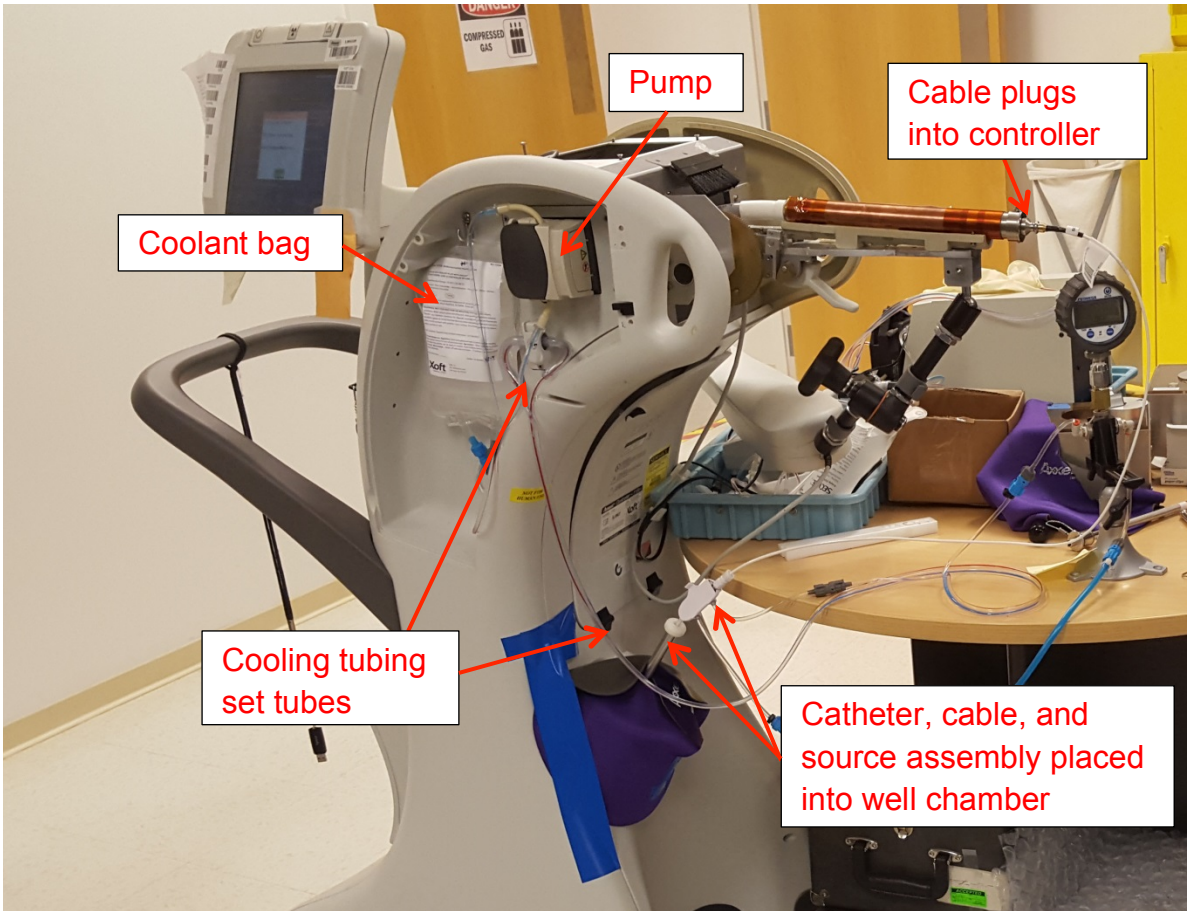

Figure 22. When the controller is fully integrated, it includes the user interface, electrometer, well chamber, pump, cooling tubing set, coolant bag, source, cable, and catheter.

1.3.5 Applicators. In addition to all the components described in previous sections, there are specific applicators for each condition the Xoft Axxent system is cleared to treat. There is a balloon applicator used in treatment of breast cancer (Figure 23), vaginal applicators used for treatment of the gynecological cancers (Figure 24), and surface applicators used for the treatment of NMSC (Figure 25).

Figure 23. The balloon applicator is designed for treatment of early stage breast cancer [35].

Figure 24. The cervical applicators are designed for treatment of gynecological cancers [35].

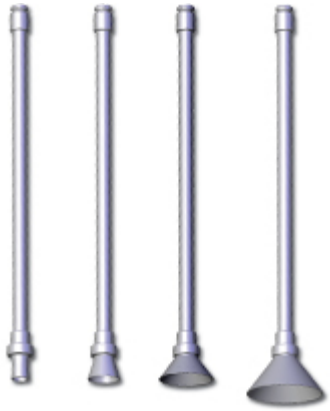

Figure 25. The skin applicators are designed for treatment of NMSC [35].

For all of the applicators, the catheter slides down the center, but the balloon applicator is unique in the fact that the radiation oncologist will slowly pull the catheter back from the fully inserted position during treatment. The applicators, despite not being a part of the core system, have one major role in the material selection criteria for the catheter. The necessary material properties, including how the applicators relate to material selection criteria for the catheter will be discussed in section 1.3.6.2.

1.3.6 Catheter Materials. As mentioned in previous sections a polymer is used to manufacture the catheter.

1.3.6.1 Current Material Limitations. Catheters made from one material are relatively strong, but some characteristics have been shown to be relatively poor in previous studies [36,37]. There are certain studies suggesting a mechanism behind this performance [37]. The catheter geometry likely plays a role in this performance characteristic as well.

1.3.6.2 Relevant Material Properties. There are three main criteria that were necessary to evaluate for the materials investigated in this report.

1.4 Summary and Aims of the Thesis

In summary, this project aimed to investigate the suitability of two materials for a radiation therapy catheter by evaluating the three main criteria outlined at the beginning of the previous section. Tensile testing, pressure testing, and coolant compatibility testing was performed.

Overall, the multiple tests performed in this report were intended to determine the best material, all criteria considered, for the Xoft Axxent eBx catheter.

2.0 MATERIALS AND METHODS

The testing for this report consisted of testing two polymers. Initial simulations in SolidWorks were also run to provide preliminary data for expected results and to model slight changes in catheter design.

2.1 Rationale for Testing Performed

Each test performed for this report was necessary to evaluate the main criteria for choosing a material for the catheter. While, there are many more tests that could be performed, the tests performed for this report captured the most relevant properties.

2.1.1 SolidWorks Simulation Rationale. The SolidWorks simulations were performed to obtain preliminary comparison data. The SolidWorks simulations allowed two materials, pressures and wall thicknesses to be compared to each other. Finally, by obtaining this initial data, it indicated general trends to expect from each type of testing.

2.1.2 Tensile Testing Rationale. Tensile testing was performed to determine how the mechanical properties of the two polymers were affected. Based on previous research, it was thought that for polymers like one of the materials tested, radiation dose would significantly affect yield strength but not elastic modulus [38,39]. Due to the alternating hard and soft segments in some polymers, the crystallinity can vary significantly, although in general, some polymers tested have lower bulk crystallinity than others [40]. Because it was unknown how the mechanical properties of two materials tested would respond, tensile testing was performed.

In addition to determining the mechanical response of the two polymers, there was also tensile testing performed on polymer samples that were soaked in Galden during the coolant compatibility testing. While testing tested the response of polymers due to Galden exposure, the tensile testing was designed to determine if Galden would cause any alterations to the structure of the polymers that would affect their mechanical properties.

2.1.3 Pressure Testing Rationale. The pressure testing was designed to examine the effect of internal pressure catheters made from two of the polymers that were tested. Testing was performed based on initial indications from prior testing that certain polymer catheters would change noticeably when pressurized internally. The testing performed for this report was designed to quantify the change, and determine how much, if at all, another polymer would change when internally pressurized. The second component of the testing was to determine the effect of increased temperature in conjunction with pressure on catheters made with both materials. Testing was not performed on irradiated catheters due to time constraints and limited availability of catheter materials. Along with these constraints, the tensile testing information, when combined with the information from the pressure testing was determined to be sufficient to predict the response of irradiated catheters to internal pressure. If tensile testing showed stiffening of a material with increasing, then les change would be seen in catheters exposed to radiation than the catheters measured in the pressure tests.

2.1.4 Coolant Compatibility Testing Rationale. The compatibility testing performed was designed to determine if Galden exposure would cause two of the polymers to break down and

lose mass. This testing is important because the catheter is in constant contact with Galden for its lifetime.

2.2 SolidWorks Simulations

SolidWorks simulations were performed on sections of the catheter solid model. The material was specified as having the relevant mechanical properties of two polymers. The properties used are given in Table 3. A quarter of the cylindrical tube was used as the model segment with the cut edges held as roller/slider fixtures. Figure 26 shows an image of the model with the roller/slider edge conditions.

Table 3. The properties for the simulation were taken from the technical datasheets for both materials. A value for Poisson's ratio was assumed based on typical values.

Property	Polymer 1	Polymer 2
Elastic Modulus	High	Low
Ultimate Tensile Strength	High	Low
Poisson's Ratio	Average	Average

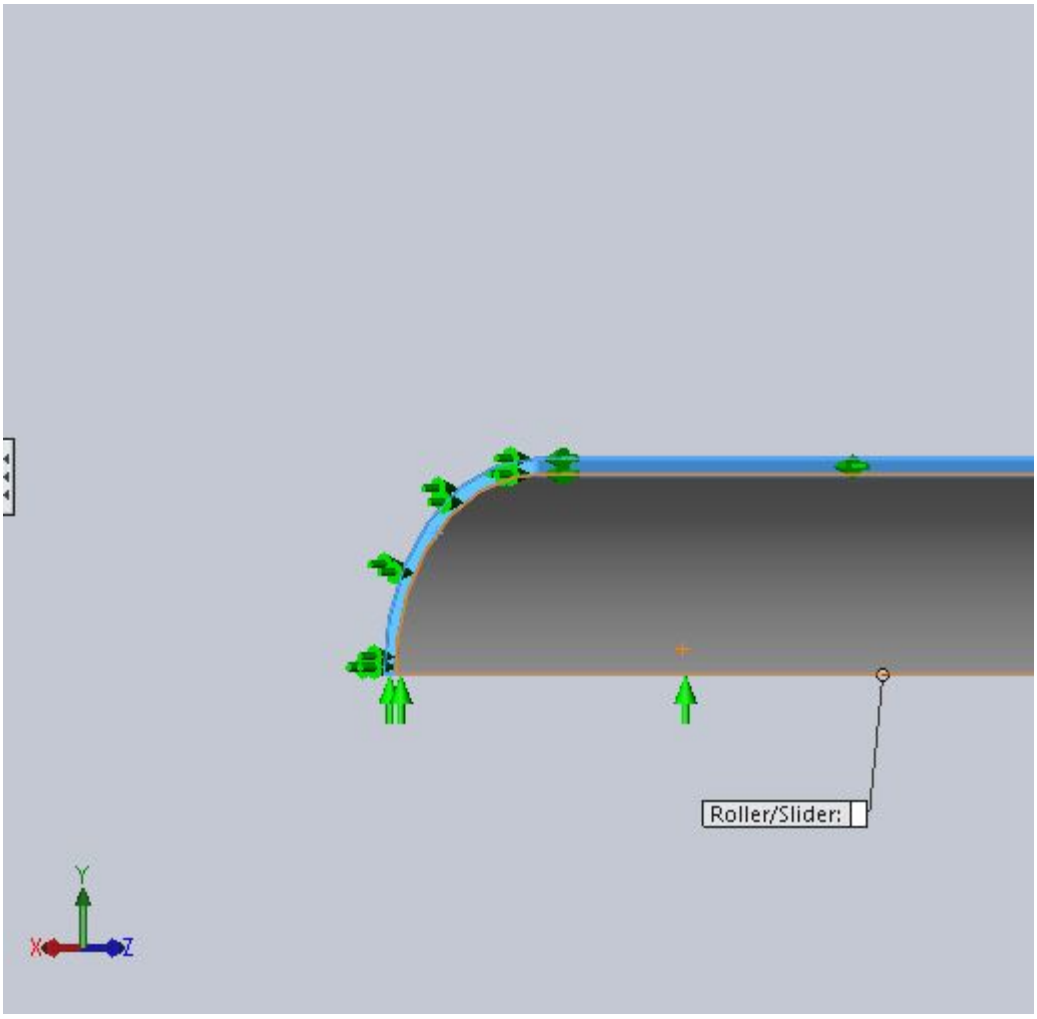

Figure 26. A quarter of the cylindrical outer catheter was used as the model segment for the SolidWorks simulations. The edges were held as roller/slider fixtures.

After the model segment was held as shown in Figure 26, a constant pressure was applied to the inside face of the quarter cylinder. A representation of the applied pressure condition is shown in Figure 27. The pressure was input as either 30 or 60 psi. The pressure values were chosen based on the maximum pressure the system is likely to experience when operating normally. In the clinic, at the most, a system will experience slightly less than 30 psi, so for this simulation, a maximum real case and an extreme case were chosen. By using such a relatively large range in pressure, more noticeable differences were observed between the two simulations for each catheter material. This also gave preliminary insight into how the catheter would react to much

higher pressures. However, because SolidWorks simulation does not handle excessive deformations as accurately as some other software, the results were only used to compare the amount of deformation between the polymer models.

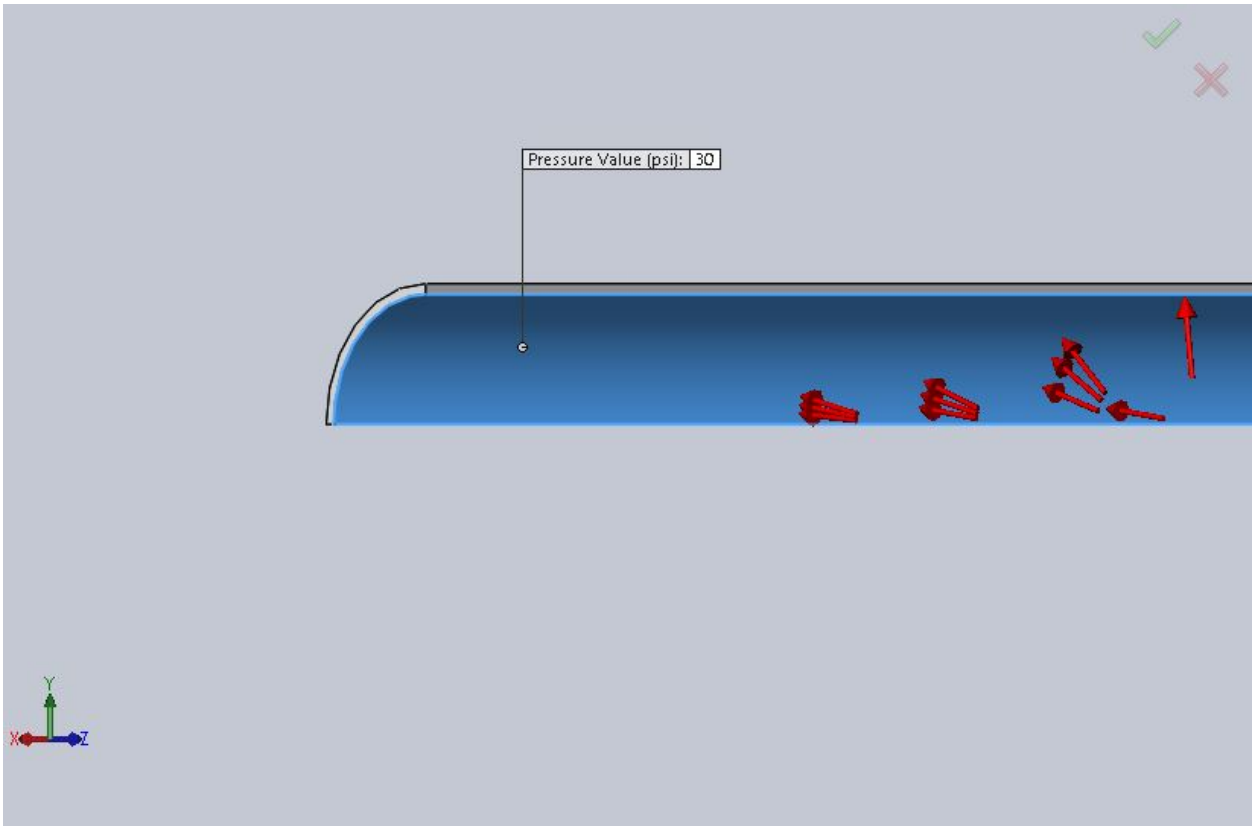

Figure 27. The models used for the pressure simulation had static pressure of either 30 or 60 psi applied to the inner wall of the tube.

The models were finally meshed using an average global element size of 0.025 inches with a tolerance of 0.00125 inches. Four pressure simulations were then run.

The values used for the material properties were based on the values given in the technical datasheets. It is important to note that Poisson's ratio was assumed based on a typical thermoplastic value [40,41], and the flexural modulus for both polymers was used instead of the

elastic modulus. The flexural moduli for the two polymers were the only moduli given, and for plastic materials, the flexural modulus is almost always very close to the elastic modulus [42]. The final assumption that was made for these simulations was the assumption of constant, static pressure. In reality, because the pump uses a peristaltic mechanism to drive flow, the pressure fluctuates by at least a few psi. For the purposes of these simulations, these assumptions were acceptable.

The other simulation that was performed in SolidWorks was to test the effect of increasing the wall thickness of one of the catheters. This simulation was specifically run for one material to determine if it was a feasible method to increase the rigidity of the catheter to a value comparable to that of another material. The simulations that were run used the same conditions as the previous simulations discussed; the only difference was the wall thickness of the models.

2.3 Sample Radiation Dosing

Cylindrical coupons of material were prepared by cutting 0.75-inch sections from the catheter as shown in Figure 28 and slitting the coupons lengthwise as shown in Figure 29. Despite the fact that one material was not one of the main materials investigated in this report, it was decided that quantitative data on the response of this material to radiation dose could be relevant to the project.

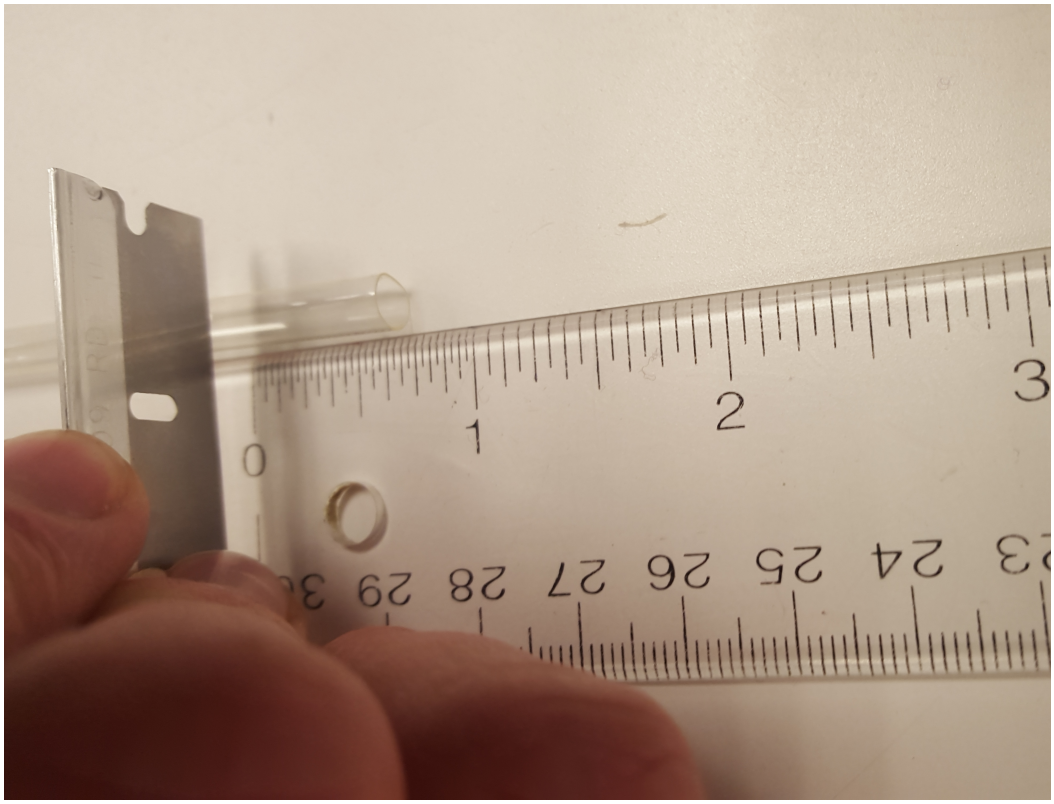

Figure 28. Coupons were cut to 0.75 inches in length from catheters.

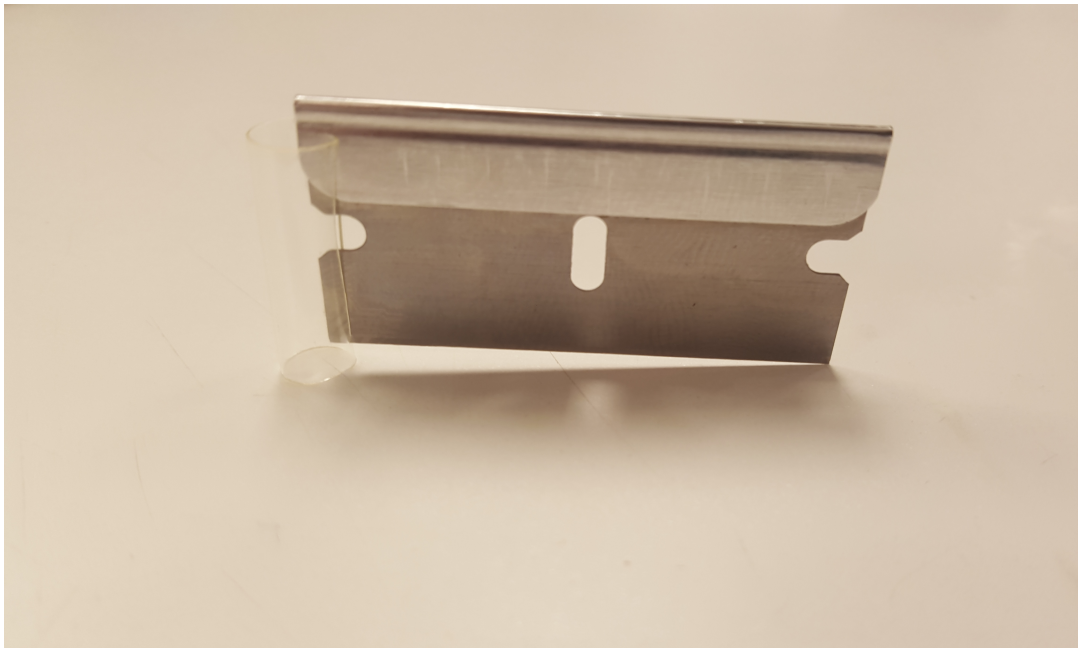

Figure 29. Coupons were slit lengthwise to allow them to wrap around the end of an intact catheter and be exposed to radiation.

Four coupons of material were wrapped concentrically around catheters (shown in Figures 30 and 31) to be exposed to radiation. Two catheters were run at the same time on an automated machine controlled by LabVIEW software. The software is designed to run the catheter for 5 minutes at a time, turn the radiation off for one minute, and then repeat the process. This test fixture is shown in Figures 32 and 33.

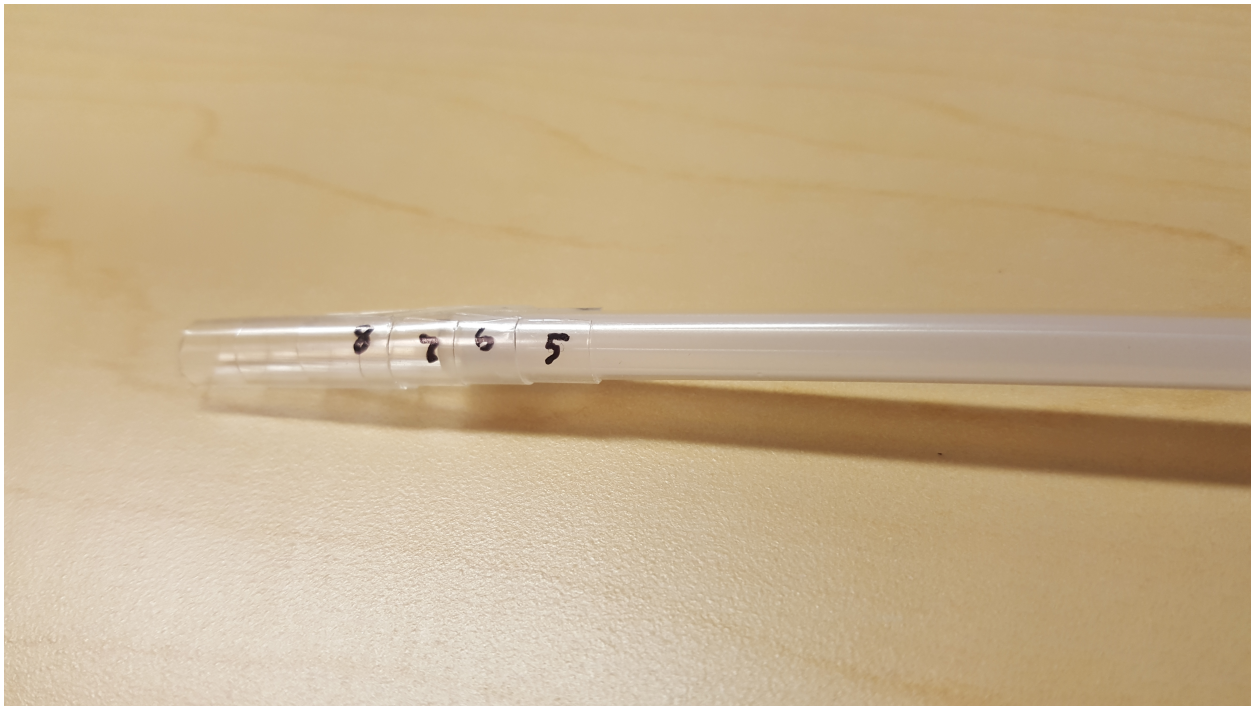

Figure 30. Coupons of material (separately) were wrapped around the end of catheters to be exposed to radiation. In this photo, the coupons are expanded to allow each coupon to show.

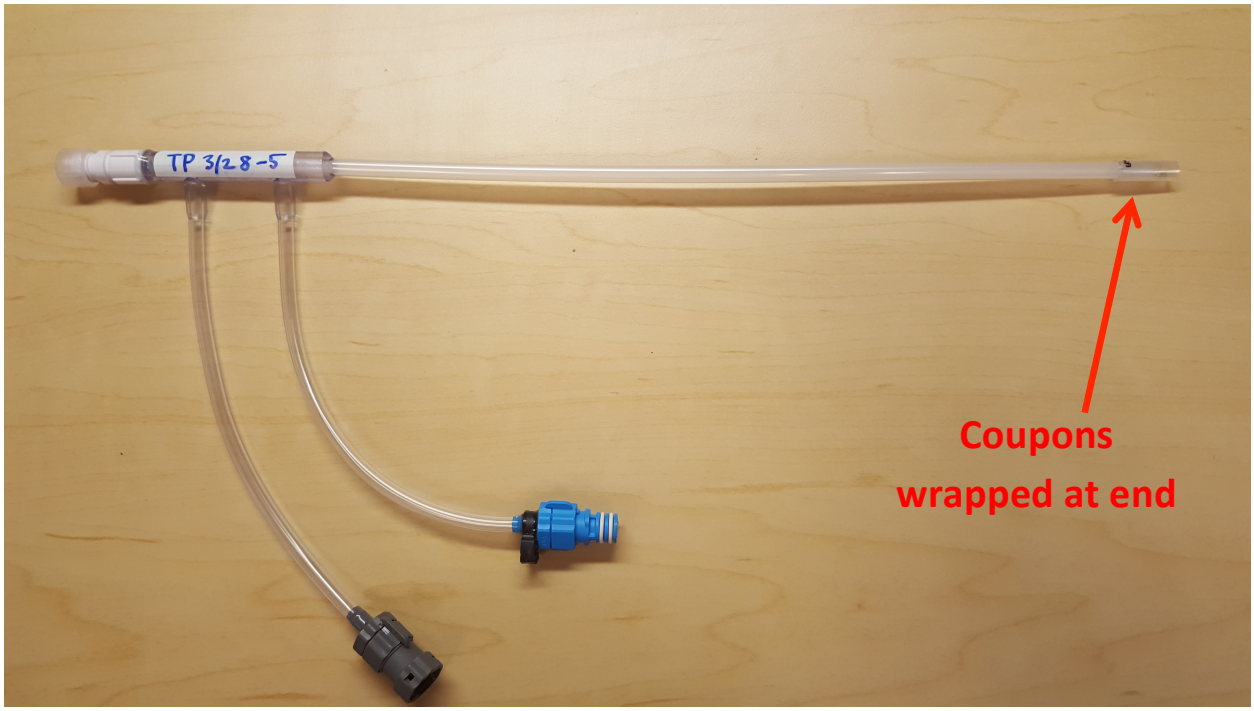

Figure 31. The coupons were aligned concentrically at the end of the catheter to allow each coupon to receive a dose of radiation.

Figure 32. The catheters were placed with the tip down into the test fixture.

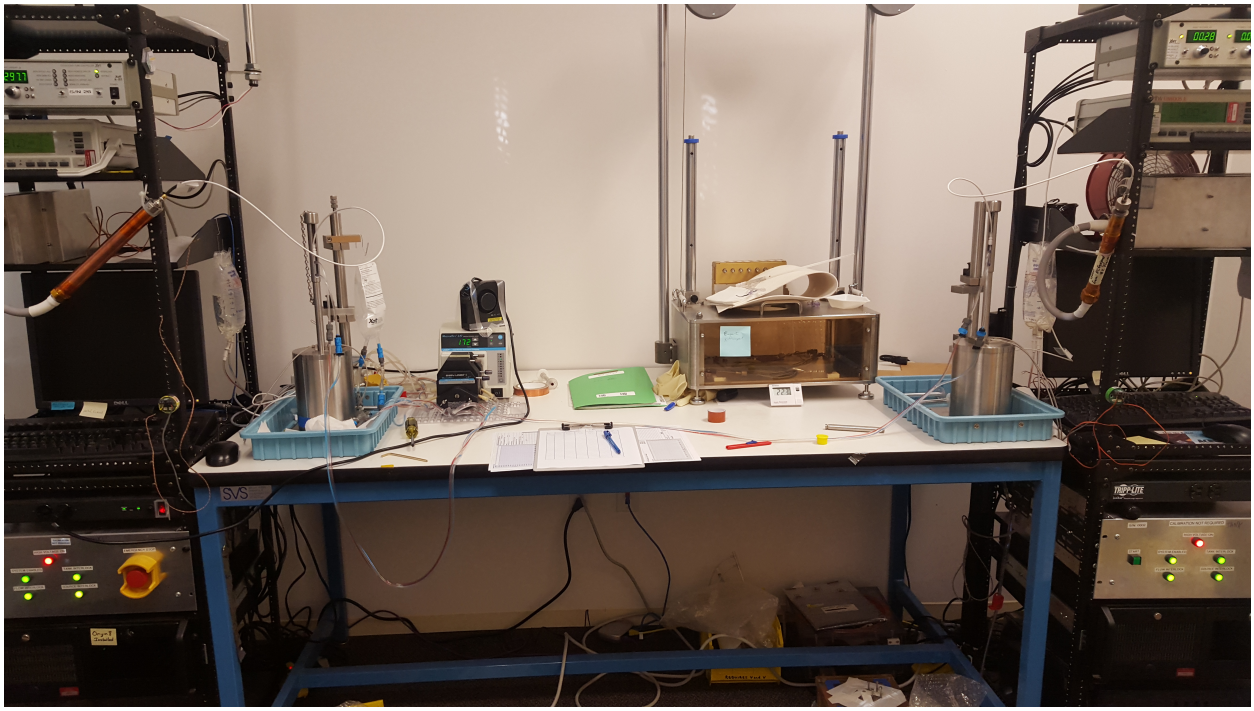

Figure 33. The test fixture has two stations for catheters to be run. This allowed for 8 samples (4 on each catheter) to be dosed at the same time.

After initially exposing one polymer to radiation in this configuration, there was difficulty with unrolling the samples into rectangles without the samples cracking (one polymer is a higher rigidity, lower ultimate elongation polymer than the other). As a result, the samples of this material were dosed in their tensile testing (notched) geometry. This geometry is shown in the next section in Figure 34.

The polymer samples were positioned on the catheter in a similar manner to the configuration for the other polymer samples shown in Figure 30. However, instead of a complete cylinder wrapping around the catheter, the layer of samples closest to the catheter were positioned at three spots around the circumference and the subsequent layers were placed on those spots as well. Only three layers were used for this configuration due to the difficulty in placing each layer on

top of the previous layer. Due to the multiple layers of samples, dose drop-offs were calculated for the different layers. A table showing the ratios for the different layers is shown in Table 4.

Table 4. The dose drop-off for each coupon layer was determined and used to estimate the radiation dose received by each coupon.

Layer	Ratio of Catheter Dose
1 (Closest to catheter)	0.85
2	0.73
3	0.63
4 (Furthest from catheter)	0.55

Sixteen polymer samples were exposed to varying levels of radiation (measured in minutes of radiation exposure). Of the 16 samples created, tensile data was obtained from 15 of the samples. Eight other polymer samples were exposed to radiation, but of the eight samples, data was only successfully obtained from one control sample and one irradiated sample. As a result, the data from these samples was not useful for the purposes of this report and is not included in the results section. Information about the tensile samples from the compatibility testing will be provided in section 2.6.

2.4 Tensile Testing Sample Preparation

All samples for tensile testing were prepared in an attempt to ensure breakage at a controlled point during tensile testing. There were two geometries that were used for tensile testing: a typical dog bone shape for two of the polymer samples, and a notched strip geometry for the other polymer samples.

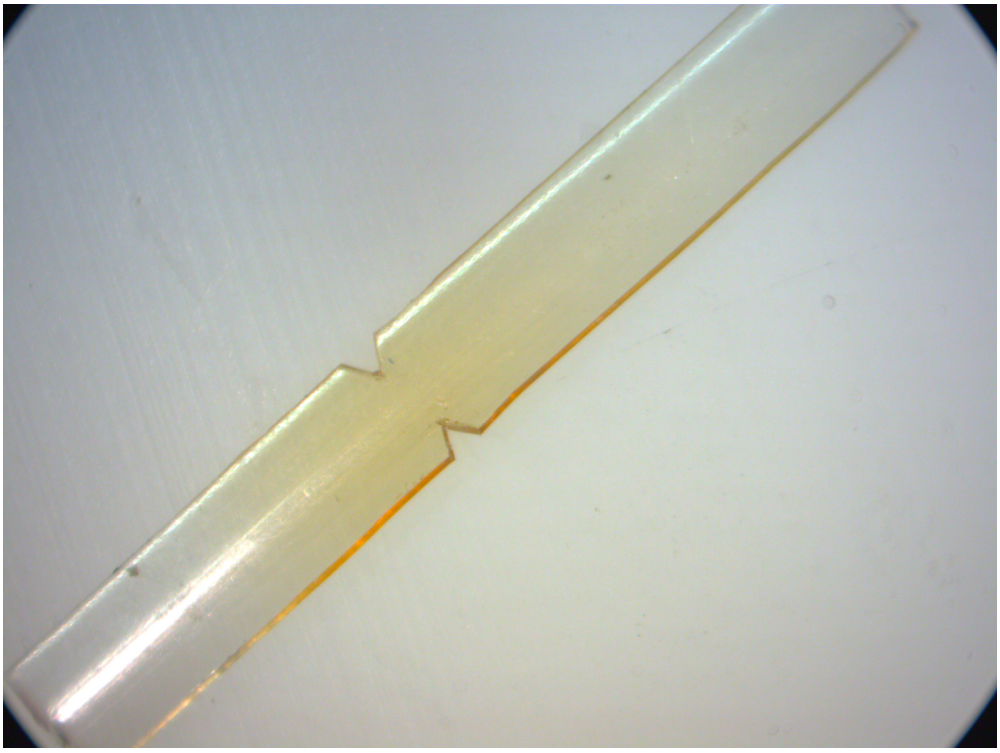

Figure 34. Some samples were cut into strips in the longitudinal direction of the catheter. They were notched under a microscope to control the breaking point during tensile testing.

The tensile samples in Figure 34 were cut before dosing using a scalpel under a microscope as shown in Figure 35. The minimum width of each sample shown in Figure 34 was measured using ImageJ with an image taken with the microscope camera. Calibration images with calipers set to a known length, shown in Figure 36, were taken to create a known pixel/inch conversion factor. The minimum cross sectional area of each sample was calculated based on this minimum width and the known thickness of the catheter.

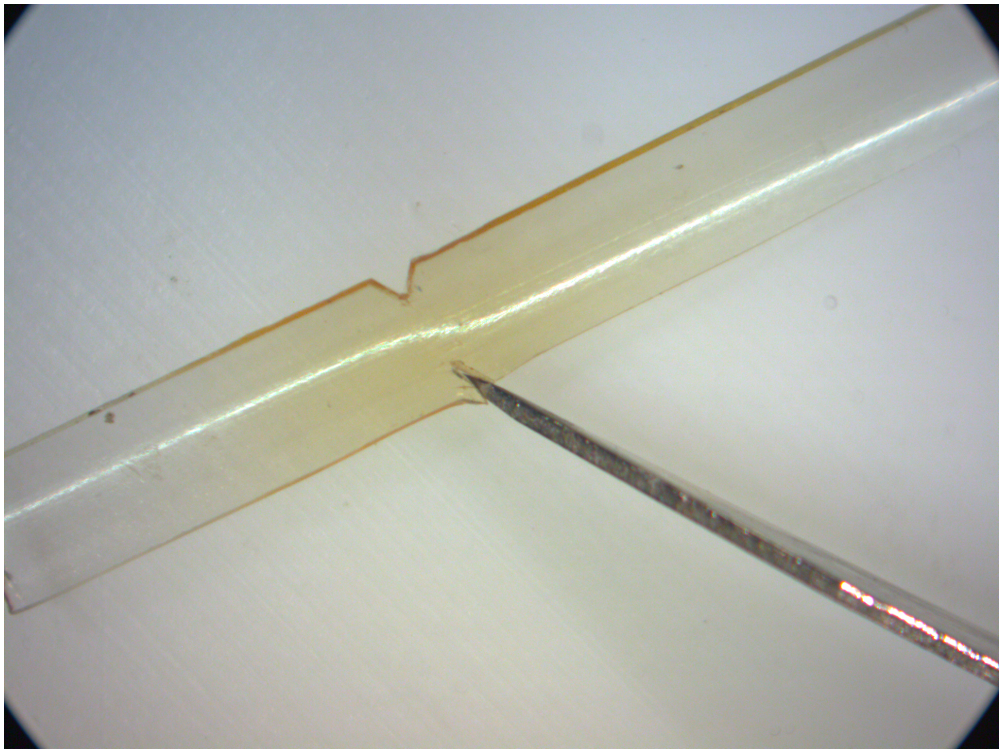

Figure 35. Polymer tensile testing specimens were created by notching polymer strips.

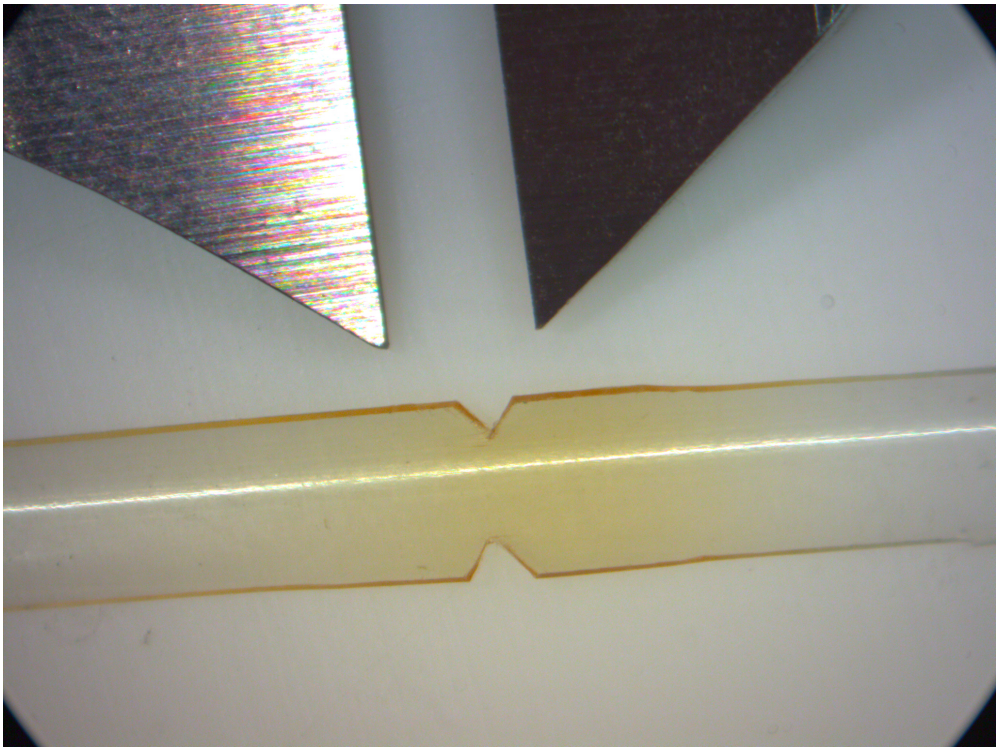

Figure 36. Images with calipers set to a known distance were taken to create a known pixel/inch conversion for ImageJ measurements of the minimum width.

Polymer tensile specimens were created after irradiation because the samples were still relatively easy to work with, even after dosing. For the creation of specimens created from two of the materials, a die was manufactured by Apple Steel Rule Die (Milwaukee, Wisconsin), and the samples were cut using a manual press (SCHMIDT 3R-03-2010). Images of the die cutting sample preparation process are shown in Figures 37-40.

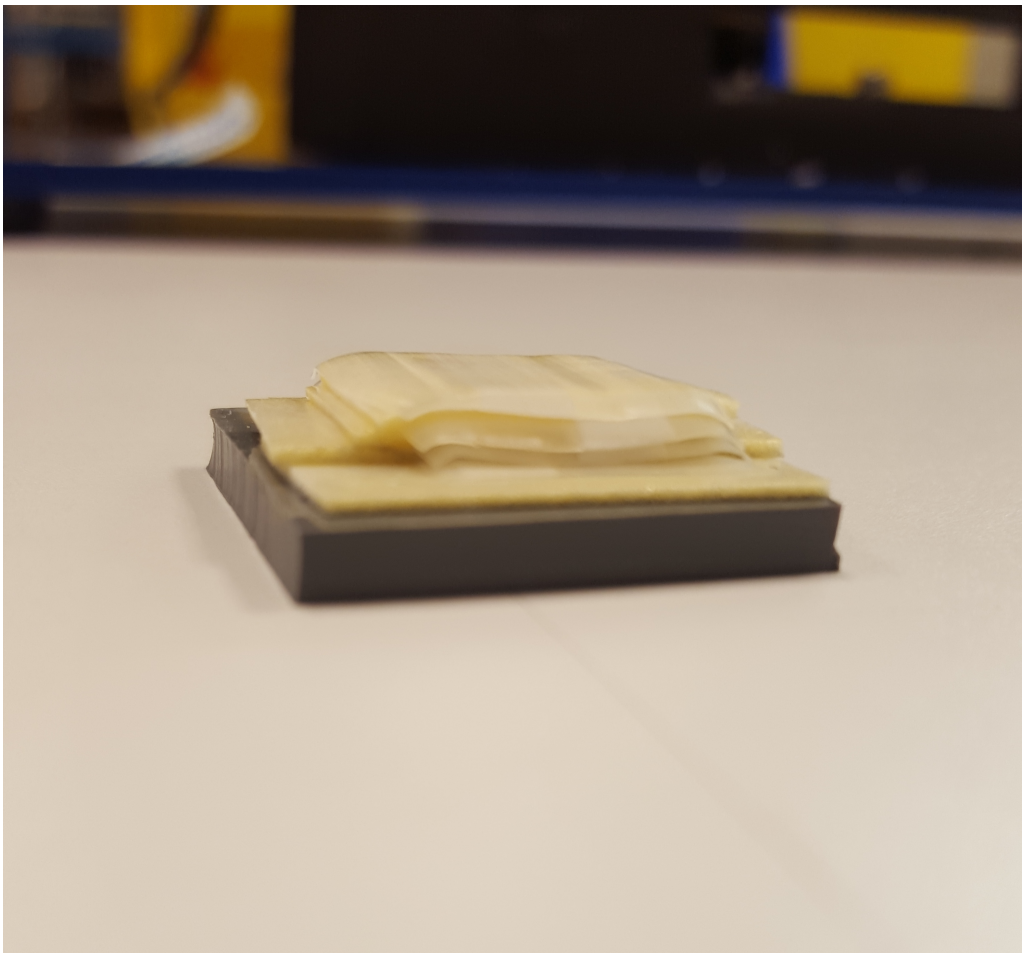

Figure 37. Unrolled coupons (rectangles) were placed on a silicone rubber sheet using double sided tape between each coupon layer and between the first coupon and the rubber sheet.

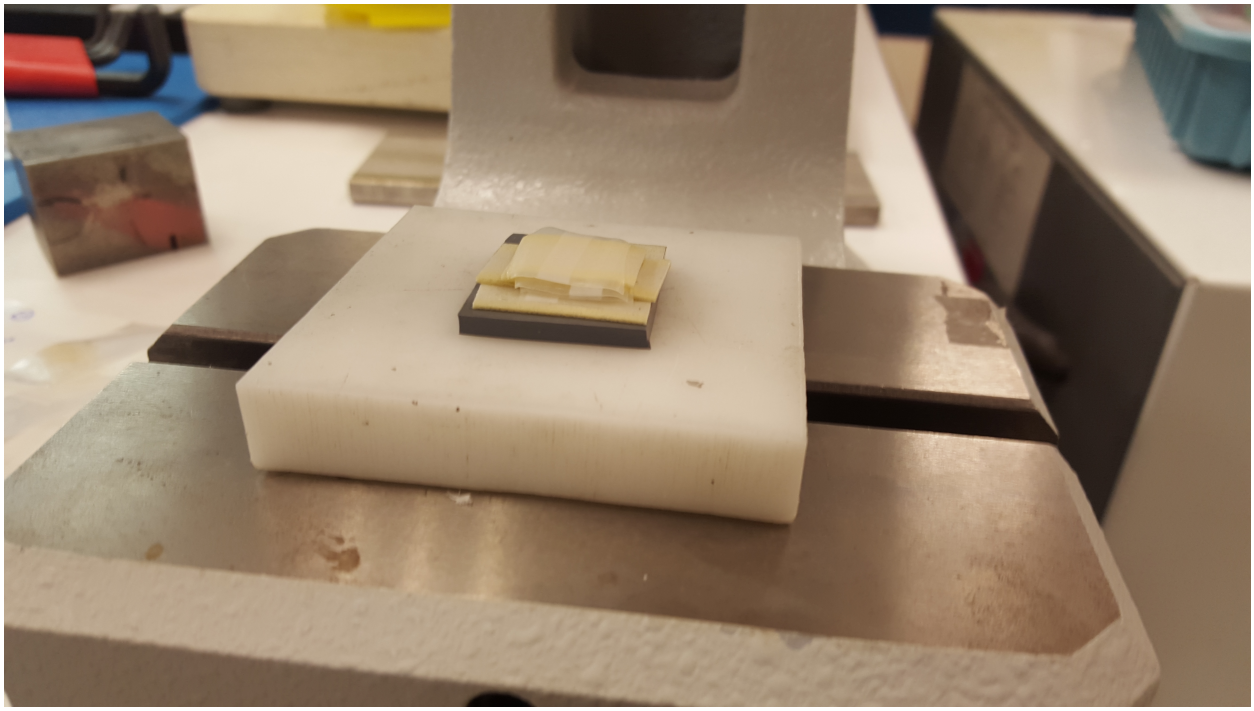

Figure 38. Four samples were cut at a time on the manual press.

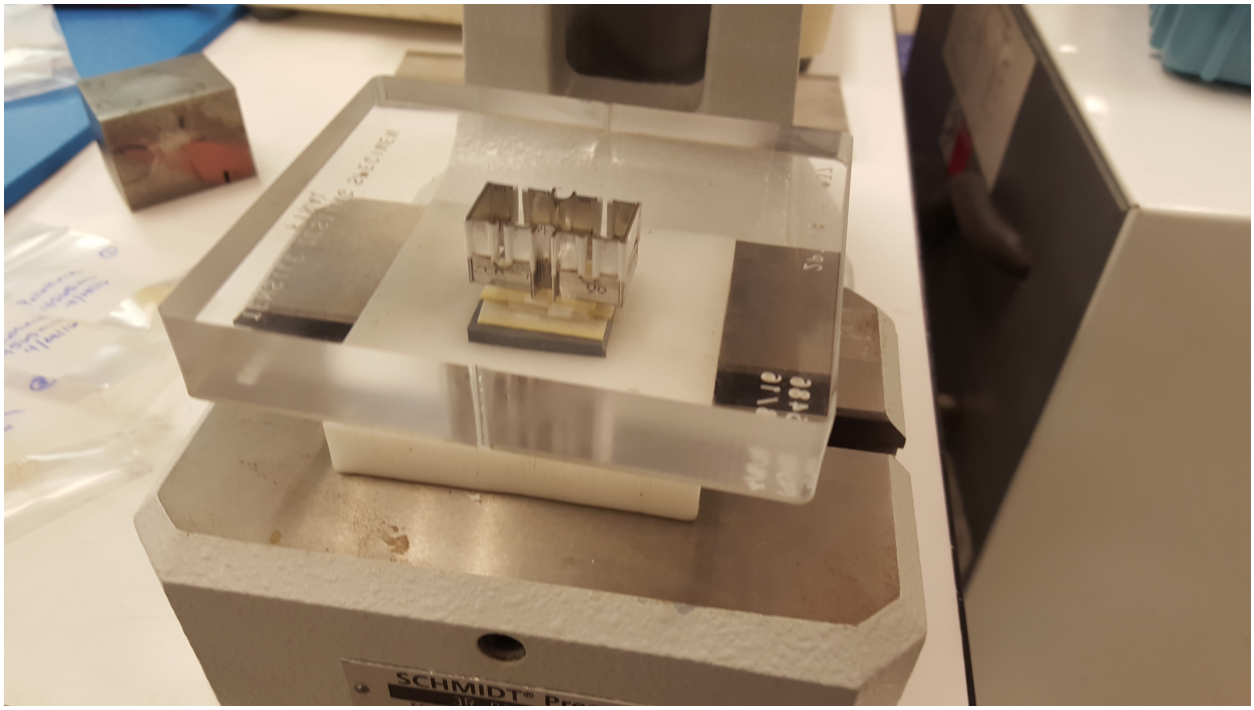

Figure 39. The die was visually centered on top of the coupons.

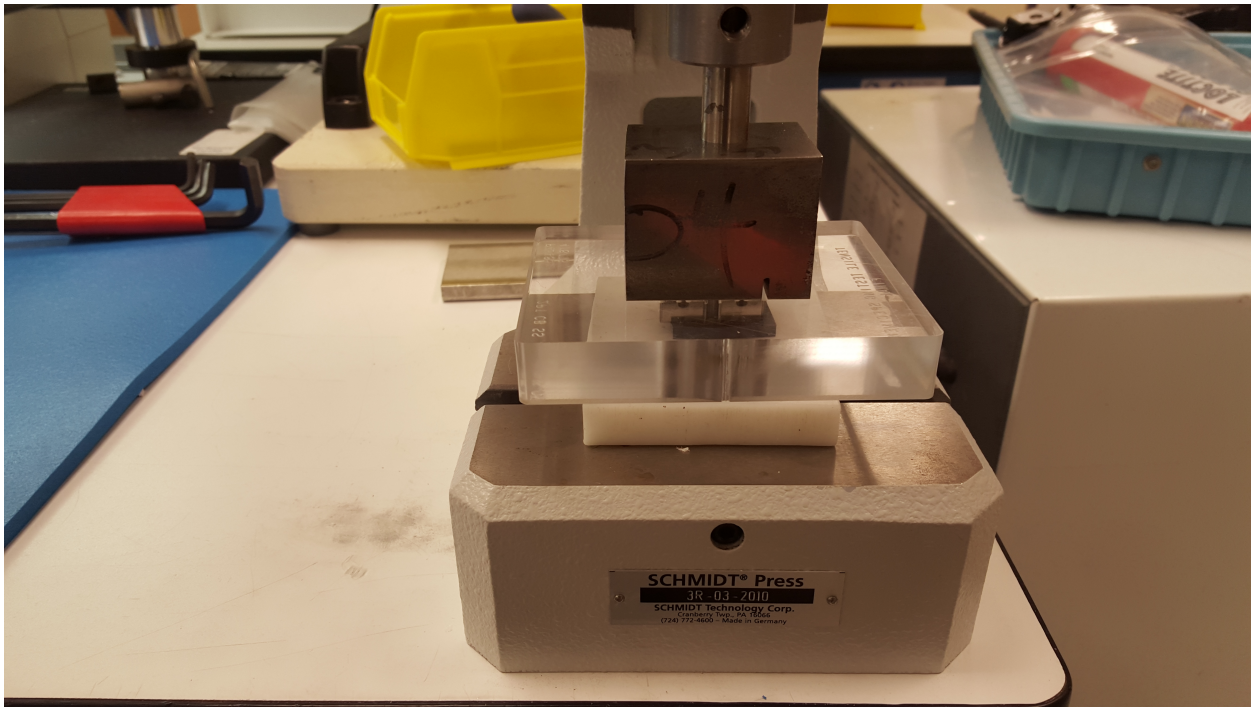

Figure 40. The press, with a steel spacer block, was used to cut through all layers of polymer coupons and the rubber sheet below the coupons.

The final geometry for the two sample types are shown in Figure 41; some polymer samples were cut to the shape on the right side of the figure, while the other polymer samples were cut to the shape on the left side of the figure.

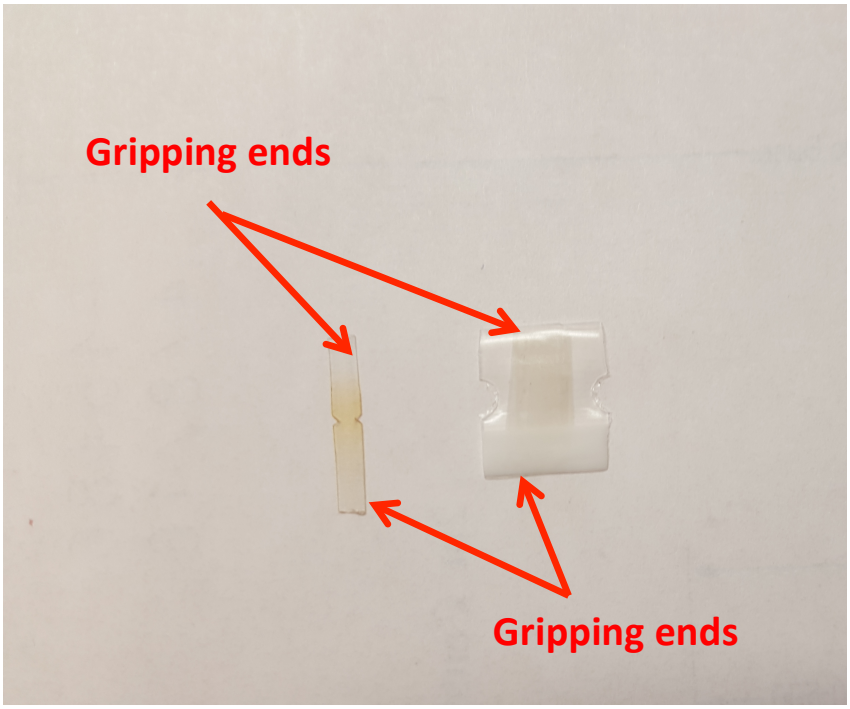

Figure 41. One tensile sample is shown on the left, and another tensile sample is shown on the right.

Due to the small size of the samples (approximately 0.6 inches x 0.5 inches for some samples, approximately 0.1 inches x 0.75 inches for the other samples) sheet metal gripping areas were added to both gripping ends (shown in the next section in Figure 42).

2.5 Tensile Testing

Tensile testing of the irradiated and Galden-soaked samples was performed at a grip separation speed of 2 inches/minute using pneumatic tensile testing grips. Testing was performed at the Westpak, Inc. San Jose testing facility. An image of a successfully tested sample is shown in Figure 42.

Figure 42. A successfully tested tensile specimen shows the breaking point at the middle of the sample. The metal glued to either end of the sample provided a place to grip the sample.

For some polymer samples, the pneumatic grips were pressurized to approximately 110 psi, and for the other samples, a pressure of approximately 140 psi was used. Due to the very brittle nature of some samples after exposure to radiation, good data was only obtained from some of the samples that were prepared. Some samples broke while gluing the metal gripping areas to the polymer, other samples broke while being loaded into the tensile testing machine, and some samples broke prematurely during testing at the interface with the glue and the metal gripping areas.

2.6 Pressure Testing

Testing was performed with 3 catheters of one material and 3 catheters of another. The first test that was performed used a gas, and the second test used a full cooling tubing set apparatus with Galden to pressurize the catheter. For both tests, a laser micrometer (BenchMike 4050G) was

used in conjunction with a 3D printed black ABS fixture (shown in Figures 43 and 44) to measure the diameter of the catheter in six locations. The blue marks on the fixture shown in Figure 44 denote 0, 60, 120, 180, 240, and 300 degrees of rotation. The catheter inlet and outlet ports were used to align the catheter to these 6 rotational positions for measurements. The concept for how the catheter fits into the fixture is shown in Figure 43. The fixture performed three main functions to enable accurate diameter measurements. First, the fixture ensured that the catheter was perpendicular to the laser measurement line. Second, the fixture allowed accurate rotation of the catheter while keeping the shaft along a straight axis of rotation. This was important because the catheter has a tendency to bend when the source and cable are inserted, and rotation of a bent catheter would have resulted in vertical translation as well. Finally, by virtue of a hard stop designed into the fixture, the measurement position along the length of the catheters was consistent.

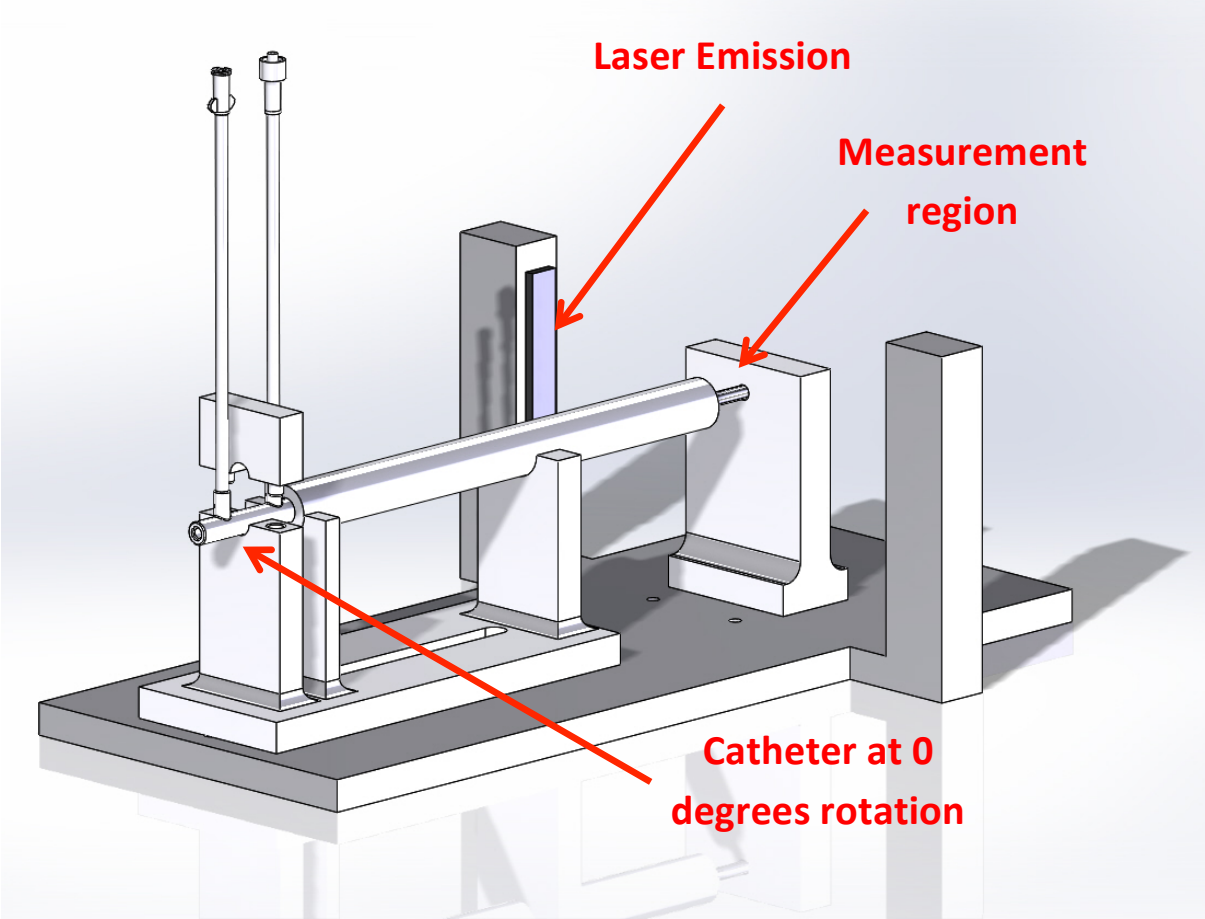

Figure 43. The fixture was designed to eliminate as much measurement error as possible. The results show that the fixture kept the measurements very consistent.

To obtain each measurement, the catheter was rotated to the proper position and held still until the measurement value stabilized at the ten thousandths (tenths) of an inch position. The value was recorded, and the catheter was rotated to the next position. Each catheter was measured twice at every rotational position for every condition to gain confidence in the measurements. In addition to evaluating the change of each catheter, by taking 6 measurements at different rotational positions, the circularity of each catheter was determined.

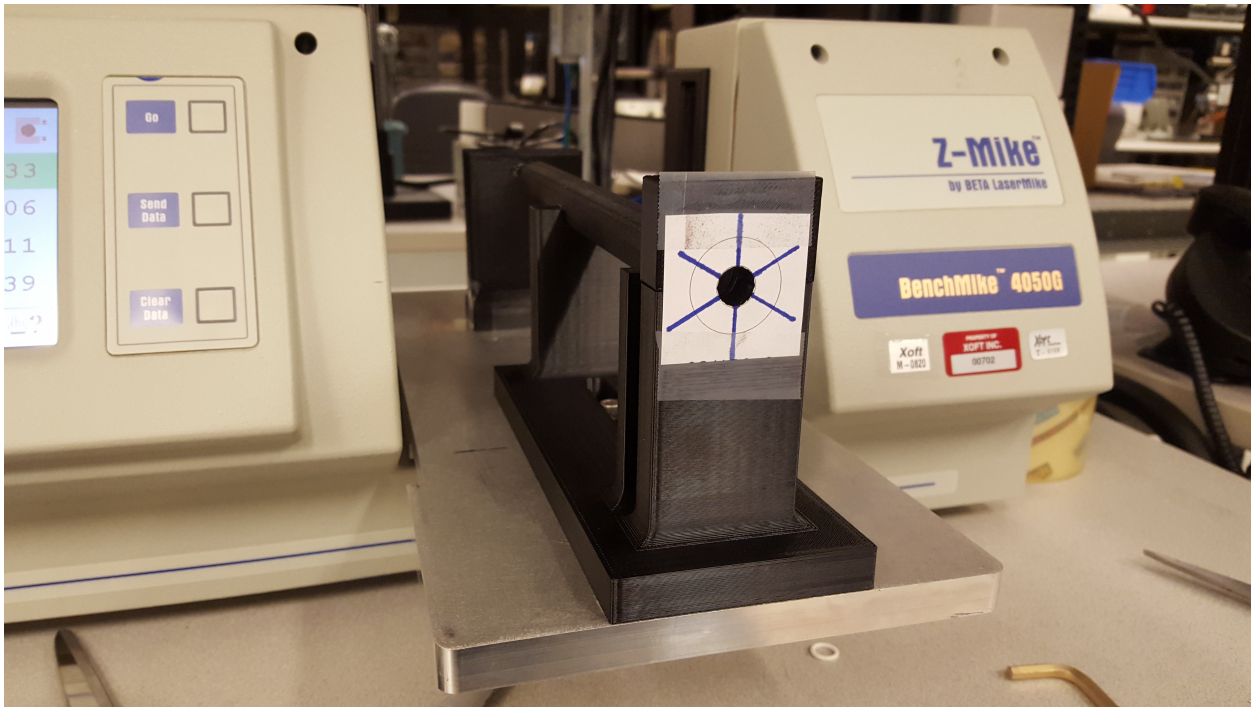

Figure 44. A 3D printed ABS fixture was used to accurately measure the diameter of the catheter at different rotational positions.

Each diameter measurement was recorded as the truncated value out to the tenths position. The specific conditions used for the nitrogen and Galden tests will be described in the next two sections.

2.6.1 Nitrogen Pressurized Testing. The testing with nitrogen was performed at various pressures. The pressure was regulated using a dual regulator system. The regulator on the wall was set to and left at 100 psi, and the regulator directly before the catheter was varied depending on the desired pressure for the test. The catheter was directly connected to the air source, and a source/cable assembly was inserted into the catheter to simulate a real use condition. Figure 45 shows a typical setup.

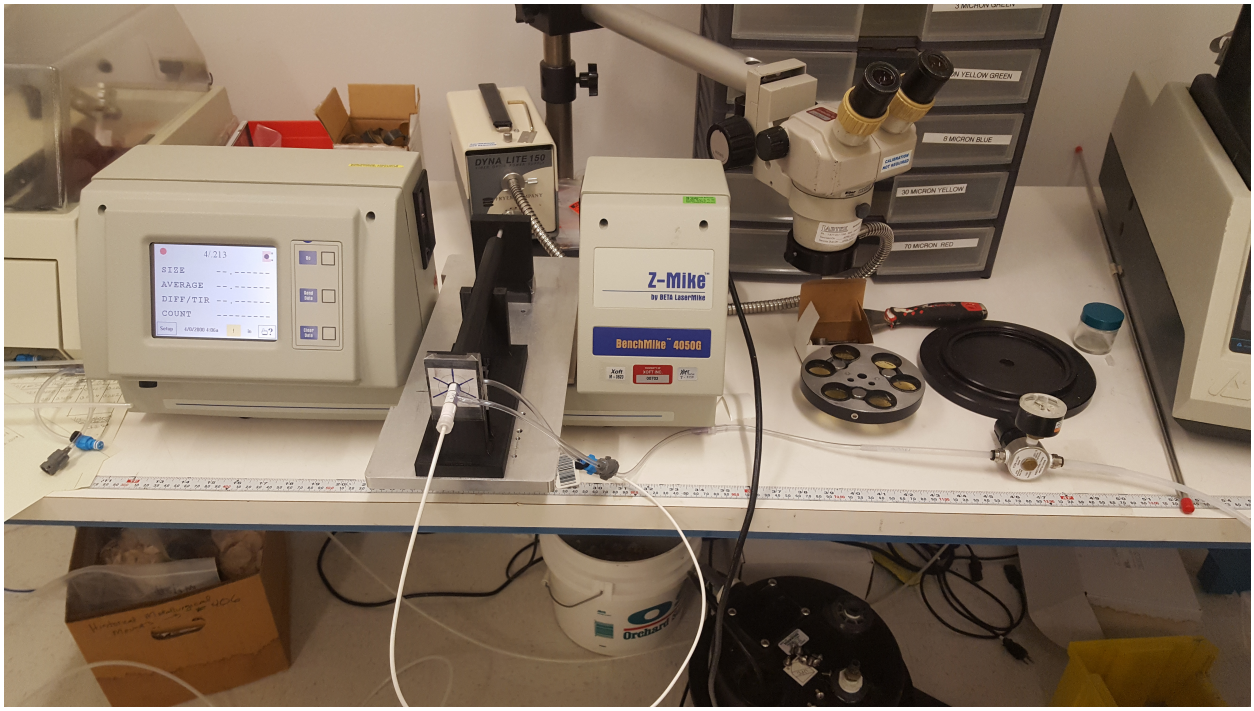

Figure 45. The catheter was connected to a nitrogen source, and diameter measurements were taken catheters at various pressures.

It is important to note that the purpose of this testing was to evaluate a simple, constant internal pressure condition, while the Galden pressure testing more accurately represents a clinical environment.

2.6.2 Galden Pressurized Testing. The testing performed with Galden was performed at multiple pressures. Because it was necessary to connect the cooling tubing set to flow Galden through the catheter, the maximum pressure that could be used without leaking was lower than initially planned. For this test, the Galden bag was placed in water heated to a higher temperature than the desired maximum coolant temperature. This simulated the increased temperature that the system experiences when the source is emitting radiation during treatment. The water heating system with the Galden bag is shown in Figure 46.

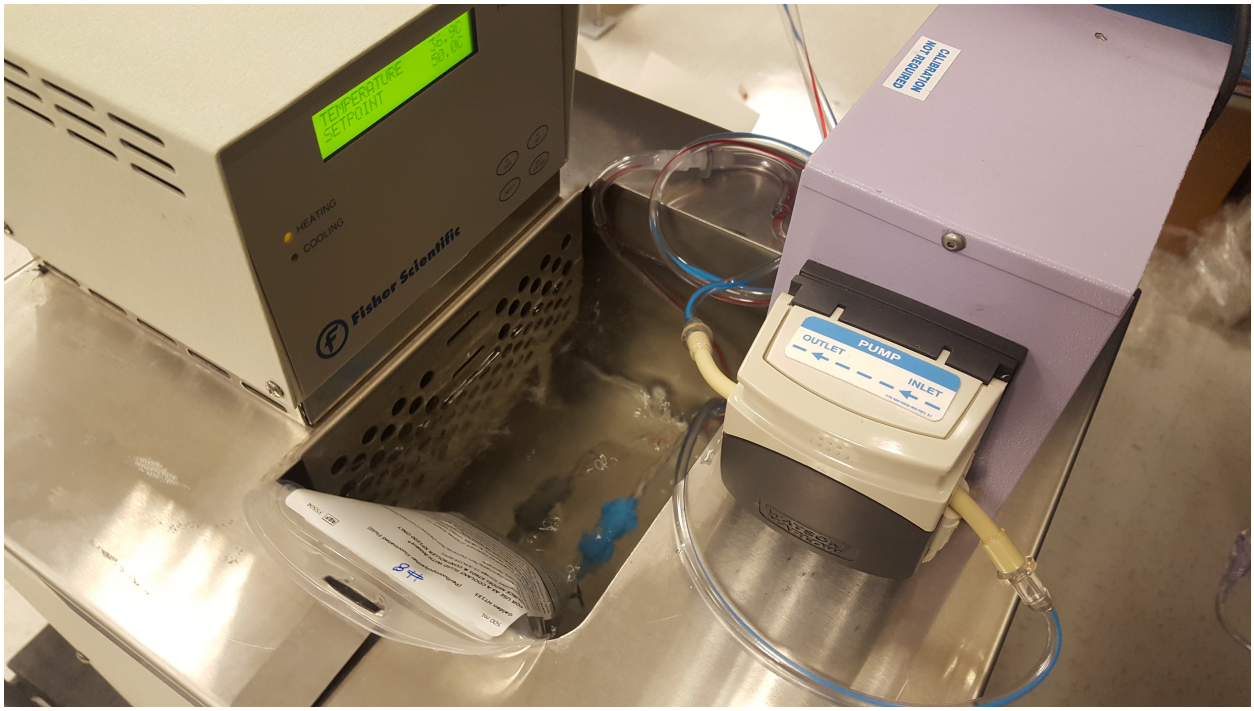

Figure 46. The Galden bag was heated by being placed in heated water.

The catheter measurements were taken when the pressure and temperature stabilized at the desired values.

2.7 Coolant Compatibility Testing

Coolant compatibility testing was performed to evaluate if any mass loss due to chemical breakdown occurred for one material when soaked in Galden. The other main material was not tested in this report because it had been tested previously by Solvay. The testing was performed using ASTM D471(16) as a guideline. Due to smaller sample geometry constraints than detailed in the ASTM standard, slight deviations from the protocol were necessary. Three square samples of one polymer had single holes poked in them, were cleaned, dried, and weighed to the nearest 0.01mg. The samples were then placed on paperclip hangers within glass bottles (Figure 47) that had been labeled and cleaned with isopropyl alcohol (IPA).

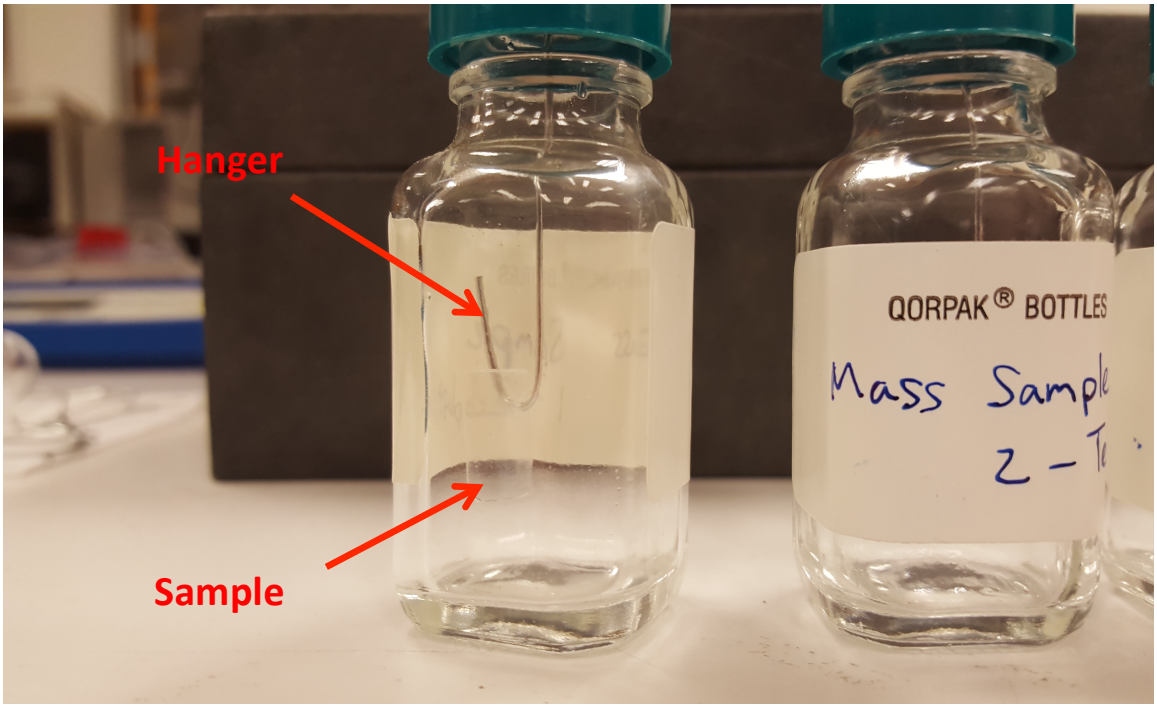

Figure 47. Some polymer samples were placed in cleaned and labeled jars for the test.

After the samples were placed in the bottles, the bottles were filled with Galden and placed in an oven at 50°C. The three samples were removed from the oven after soaking for 168 hours, dipped briefly in IPA, and placed in new, clean bottles before being weighed. The samples were weighed to the nearest 0.01 mg, and the values were recorded. The Galden from this test was saved for Fourier transform infrared spectroscopy (FTIR) analysis.

FTIR analysis was performed at Cal Poly San Luis Obispo using the Chemistry Department's machine. A sample of pure Galden was evaluated, and the FTIR spectra from the three samples of Galden from the compatibility test were compared to the spectrum from the pure Galden to look for different peaks that would indicate polymer functional groups in the Galden.

Six tensile-shaped specimens of one polymer were soaked in Galden for 168 and 381 hours at 50°C (three for each length of time). The procedure was the same as for the mass evaluation samples, but no mass measurements were taken. The samples soaked for 381 hours were originally going to be soaked for 336 hours, but a work holiday prevented removal of the samples from the oven at the planned time. Six tensile samples of another polymer were soaked in Galden for 168 and 336 hours at 50°C. No data was recorded for the Galden samples due to cracking when loading test samples into the tensile testing machine. For the second polymer, five of the six samples were successfully tested.

2.8 Life Testing

Life testing was not specifically performed as a separate test for this report, but observations were taken while dosing the coupons. The test system is specifically designed to simulate a very extreme clinical situation. For the catheters of one material, this system was used to gain initial experience with how the material reacted to a set of conditions. The dose on each catheter (in minutes) was recorded, and catheters were run for a predetermined length of time – much longer than a typical clinical environment. Overall, the observations from this simulated clinical environment testing combined with the SolidWorks simulations, tensile, pressure, and coolant compatibility testing were used to determine which material is a better material for the catheter.

2.9 Statistical Methods

Simple linear regression was performed to analyze the relationship between radiation dose and ultimate tensile strength (UTS) for two polymers. The residuals were analyzed to determine the

validity of the model used. An ANOVA was also used to determine if there were any differences in UTS between groups for the polymer samples soaked in Galden.

3.0 RESULTS AND DISCUSSION

In this section, the results from the tests described in the previous section will be presented. When applicable, statistical results will also be given. The results of the testing and the statistics are discussed and potential reasons for the test findings are given. The results are also discussed in terms of deciding the best material for the catheter.

3.1 SolidWorks Simulations

A sample image from the typical wall thickness simulations of a deformed model with the original model overlaid in pink and the maximum deformation displayed is shown in Figure 48. A sample image from the increased wall thickness simulations is shown in Figure 49. It is important to note that the deformation is not to scale to allow for easier visualization of the deformation direction. All simulation images are presented in Appendix C

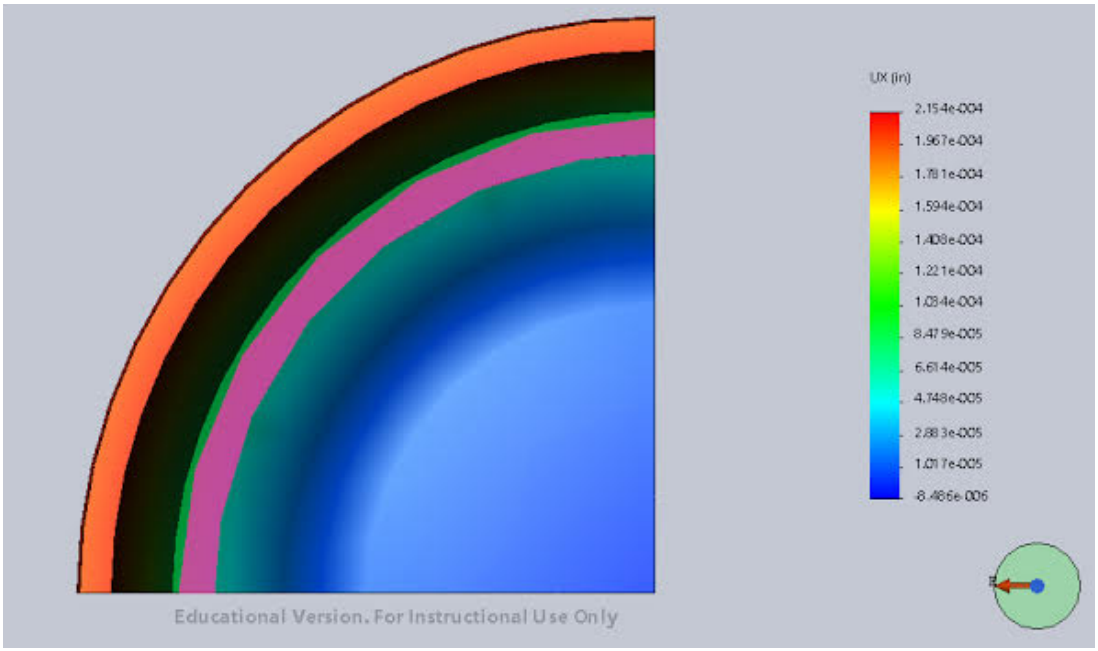

Figure 48. A segment of a model of a catheter was analyzed after simulating an internal pressure. This same deformation geometry was seen for both polymer catheter simulations.

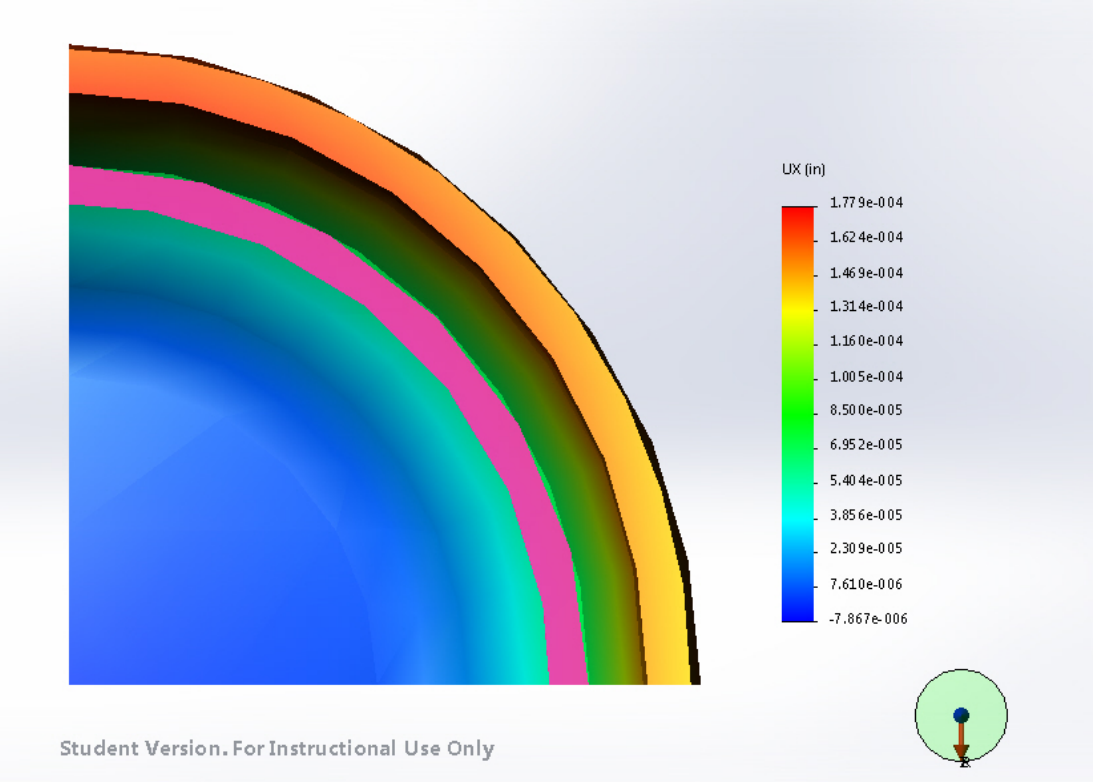

Figure 49. The effect of increasing the wall thickness was simulated in SolidWorks.

Maximum deformations for the normal wall thickness simulations are given in Table 5, along with percent differences between the two main polymers. In Table 6, maximum deformations are given for both of the different wall thickness catheters. The percent decrease in change when the wall thickness was increased is also given.

Table 5. Initial SolidWorks simulations indicated a difference between two polymers.

Material	Pressure	Max Deformation (in)	Percent Decrease from Polymer 1 to Polymer 2
Polymer 1	Low	2.154E-04	36.7%
Polymer 2	Low	1.364E-04	
Polymer 1	High	4.308E-04	36.7%
Polymer 2	High	2.728E-04	

Table 6. Initial SolidWorks simulations suggested that an increase in wall thickness would decrease catheter change.

Material	Wall Thickness	Pressure (psi)	Max Deformation (in)	Percent Decrease in Change Due to Increased Wall Thickness
Polymer 1	Thin	Low	2.326E-04	23.5%
Polymer 2	Thick	Low	1.779E-04	
Polymer 1	Thin	High	4.652E-04	23.5%
Polymer 2	Thick	High	3.557E-04	

The SolidWorks simulations, while not as definitive or accurate as validation testing, are good initial indications in this case because the simulations are based on relatively simple models. Based on the approximately 25% reduction in change with a wall thickness increase of a small amount, this design change would become a viable option if this polymer proves to be the best catheter material. Overall, these simulations gave good indications about what to expect when performing testing with the real materials.

3.2 Tensile Testing

The tensile testing performed for this report was very important because it showed how well the two main polymers resist radiation, and it allowed the two materials to be compared. With more data, the dose-strength curve could be used to determine the acceptable lifetime of the catheter in a clinical setting. The tensile testing data was also important because it gave valuable information about the mechanical integrity of the polymers at higher radiation doses, which is important to know in conjunction with the pressure data. Together, the pressure testing data and the tensile testing data will help determine if change is expected to increase, decrease, or stay the same over the lifetime of the catheter.

3.2.1 Dose-Strength Curves. Based on ultimate tensile strengths from tensile testing, dose strength curves were created for the two main polymers. For some dose levels, there were multiple samples of one polymer that were successfully tested, and some results are average tensile strength values. Simple linear regression results are given after the dose-strength curve plot.

There was a data point that is a potential outlier. Due to the overall variability in the data, however, this data point was kept in the analysis. It is likely that this sample had been affected in some way by the sample preparation process or by loading the sample into the testing machine. Because the metal that was used as gripping handles on either end of the specimens created a sharp edge that was significantly stronger than either of the polymers, many samples broke at the edge of the metal where they were glued. Some of this may have been due to off-axis loading. In tensile testing, to obtain accurate results, it is important to pull in a single axis. To achieve this, the tensile specimen must be as close to vertical as possible. The tensile grips at Westpak are self-centering, meaning that they will automatically line up on the same vertical axis as they pull. This greatly reduced the chance of off-axis pulling during tensile testing. Despite this self-centering feature, the grips had a tendency to clamp down on the samples quickly, and at times the samples were slightly bent off the intended axis of pull by the jaws.

There was a noticeable negative relationship between the independent and dependent variables that were recorded. The results plotted in this graph are consistent with observations about one of the polymers during the dosing of samples – before this polymer is exposed to radiation, it is noticeably stronger than the other, but over time, with testing, its strength decreased rapidly.

To quantitatively evaluate the response to radiation, linear regression was performed. The linear regression equation is given in Equation 1.

$$Y = Dose + Material + Dose * Material \qquad \text{Eq. 1}$$

This linear regression was designed to evaluate the relationship between dose and Y as well as the unique responses of both polymers to radiation dose. The ANOVA results from the linear regression are given in Table 7 and the effect tests are given in Table 8.

Table 7. Based on the results of the ANOVA, the model is statistically significant.

Analysis of Variance				
Source	**DF**	**Sum of Squares**	**Mean Square**	**F Ratio**
Model	3	69519107	23173036	19.3535
Error	23	27539133	1197353.6	**Prob > F**
C. Total	26	97058240		**<.0001***

Table 8. The effect tests show that both variables are significant predictors of the response.

Effect Tests					
Source	**Nparm**	**DF**	**Sum of Squares**	**F Ratio**	**Prob > F**
Dose (min)	1	1	65576130	54.7676	**<.0001***
Material	1	1	4022476	3.3595	**0.0798**
Dose (min)*Material	1	1	20408971	17.0451	**0.0004***

Table 9. R-square and adjusted R-square values were evaluated for the statistical model.

RSquare	**RSquare Adj**	**Root Mean Square Error**	**Mean of Response**	**Observations (or Sum Wgts)**
0.716262	0.679252	1094.237	5311.119	27

Based on the ANOVA, at least one of the terms in the model explains a statistically significant portion of the variability in UTS ($F(3,23) = 19.35$, p-value <.0001). The effect tests show that

one dependent variable and the material are significant in the model with p-values of <.0001 and 0.0004 respectively (material is significant because of the significant interaction). One of the most important things that the statistics show is the significant interaction, which means that the relationship between one of the dependent variables and the response is different for one polymer than it is for the other. Both materials exhibit a negative relationship between the dependent variable and the response, but the slopes of the regression lines are significantly different. Due to the shallower nature of the slope for one polymer, it can be the response for this polymer will be less affected by one of the conditions than the response of the other polymer for the range of conditions evaluated in the tensile testing.

The adjusted r-square in Table 9 value shows that the model accounts for approximately 68% of the data variability around the mean. In this case the adjusted r-square and r-square values are similar, which also suggests that all variables in this model are significant. While the predictors in this model only account for 68% of the variability about the mean, because they are all significant predictors, the model is still a good model to investigate the research questions for this project [43].

The statistical model used for this analysis is an appropriate model based on the residuals. There is no clear pattern seen in Figure 50 that would suggest that a different model should be used, and the residuals are relatively evenly distributed about the blue line in the figure.

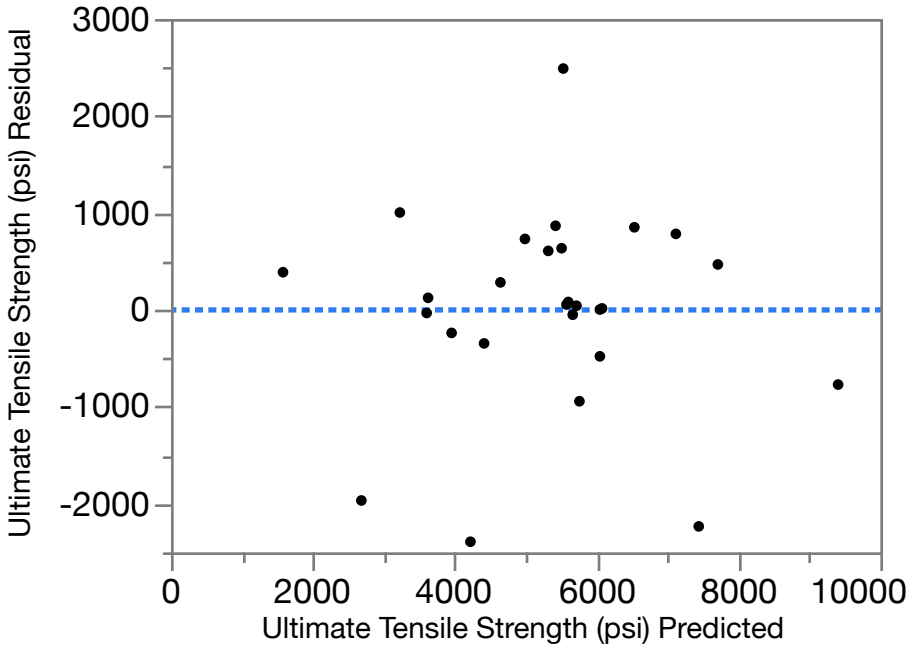

Figure 50. The residuals for this model suggest that the model is an appropriate one for the data.

Finally, the distribution of the residuals is important to determine if the model is appropriate. Ideally, the residuals would follow a normal distribution. A normal quartile plot is shown in Figure 51.

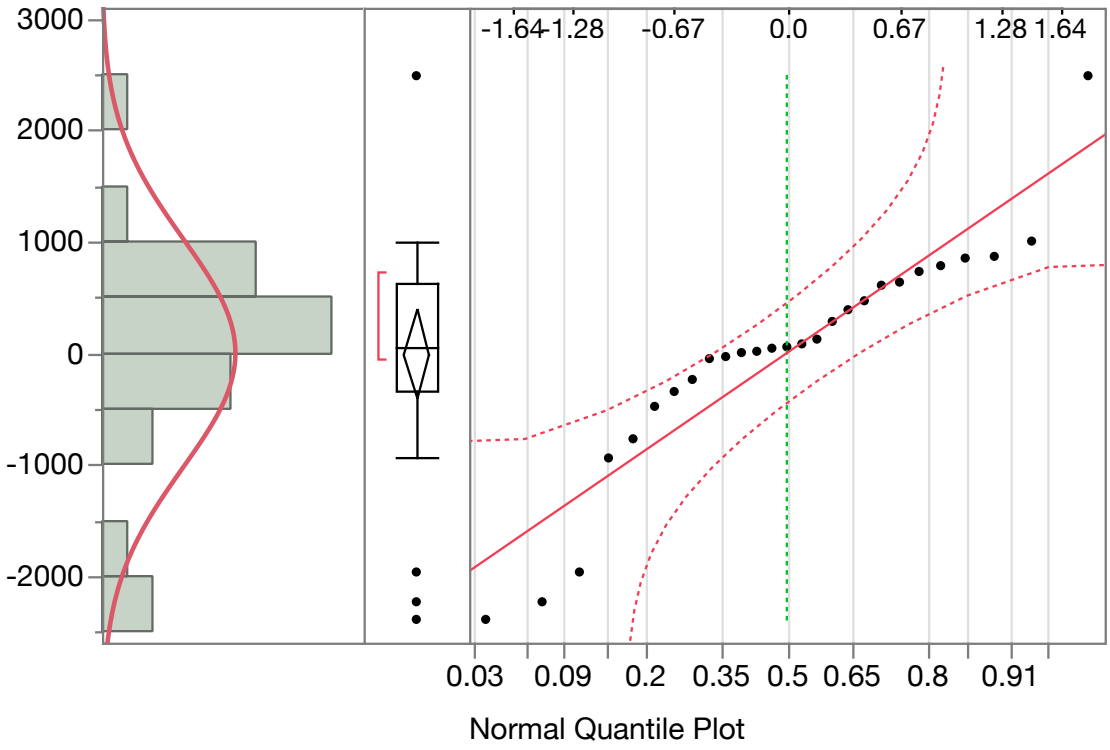

Figure 51. The residual distribution appears to be fairly normal, however there are some outliers that will leverage the distribution away from normal.

To analyze the distribution of the residuals, a goodness of fit test was performed. The results from this test are presented in Table 10.

Table 10. A goodness of fit test was performed to determine the distribution of the residuals.

Goodness-of-Fit Test	
Shapiro-Wilk W Test	
W	**Prob<W**
0.911116	**0.0242***
Note: Ho = The data is from the Normal distribution. Small p-values reject Ho.	

The significant p-value means that there is evidence against normality of the residuals. However, because this is likely caused by one or two outliers, and the p-value for the Goodness-of-Fit Test only provides moderate evidence against normality, it is a reasonable model to use for this data.

3.2.1.1 Polymer Soaked in Galden. A plot comparing the ultimate tensile strengths for control samples and samples soaked in Galden for 168 and 336 hours was created based on the data from Westpak. This plot is shown in Figure 58.

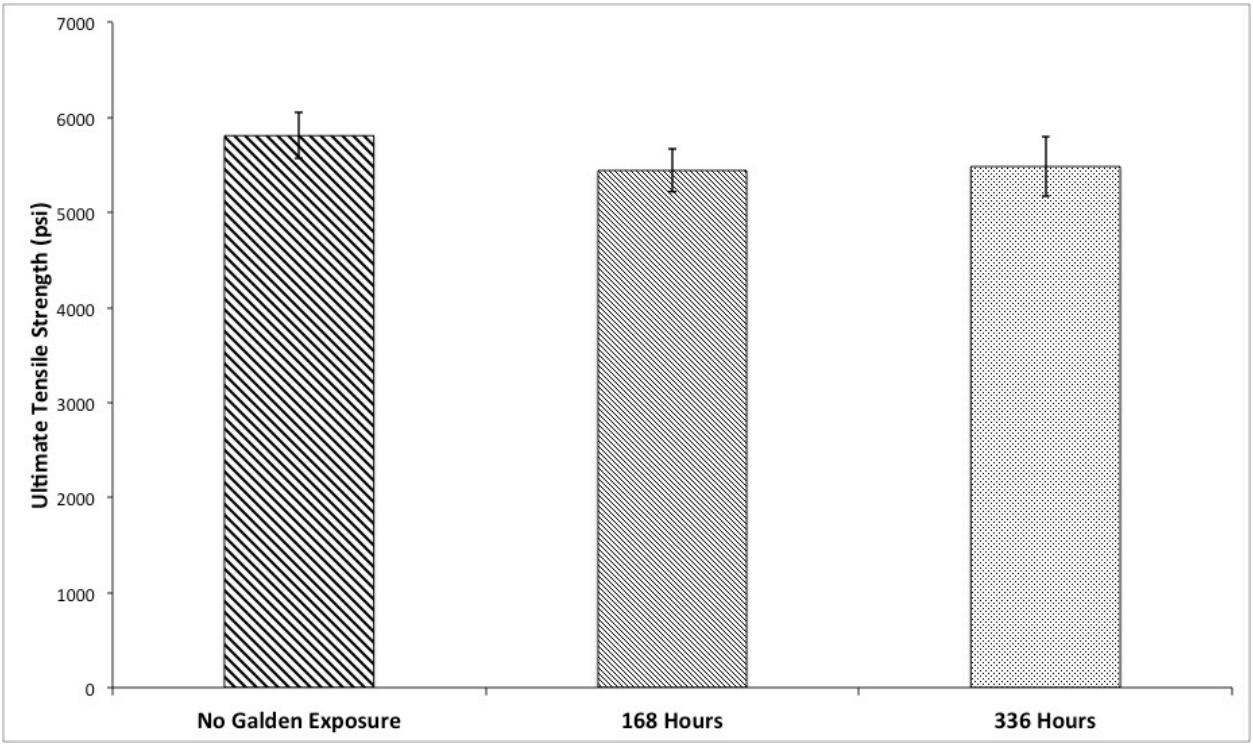

Figure 52. The ultimate tensile strengths for samples soaked in Galden for 0 (control, n = 2), 168 (n = 2) and 336 (n = 3) hours were determined through tensile testing.

Table 11. The ANOVA shows that there is no statistically significant difference between the means for the three groups.

Analysis of Variance					
Source	**DF**	**Sum of Squares**	**Mean Square**	**F Ratio**	**Prob > F**
Time (hrs)	2	167988.28	83994	0.4163	0.6851
Error	4	807080.18	201770		
C. Total	6	975068.46			

Table 12. Tukey-Kramer Honest Significant Difference showed no difference between the three groups.

Connecting Letters Report		
Level (hours of exposure)	**Group**	**Mean**
0	A	5808.7189
336	A	5483.9293
168	A	5443.6052
Levels not connected by the same letter are significantly different.		

Based on the results presented in Tables 11 and 12, the tensile strength of one of the polymersis not significantly altered by prolonged exposure to Galden. No samples of the other maine polymer that had been soaked in Galden were successfully tested – all samples broke while being loaded into the tensile testing machine. Based on the results for the polymers, it appears that one material retains its tensile strength when exposed to Galden, while the other material appears to become significantly weaker.

3.2.1.2 Dose-Elastic Modulus Curves. The tensile test results also provided elastic modulus calculations for samples of both materials. For some dose levels, there were multiple samples that were successfully tested, and some results are average elastic modulus values.

There is a very large amount of variability in the data for one polymer, and there is very little variability in the data for the other polymer. The larger variability in the data is likely due to the tensile testing geometry (notched strips) that was used; the stress-strain curves were very short, so a reliable slope calculation for the linear portion of the curve was difficult. The other polymer results show very little variability, suggesting that the testing produced consistent and comparable data, however, the values are extremely low compared to the datasheet values. This

suggests that while the data points are comparable to one another, they are not reliable absolute values. The trends for both sets of data were analyzed using simple linear regression, and the statistical results are given in the following tables and figures. The model used for the linear regression is given by Equation 2.

$$Elastic\ Modulus = Independent\ variable + Material + Dose * Material \quad \text{Eq. 2}$$

Table 13. Based on the ANOVA results, the model is statistically significant.

Source	DF	Sum of Squares	Mean Square	F Ratio	Prob > F
Model	3	4.59e+11	1.53e+11	41.8214	**<.0001***
Error	23	8.4144e+10	3.6585e+9		
C. Total	26	5.4315e+11			

Table 14. Effect tests for the model show that when all predictors are taken into account, the material is the only significant linear predictor of elastic modulus.

Source	Nparm	DF	Sum of Squares	F Ratio	Prob > F
Independent variable	1	1	2131977749	0.5828	**0.4530**
Material	1	1	4.557e+11	124.5610	**<.0001***
Independent variable*Material	1	1	4523058963	1.2363	**0.2777**

As Tables 13 and 14 show, the overall model given in Equation 2 is significant, but the only significant predictor, when all predictors are accounted for, is material. These conclusions seem to be valid. There did not appear to be a significant linear trend to either of the polymer data sets. This conclusion is supported by the statistical results, and it can be concluded that for this study, elastic modulus did not appear to be significantly affected by radiation dose.

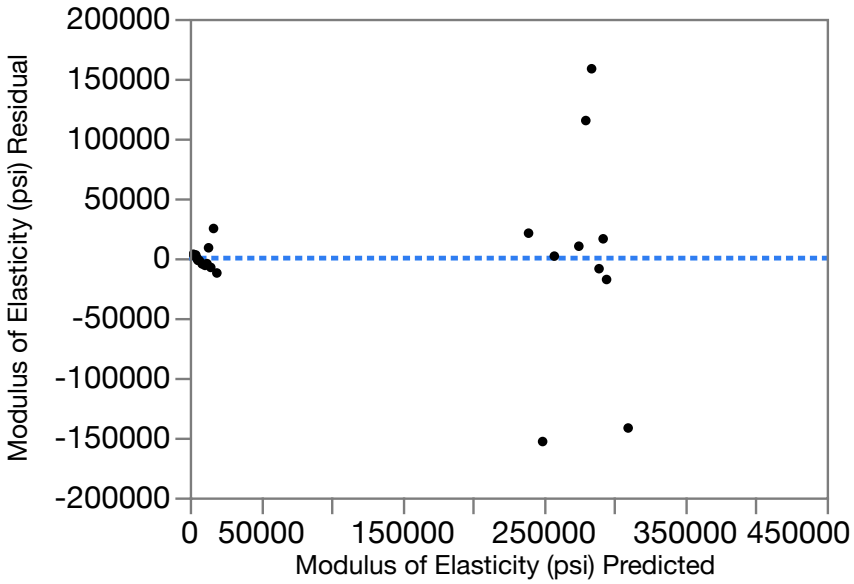

Figure 53. The residuals were plotted against predicted values for the elastic modulus statistical model.

The residuals against predicted plot, shown in Figure 53, shows no significant pattern, and the residuals appear to be relatively evenly distributed about zero. Based on this plot, the model appears to be valid. The final important check, is to check the distribution of the residuals.

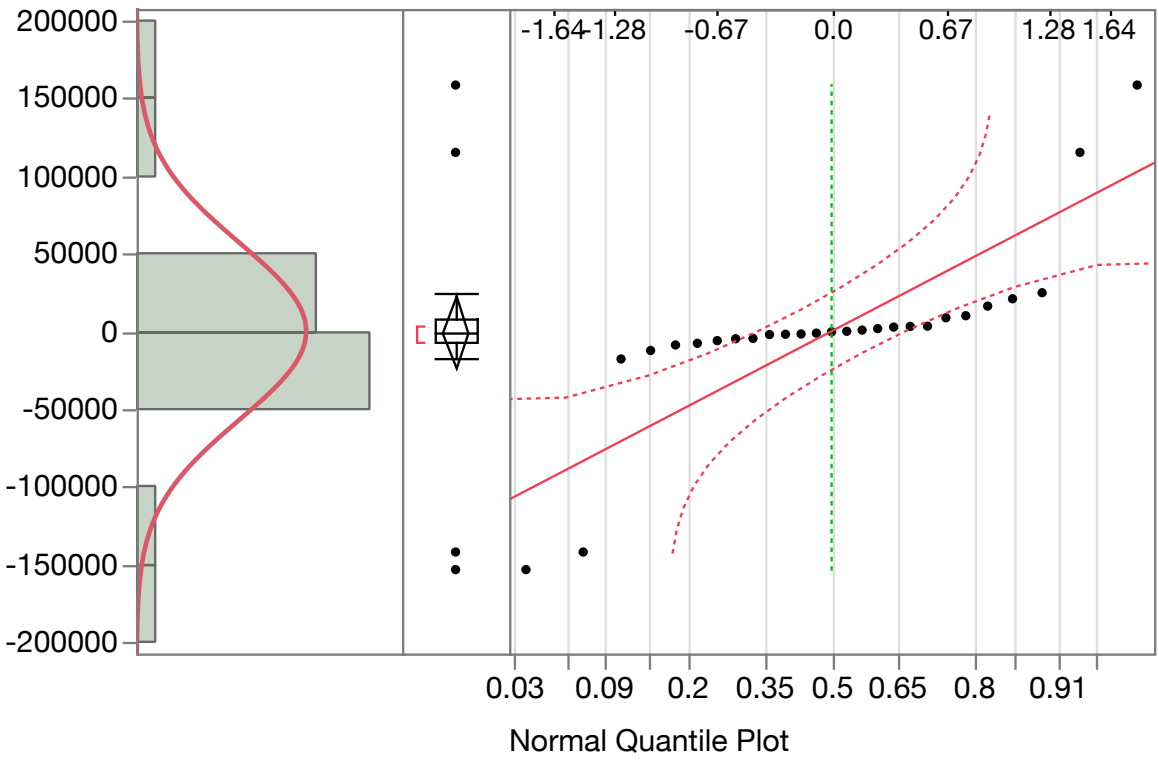

Figure 54. Similar to the residuals for the UTS results, the residuals for the elastic modulus appear to be mostly normal, with the exception of a few outliers that will leverage the distribution away from normal.

Table 15. The goodness of fit test presented strong evidence that the residuals are not from a normal distribution.

Goodness-of-Fit Test	
Shapiro-Wilk W Test	
W	**Prob<W**
0.700598	**<.0001***
Note: Ho = The data is from the Normal distribution. Small p-values reject Ho.	

Based on the normal quantile plot of the residuals and the goodness-of-fit test, there is strong evidence that the residuals are not from a normal distribution. This apparent lack of normality is likely due to the outliers seen on the normal quantile plot. Based on the plot of the residuals against the predicted values, and the fact that the model is highly significant (p-value <.0001) the

model is reasonable. Overall, based on all the tensile testing results, the lower ductility polymer appears to be a more radiation resistant and Galden compatible material.

3.3 Pressure Testing Results

Pressure testing was performed to evaluate the resistance of both polymers to change due to internal pressure. Based on the results from the SolidWorks simulations, one polymer should swell less than the other. Polar plots mapping the catheter diameter based on the 6 measurements were created for each catheter. The plots from the tests with nitrogen show similar patterns as the plots from the tests with Galden (the smaller diameter areas change first until the catheter becomes nearly circular), but the change seen with nitrogen is less for one polymer and approximately the same for the other polymer.

The diameters of the unpressurized catheters varied but as the pressure increased, the catheter became more circular. In all of the catheters of one polymer, with applied internal pressure, the catheters became very circular despite any non-circularities. Based on the results, the catheters, when unpressurized, are very non-circular, but when internal pressure is applied, the larger diameter areas shrink and the smaller diameter areas balloon to become circular. This movement is especially seen in some catheters. It is important to note, when viewing the plots, some plots have concentric gridlines spaced at larger intervals, while other have gridlines spaced at smaller intervals.

One important result of the discovery is that depending on where the diameter of the catheter is measured, the catheter could appear to be within the tolerance specification. However, if the

diameter is measured in a different area, the dimension could be outside of the tolerance for the part. The part calls out the diameter of the catheter as a specific dimension. As a result, problems with certain catheters could be seen. There are other examples where the catheter is above the upper end of the specification, and this is a greater concern. It is possible that if the catheter is too far above the upper specification it might not fit within the applicators properly. As Table 16 shows, certain catheters undergo significant change when compared to the catheters made from the other polymer. Another important result from the testing is the increased change seen in one polymer when Galden is the pressurizing agent. The maximum % change in average diameter is the data point that is presented from the testing. This is a more accurate data point because a larger diameter unpressurized catheter will expand more than a small catheter. This allows this data to be extended to other catheters than solely the ones used in this study.

Table 16. Maximum average diameters at the lowest and highest pressures for the nitrogen and Galden tests, respectively, were calculated, and a percent change was determined.

Catheter	MAX % CHANGE IN AVG DIAMETER - NITROGEN (%)	MAX % CHANGE IN AVG DIAMETER - GALDEN (%)
Polymer 1-1	0.200	0.157
Polymer 1-2	0.235	0.212
Polymer 1-3	0.216	0.204
Polymer 2-1	0.951	1.217
Polymer 2-2	1.035	1.233
Polymer 2-3	1.123	1.610

It is interesting to note that the maximum Galden pressure produced more change in certain catheters at just over half the pressure of the maximum nitrogen pressure. There were two main theories that attempted to explain this. The first is that the fluctuating pressure produced by the peristaltic pump causes the material to expand more than a constant pressure, due to a fatigue-like mechanism. This could be possible, but from the testing that was performed, all of the

catheters returned to their original baseline diameters after the Galden pressure was removed. If it were to be fatigue-induced change, there would likely be plastic deformation of the catheter. The second, more likely theory is that the increased temperature variable that was added during the Galden testing caused one polymer to become more flexible. This is likely because it was observed during coolant compatibility testing that when the samples were removed from the oven at 50°C the flexibility of the polymer was significantly increased. Especially considering the significantly lower pressure generated in the Galden tests, it is likely that increased temperature significantly increases change of catheters made from one of the polymers.

3.4 Coolant Compatibility Testing Results

The test performed on the samples confirmed that there was no significant amount of the material in Galden after exposure at 50°C for 168 hours. Table 17 shows the mass measurements taken for the samples used in the test.

Table 17. Mass measurements were taken before and after one polymer was soaked in Galden.

		Before Soaking	After Soaking	Percent Change in Mass After Soaking Time
Sample	Soaking Time (hr)	Average Mass (g)	Average Mass (g)	
T1	168	0.035193	0.03395	-3.53
T2	168	0.034330	0.03468	1.02
T3	168	0.034877	0.03456	-0.91

As the table shows, none of the samples lost significant mass after soaking in Galden for a week. Sample T1 lost approximately 3.5% of its mass, but when these results are combined with the FTIR results, it is clear that there is no significant change in the Galden. The FTIR spectra for pure Galden and the pure polymer are shown in Figures 55 and 56.

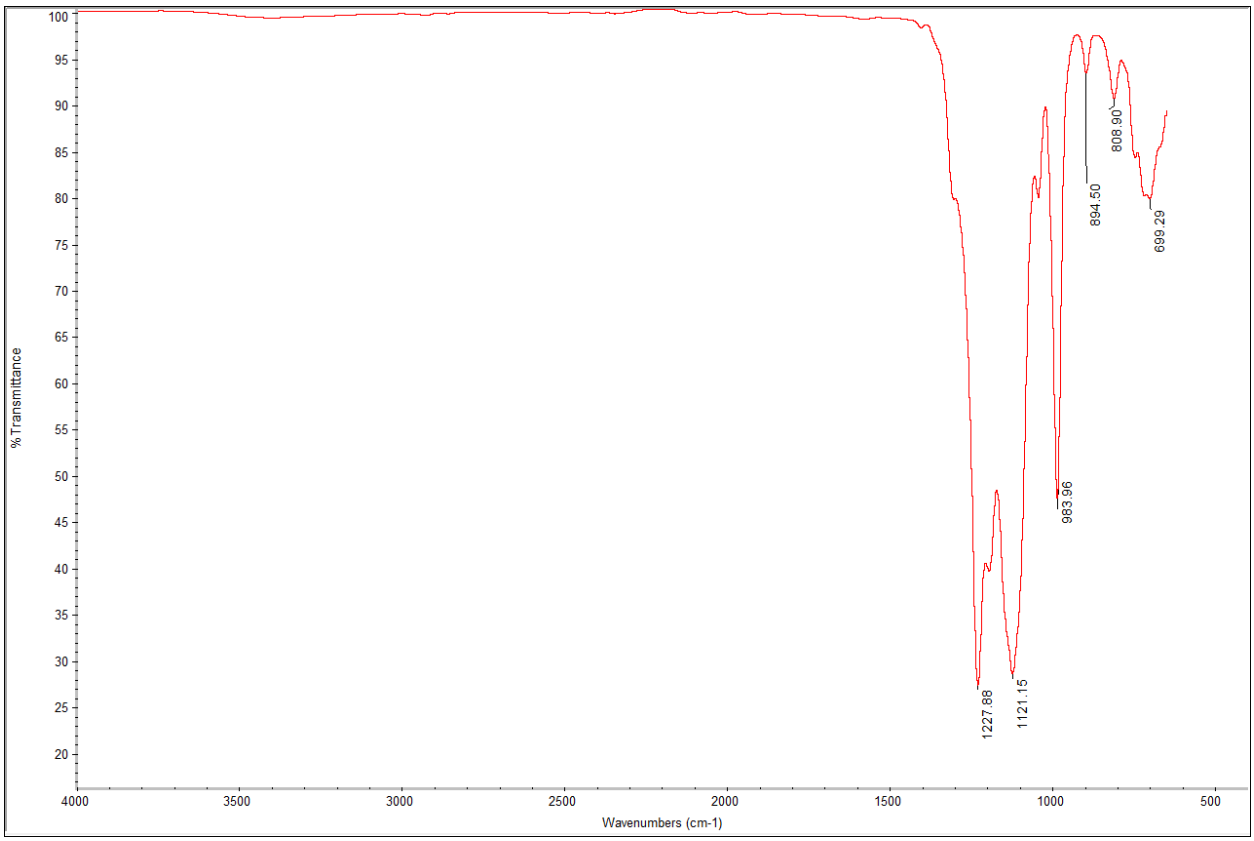

Figure 55. An FTIR spectrum was obtained for pure Galden for comparison with the polymer-exposed Galden spectra.

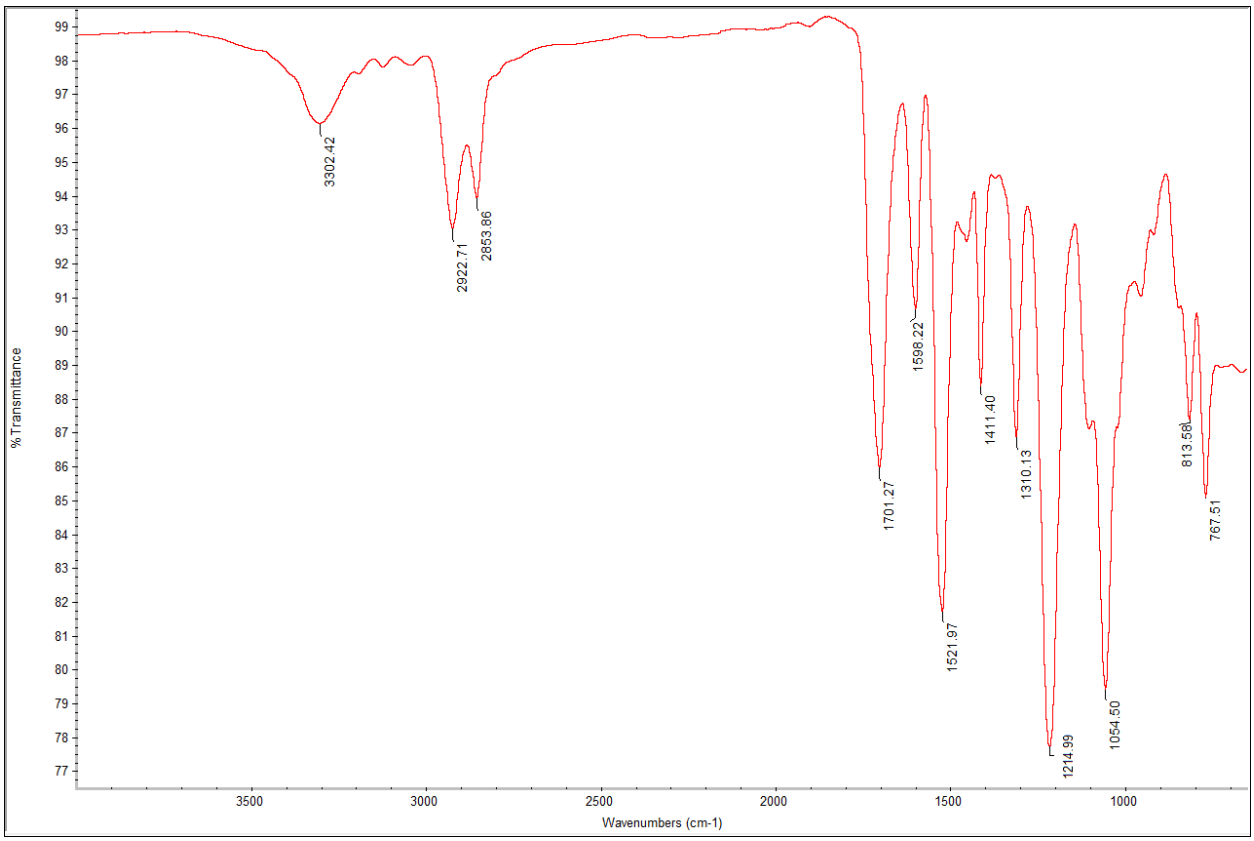

Figure 56. An FTIR spectrum was obtained for a polymer. The functional groups that would be seen if there was significant change would be the higher wavenumber peaks [44].

NH bonds, which are seen in urethane groups, show as peaks in the 3300-3700 wavenumber range [44]. Peaks in this range would indicate change in Galden composition. The three spectra taken from Galden samples containing the specimens T1-T3 are shown in Figures 59-61.

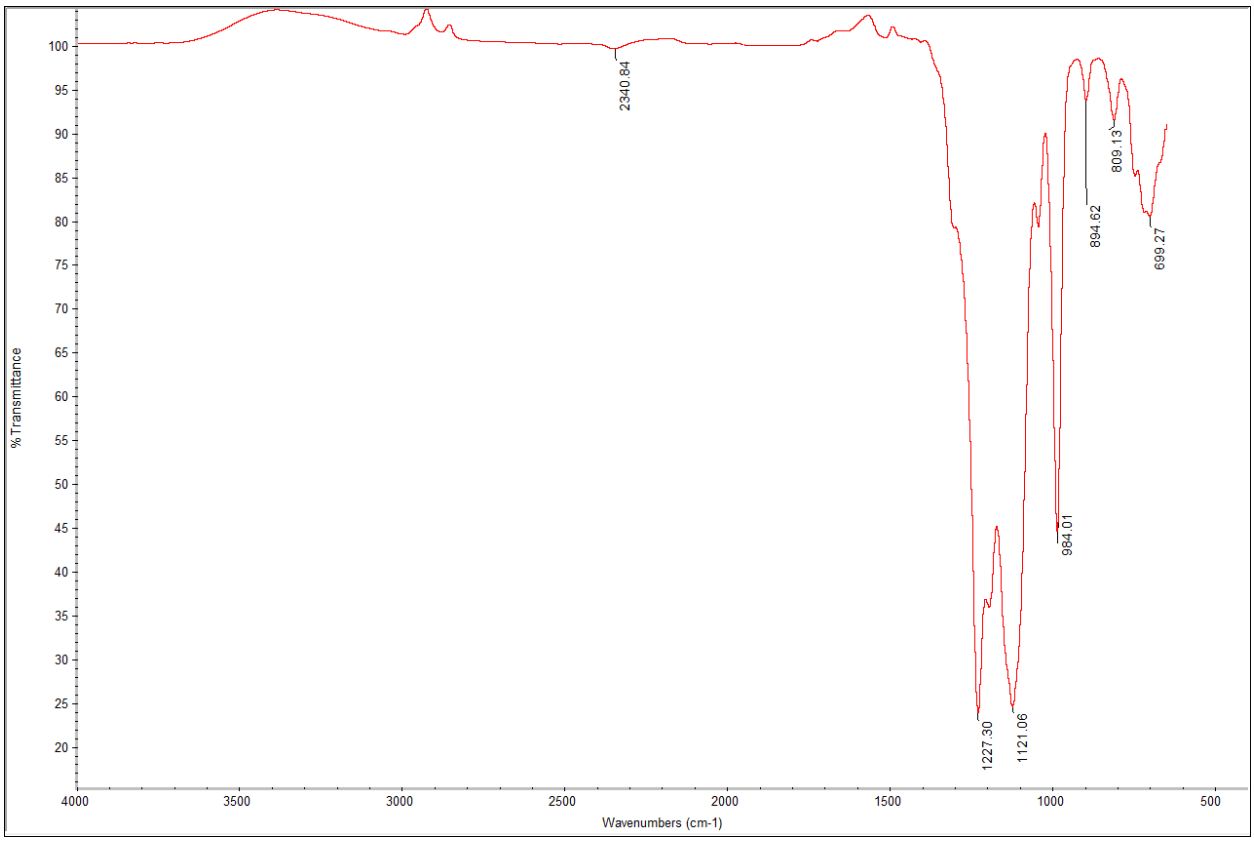

Figure 57. An FTIR spectrum was obtained from Galden that had contained the polymer sample sample T1 from the testing.

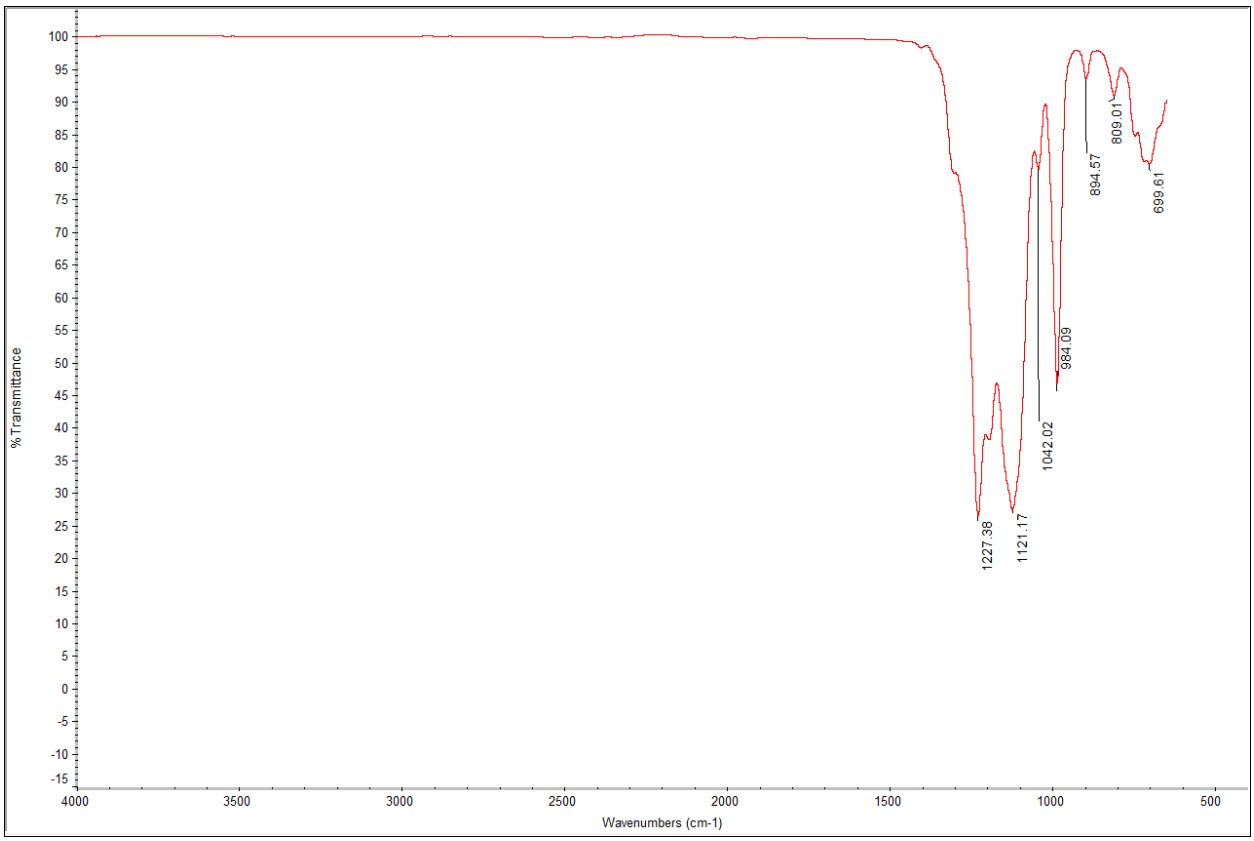

Figure 58. An FTIR spectrum was obtained from Galden that had contained the polymer sample T2 from the testing.

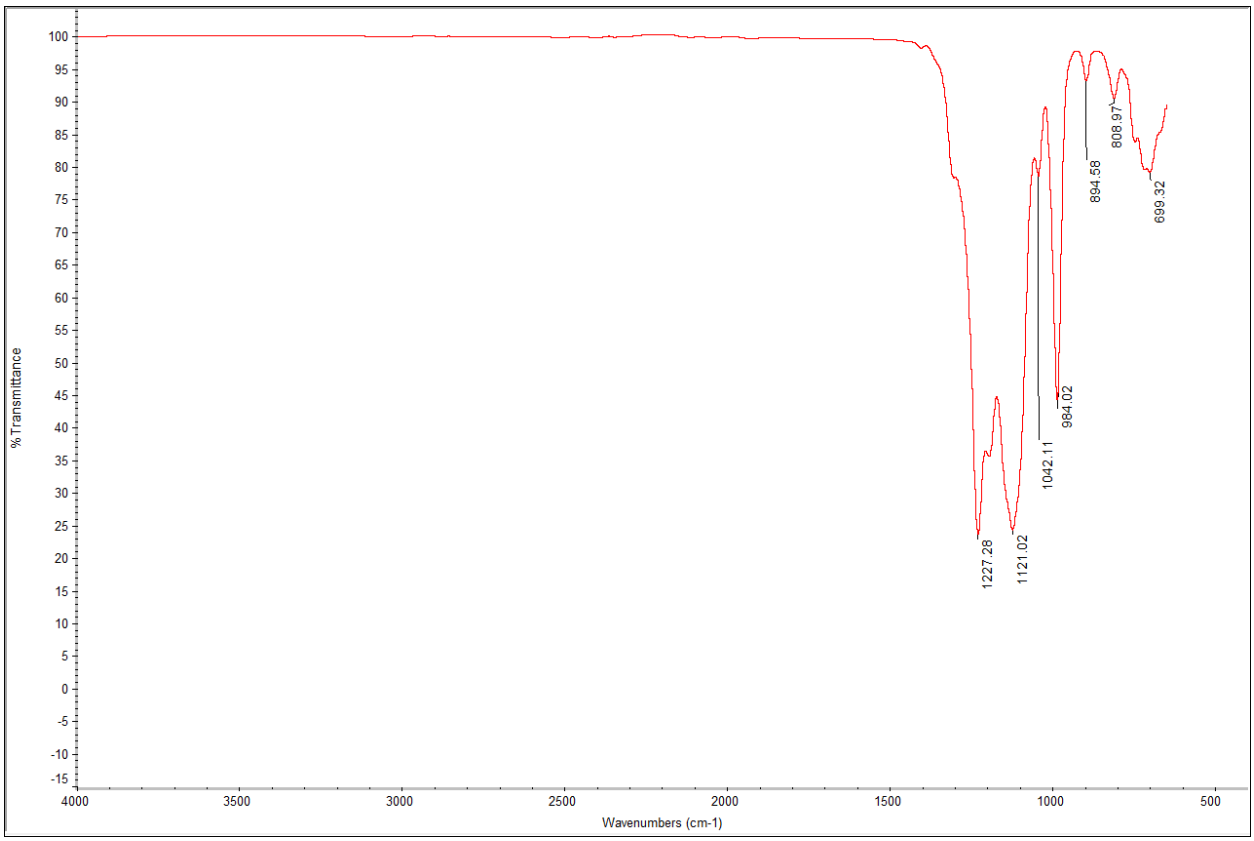

Figure 59. An FTIR spectrum was obtained from Galden that had contained the polymer sample T3 from the testing.

As the spectra show, no clear peaks suggesting change of Galden composition were seen during FTIR testing. There were some inverted peaks in the spectrum from the Galden associated with the T1 sample. Inverted peaks are not definitive, and at best these peaks suggest that something might be there. Based on the next two spectra that show no sign of anything other than pure Galden, it is very unlikely that there was significant change cause by any of the samples. Based on these results, the polymer tested is just as compatible with Galden as the other polymer is.

3.5 Life Testing Results

Based on simulated life testing while dosing coupons, one polymer becomes very brittle. There were also at least two material-related leaks during tensile coupon dosing. This initial simulated

life testing showed one massive limitation of one polymer that had been previously exposed through coupon dosing; this, when exposed to certain conditions is extremely susceptible to cracking.

4.0 LIMITATIONS

As with all studies, there were some limitations to this project. The main limitation to this project was the large number of possible factors that could potentially be affecting the system in ways that are not currently known. Because the system is small, and most of the problems dealt with in this project occur within the catheter, it is often difficult to determine exactly what the main problems are. As a result, the best evidence available was used to create a problem statement, and the problem statement was constantly evolving slightly throughout the project. Because the system is so complex and has so many components, there was not time to test every possible configuration to determine everything that could possible impact the issue studied in this report. To mitigate this issue, the most important aspects that could impact the problems this project sought to address were chosen as priorities. Choosing a specific set of variables that could impact the issues studied in this report allowed the report to stay focused and the results to remain meaningful and clear.

Another limitation on this project was the geometries that were necessary to work with for tensile testing. The best tensile testing data comes from completely consistent samples that can be easily gripped and are in a perfect “dog bone” configuration. Because the samples needed to be exposed to radiation, the geometries that would work with the current fixture for irradiating samples needed to be used. These geometries limited was tensile specimens could be prepared. To mitigate the fact that the tensile data might not be perfect, the purpose of the tensile testing was to compare the samples prepared to each other. For example, even though the notched configuration used for some samples that were irradiated is not an ideal tensile testing configuration, because all of the same material samples were the same configuration, the dose-

strength curve for this material should still be the correct trend. Also, as a check, the ultimate tensile strength values on the technical datasheets were compared to the UTS values for the control samples. The values were found to match relatively well, suggesting that the tensile testing results are very reasonable.

Finally, a third limitation was the assumptions made for the SolidWorks simulation. First of all, Poisson's ratio was assumed to be an average value. Second, the flexural modulus was used instead of the elastic modulus; based on previous research, however, this was a reasonable assumption to make. Lastly, SolidWorks, while good for general trends, does not always mimic reality perfectly, so any simulations performed may have neglected important real world conditions. Again, to mitigate these limitations, the SolidWorks simulations were used as comparative study tools so that all simulations considered would have similar errors that would essentially be cancelled out when comparing the results.

5.0 RECOMMENDATIONS AND FUTURE WORK

Based on the results from the tests, there is a material that is best for the catheter. One polymer is too easily altered to make it a viable option for a catheter that will be continuously inserted and removed from various applicators and well chambers. This would likely cause the catheters to fail well short of the desired lifetime. Because there is significant change of the catheters, it would be good to find a way to reduce the change as much as possible. One option that was simulated in this experiment was simply increasing the wall thickness. Other options that could reinforce the catheter would be to add some type structure to the catheter to increase the resistance to hoop stress. Finally, if absolutely necessary, a new catheter material could be tested in the same way that materials were tested in this report. There are many different types of molecules use to synthesis polymers and they all have varying degrees of radiation resistance.

Based on this study it is clear that if a new material were to be investigated, a material that has different properties than one of the polymers that was tested, while maintaining other properties would be ideal. The final recommendation based on the testing in this report, is to have the manufacturer of the catheter ensure that they measure the diameter of the catheter in more than one spot around the cri. By ensuring a more consistent, circular diameter, known behavior could be accounted for.

Despite the many tests that were performed in this project, there are still many potential tests that could be performed to gain a better understanding of the catheter behavior to certain conditions. One of the next specific tests that could be performed would be to conduct testing with irradiated catheters. Another test that could be performed would be a test to determine the effect of a

condition not tested in this study on the mechanical properties of one of the polymers that was tested. For the future, a completely new catheter and applicator design could be investigated to negate one of the issues seen in this study. Finally, an in depth materials science study to determine what makes specific materials react differently to x-ray radiation specifically would provide useful information for determining what the best material to use would be.

6.0 CONCLUSION

In summary, this thesis investigated two polymers for use as an x-ray catheter for electronic brachytherapy. Testing was performed to evaluate certain properties and coolant (Galden HT 135) compatibility for both materials. Specific types of testing included tensile, pressure, coolant compatibility, and simulated life testing. Based on all the testing that was performed, one polymer was determined to be too brittle, especially after exposure to certain conditions. This polymer did change significantly less than another when exposed to other conditions, but the second polymer was less affected by a different set of conditions than the first polymer was. Prior testing with Galden and the second polymer had shown that the material is compatible with Galden, and similar tests with the first polymer showed the same results. In the end, the second polymer was chosen as the better option because of its better durability when exposed to Galden and other conditions. The Xoft Axxent eBx system is an exciting and relatively new form of radiation therapy for cancer patients. Through constant improvement to the components that the device is comprised of, the Axxent system will remain at the forefront of minimal impact radiation therapies.

REFERENCES

[1] ICAD Inc. *K122951*. Silver Spring: FDA, 17 Jan. 2013. PDF.

[2] American Cancer Society. *Cancer Facts & Figures 2016*. Atlanta: American Cancer Society; 2016.

[3] National Cancer Institute. "SEER Stat Fact Sheets: Female Breast Cancer." *Seer.cancer.gov*. National Cancer Institute, n.d. Web. 24 Mar. 2016.

[4] Breast Cancer.org. "Image - Range of Ductal Carcinoma in Situ (DCIS)." *Breastcancer.org*. N.p., n.d. Web. 24 Mar. 2016.

[5] American Cancer Society. "What Are Basal and Squamous Cell Skin Cancers?" *Cancer.org*. American Cancer Society, 10 May 2016. Web. 28 June 2016.

[6] Mayo Clinic. "Where Skin Cancer Develops." *Mayo Clinic*. Mayo Foundation for Medical Education and Research, n.d. Web. 28 June 2016.

[7] Rogers HW, Weinstock MA, Harris AR, et al. Incidence Estimate of Nonmelanoma Skin Cancer in the United States, 2006. *Arch Dermatol.* 2010;146(3):283-287.

[8] American Cancer Society. "The History of Cancer." *Cancer.org*. American Cancer Society, 2014. Web. Apr. 2016.

[9] National Cancer Institute. "CAR T-Cell Immunotherapy for ALL." *National Cancer Institute*. National Institutes of Health, 2014. Web. Apr. 2016.

[10] American Cancer Society. "The Science Behind Radiation Therapy." *Cancer.org*. American Cancer Society, 2014. Web. Apr. 2016.

[11] Mirion Technologies. "Types of Radiation: Gamma, Alpha, Neutron, Beta & X-Ray Radiation Basics." *Mirion*. Mirion Technologies, n.d. Web. Apr. 2016.

[12] Smith, Alfred, Ph.D. "Proton Physics and Technology." Houston. Web. Apr. 2016.

[13] American Cancer Society. "Radiation Therapy for Breast Cancer." *Cancer.org*. American Cancer Society, 4 Apr. 2016. Web. Apr. 2016.

[14] Dooley, William, Wurzer, Megahy, Schreiber, Roy, Proulx, Kugler, Lane, Dalzell, Dowlatshahi, Simmons, Thropay, Ahuja, Peter Beitsch, Holt, and Lee. "Electronic Brachytherapy as Adjuvant Therapy for Early Stage Breast Cancer: A Retrospective Analysis." *OTT OncoTargets and Therapy* (2011): 13. Web. Apr. 2016.

[15] American Cancer Society. "Radiation Therapy for Vaginal Cancer." *Cancer.org*. American Cancer Society, 16 Feb. 2016. Web. Apr. 2016.

[16] American Cancer Society. "Radiation therapy for uterine sarcomas." *Cancer.org*. American Cancer Society, 15 Feb. 2016. Web. Apr. 2016.

[17] American Cancer Society. "Radiation therapy for cervical cancer." *Cancer.org*. American Cancer Society, 29 Jan. 2016. Web. Apr. 2016.

[18] American Cancer Society. “Skin Cancer: Basal and Squamous Cell.” *Cancer.org*. American Cancer Society, 1 Feb. 2016. Web. Apr. 2016.

[19] Cancer Research UK. "Internal Radiotherapy (brachytherapy) for Prostate Cancer." *Cancer Research UK*. Cancer Research UK, n.d. Web. 31 July 2016.

[20] Breastcancer.og. "Studies Show Risks and Benefits of Intraoperative Radiation Therapy." *Breastcancer.org*. Breastcancer.org, 3 Dec. 2013. Web. Apr. 2016.

[21] Vaidya, Jayant S., Frederik Wenz, Max Bulsara, Jeffrey S. Tobias, David J. Joseph, Mohammed Keshtgar, Henrik L. Flyger, Samuele Massarut, Michael Alvarado, Christobel Saunders, Wolfgang Eiermann, Marinos Metaxas, Elena Sperk, Marc Sütterlin, Douglas Brown, Laura Esserman, Mario Roncadin, Alastair Thompson, John A. Dewar, Helle M R Holtveg, Steffi Pigorsch, Mary Falzon, Eleanor Harris, April Matthews, Chris Brew-Graves, Ingrid Potyka, Tammy Corica, Norman R. Williams, and Michael Baum. "Risk-adapted Targeted Intraoperative Radiotherapy versus Whole-breast Radiotherapy for Breast Cancer: 5-year Results for Local Control and Overall Survival from the TARGIT-A Randomised Trial." *The Lancet* 383.9917 (2014): 603-13. Web. Apr. 2016.

[22] Veronesi, Umberto, Roberto Orecchia, Patrick Maisonneuve, Giuseppe Viale, Nicole Rotmensz, Claudia Sangalli, Alberto Luini, Paolo Veronesi, Viviana Galimberti, Stefano Zurrida, Maria Cristina Leonardi, Roberta Lazzari, Federica Cattani, Oreste Gentilini, Mattia Intra, Pietro Caldarella, and Bettina Ballardini. "Intraoperative Radiotherapy versus External Radiotherapy for Early Breast Cancer (ELIOT): A Randomised Controlled Equivalence Trial." *The Lancet Oncology* 14.13 (2013): 1269-277. Web. Apr. 2016.

[23] Dickler, A., O. Ivanov, M.c. Baird, and D. Francescatti. "Initial Results of a Multi-center Trial Utilizing Xoft Axxent Electronic Brachytherapy to Deliver Intraoperative Radiation Therapy in the Treatment of Early-stage Breast Cancer." *International Journal of Radiation Oncology*Biology*Physics* 78.3 (2010): n. pag. Web. Apr. 2016.

[24] Ivanov, Olga, Adam Dickler, Bennett Y. F. Lum, James V. Pellicane, and Darius S. Francescatti. "Twelve-Month Follow-Up Results of a Trial Utilizing Axxent Electronic Brachytherapy to Deliver Intraoperative Radiation Therapy for Early-Stage Breast Cancer." *Annals of Surgical Oncology Ann Surg Oncol* 18.2 (2010): 453-58. Web. Apr. 2016.

[25] Applied Radiation Oncology. *November 16 - Researchers Present Clinical Data Supporting Xoft System for Early Stage Breast Cancer and Nonmelanoma*. *Appliedradiationoncology.com*. Anderson Publishing, 16 Nov. 2015. Web. Apr. 2016.

[26] Dooley, William C., Ozer Algan, Kambiz Dowlatshahi, Darius Francescatti, Elizabeth Tito, J. David Beatty, Art G. Lerner, Betsy Ballard, and Susan K. Boolbol. "Surgical Perspectives from a Prospective, Nonrandomized, Multicenter Study of Breast Conserving Surgery and Adjuvant Electronic Brachytherapy for the Treatment of Breast Cancer." *World J Surg Onc World Journal of Surgical Oncology* 9.1 (2011): 30. Web. Apr. 2016.

[27] Kasper, Michael, and Ahmed Chaudhary. "Novel Treatment Options for Nonmelanoma Skin Cancer: Focus on Electronic Brachytherapy." *MDER Medical Devices: Evidence and Research* (2015): 493. Web. Apr. 2016.

[28] Williams, Norman R., Katharine H. Pigott, Chris Brew-Graves, and Mohammed R. S. Keshtgar. "Intraoperative Radiotherapy for Breast Cancer." *Gland Surgery* 3.2 (2014): 109-19. Web. Apr. 2016.

[29] Mehta, Vivek K., Ozer Algan, Katherine L. Griem, Adam Dickler, Kenneth Haile, David E. Wazer, Randy E. Stevens, Manjeet Chadha, Steve Kurtzman, Sheela D. Modin, Kambiz Dowlatshahi, Kelly W. Elliott, and Thomas W. Rusch. "Experience With an Electronic Brachytherapy Technique for Intracavitary Accelerated Partial Breast Irradiation." *American Journal of Clinical Oncology* 33.4 (2010): 327-35. Web. Apr. 2016.

[30] Bhatnagar, Ajay. "Nonmelanoma Skin Cancer Treated with Electronic Brachytherapy: Results at 1 Year." *Brachytherapy* 12.2 (2013): 134-40. Web. Apr. 2016.

[31] Doggett, Stephen, M.D. *Electronic Brachytherapy for Non-Melanomatous Skin Cancer: Report of Failures and Adverse Events; Annual Follow-Up Report of First 565 Lesions*. Publication. N.p.: n.p., n.d. *Brachyjournal.com*. Web. Mar. 2016.

[32] Kurt J. Lesker Company. "Galden® Heat Transfer Fluids." *Kurt J. Lesker Company*. Kurt J. Lesker Company, n.d. Web. Mar. 2016. <http://www.lesker.com/newweb/fluids/heattransfer_galden_ht.cfm?pgid=0#fragment-1>.

[33] Clark Solutions. N.p.: Clark Solutions, n.d. *Clarksol.com*. Clark Solutions. Web. Mar. 2016.

[34] Watson-Marlow.*Rapid load pumpheads.* N.p: Watson-Marlow, n.d. Watson-Marlow. Web. Mar. 2016.

[35] Xoft, Inc. "Axxent® Applicators." *Xoftinc.com*. Xoft, Inc, 2010. Web. Apr. 2016.

[36] Hanks, C. L., and D. J. Hamman. *RADIATION EFFECTS DESIGN HANDBOOK*. Tech. no. CR-1787. Columbus: RADIATION EFFECTS INFORMATION CENTER, 1971. *Nasa Technical Reports Server*. Web. May 2016.

[37] Idesaki, Akira, Akihiko Shimada, Norio Morishita, Masaki Suimoto, and Masahito Yoshikawa. "Evaluation of Radiation Resistance for Organic Materials Used in Atomic Energy-related Facilities." *Princeton.edu*. Web. May 2016.

[38] Ghaemy, Mousa, Mohammad R. Hadjmohammadi, and Reza Tabaraki. "Study of Crystallinity of High-density [polymer] by Inverse Gas Chromatography."*Iranian Polymer Journal* 9.2 (2000): 117-24. *Elsevier*. Web. 20 Aug. 2014.

[39] Fayolle, B., L. Audouin, and J. Verdu. "Radiation Induced Embrittlement of PTFE." Polymer 44.9 (2003): 2773-780. Elsevier. Web. 20 Aug. 2014.

[40] Qi, H.J., and M.C. Boyce. "Stress–strain Behavior of Thermoplastic [polymer]s." *Mechanics of Materials* 37.8 (2005): 817-39. *ResearchGate*. Web. Mar. 2016.

[41] Covestro. "Poisons Ratio." *Poisson's Ratio (Hencky Ratio)*. Covestro AG, 1 Sept. 2015. Web. 06 Aug. 2016. <http://www.covestro.com/Technologies/Properties/Mechanical-Properties/Poisons-Ratio.aspx>.

[42] Pedersen, Keith. "Frequently Asked Questions on Material Properties for Simulation Answered." *CAPUniversity*. CAPUNIVERSITY, 25 Sept. 2013. Web. Mar. 2016.

[43] Frost, Jim. "Regression Analysis: How Do I Interpret R-squared and Assess the Goodness-of-Fit?" *The Minitab Blog*. Minitab, 30 May 2013. Web. July 2016.

[44] Merlic, Craig A., and Jane Strouse. "IR Absorption Table." *WebSpectra*. Cambridge Isotope Laboratories & UCLA Department of Chemistry and Biochemistry, 1997. Web. June 2016. <http://webspectra.chem.ucla.edu//irtable.html>.

APPENDICES

Appendix A: Cosmetic NMSC Images

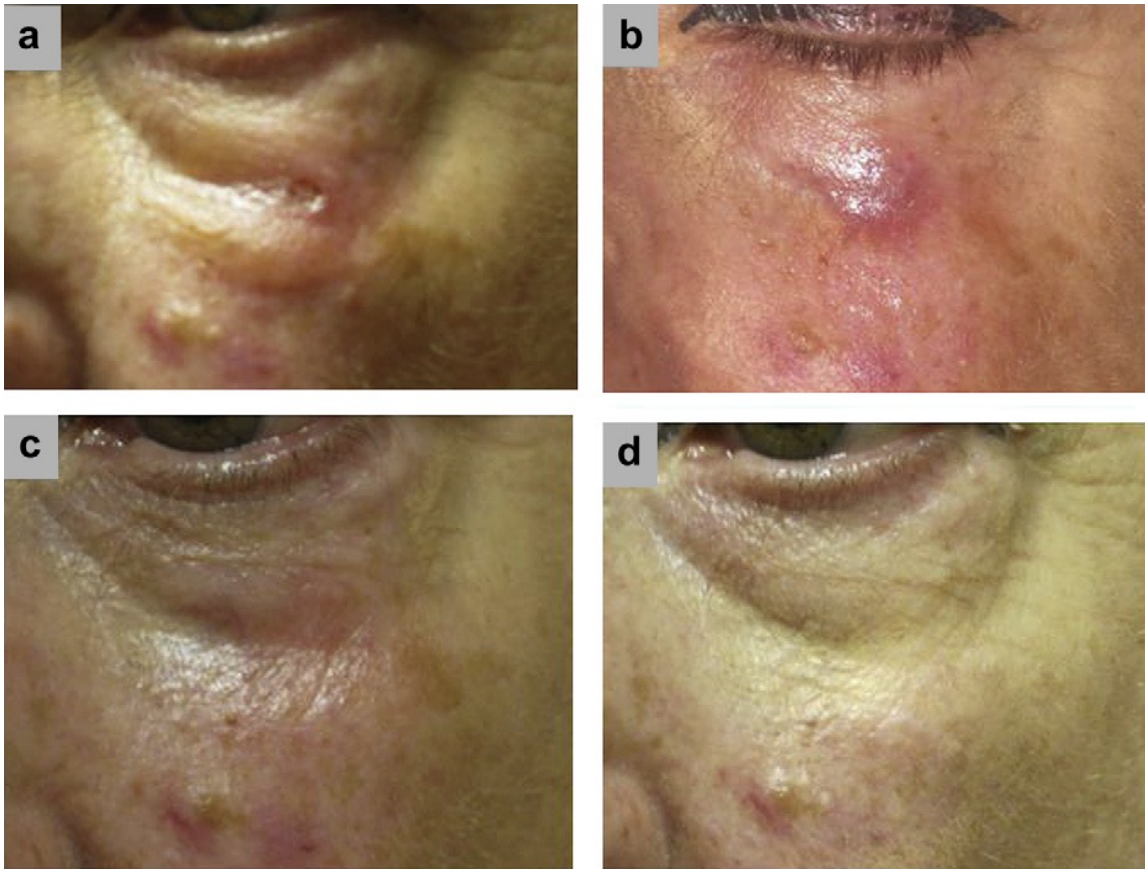

Figure 60. A 68 year old woman with squamous cell carcinoma pre-treatment (a) and 1 (b), 2.5 (c), and 20 (d) months post treatment [26].

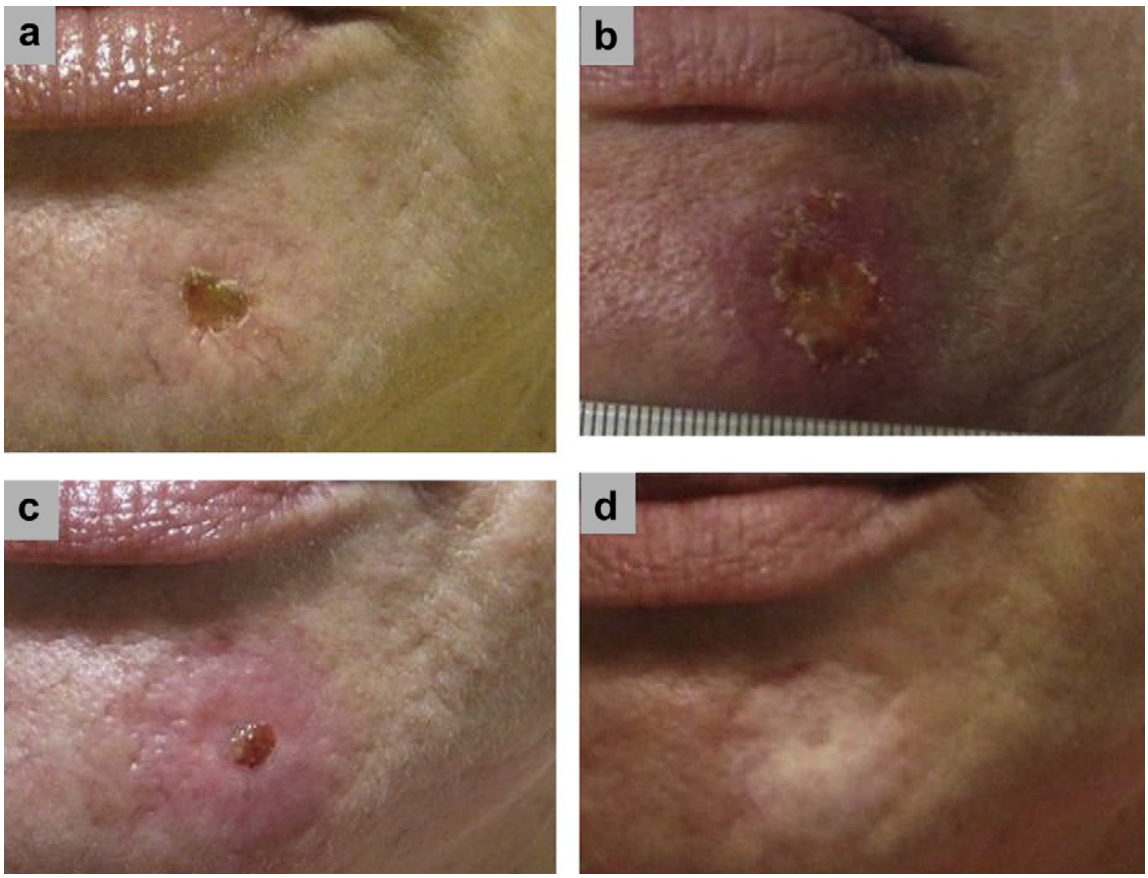

Figure 61. A 56 year old woman with basal cell carcinoma pre- (a) and post-treatment (b); 1 (c) and 12 (d) months post treatment [26].

Table 18. Galden HT135 is the current coolant used in the Xoft Axxent system.

Specifications Table

Grade	HT55	HT70	HT80	HT110	HT135	HT170	HT200	HT230	HT270
Vapor Pressure (Torr)	225	141	105	17	5.8	0.8	0.2	0.03	<10-2
Pour Point	<-125°C	<-110°C	-110°C	-100°C	-100°C	-97°C	-85°C	-77°C	-66°C
Boiling Point	55°C	70°C	80°C	110°C	135°C	170°C	200°C	230°C	270°C
Specific Heat (Cal/g•°C)	0.23	0.23	0.23	0.23	0.23	0.23	0.23	0.23	0.23
Surface Tension	14 (dyne/cm)	14 (dyne/cm)	16 (dyne/cm)	16 (dyne/cm)	17 (dyne/cm)	18 (dyne/cm)	19 (dyne/cm)	19 (dyne/cm)	20 (dyne/cm)
Molecular Weight (average)	340	410	430	580	610	760	870	1020	1550
Heat of Vaporization	22 (Cal/g)	17 (Cal/g)	17 (Cal/g)	17 (Cal/g)	16 (Cal/g)	16 (Cal/g)	15 (Cal/g)	15 (Cal/g)	15 (Cal/g)
Kinematic Viscosity (cSt)	0.45	0.5	0.57	0.77	1	1.8	2.4	4.4	14
Thermal Conductivity	0.065 (W/m•K)	0.065 (W/m•K)	0.065 (W/m•K)	0.065 (W/m•K)	0.065 (W/m•K)	0.065 (W/m•K)	0.065 (W/m•K)	0.065 (W/m•K)	0.065 (W/m•K)
Relative Density	1.65 (g/cm^3)	1.68 (g/cm^3)	1.69 (g/cm^3)	1.71 (g/cm^3)	1.72 (g/cm^3)	1.77 (g/cm^3)	1.79 (g/cm^3)	1.82 (g/cm^3)	1.85 (g/cm^3)
Coeff. of Expansion	0.0011 (cm^3/cm^3•°C)	0.0011 (cm^3/cm^3•°C)	0.0011 (cm^3/cm^3•°C)	0.0011 (cm^3/cm^3•°C)	0.0011 (cm^3/cm^3•°C)	0.0011 (cm^3/cm^3•°C)	0.0011 (cm^3/cm^3•°C)	0.0011 (cm^3/cm^3•°C)	0.0011 (cm^3/cm^3•°C)
Volume Resistivity	1×10^{12} (ohm•cm)	1×10^{15} (ohm•cm)	1.5×10^{15} (ohm•cm)	1.5×10^{15} (ohm•cm)	1.5×10^{15} (ohm•cm)	1.5×10^{15} (ohm•cm)	6×10^{15} (ohm•cm)	6×10^{15} (ohm•cm)	6×10^{15} (ohm•cm)
Solubility of Water (ppm by wt)	<10	<10	<10	<10	<10	<10	<10	<10	<10
Dielectric Strength	40 (kV)	40 (kV)	40 (kV)	40 (kV)	40 (kV)	40 (kV)	40 (kV)	40 (kV)	40 (kV)
Dielectric Constant	1.86	1.86	1.89	1.92	1.92	1.94	1.94	1.94	1.94
Dissipation Factor	$2x10^{-4}$ (1 Khz)	$2x10^{-4}$ (1 Khz)	$2x10^{-4}$ (1 Khz)	$2x10^{-4}$ (1 Khz)	$2x10^{-4}$ (1 Khz)	$2x10^{-4}$ (1 Khz)	$2x10^{-4}$ (1 Khz)	$2x10^{-4}$ (1 Khz)	$2x10^{-4}$ (1 Khz)
Refractive Index	1.280	1.280	1.280	1.280	1.280	1.280	1.281	1.283	1.283
Solubility of Air (cm^3 gas/100 cm^3 liquid)	26	26	26	26	26	26	26	26	26
Operating Range	-90 to 45 °C	-75 to 60 °C	-70 to 70 °C	-60 to 100 °C	-50 to 125 °C	-30 to 160 °C	-20 to 190 °C	0 to 220 °C	25 to 260 °C

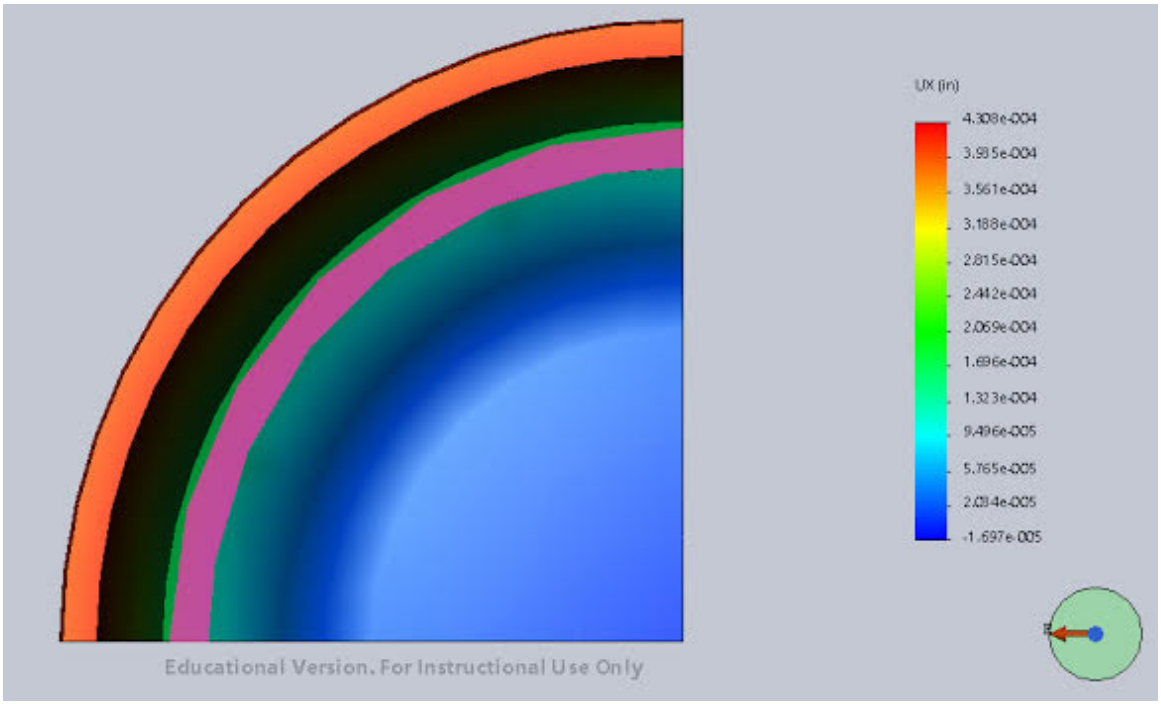

Figure 62. A segment of a model of a catheter was analyzed after simulating an internal pressure.

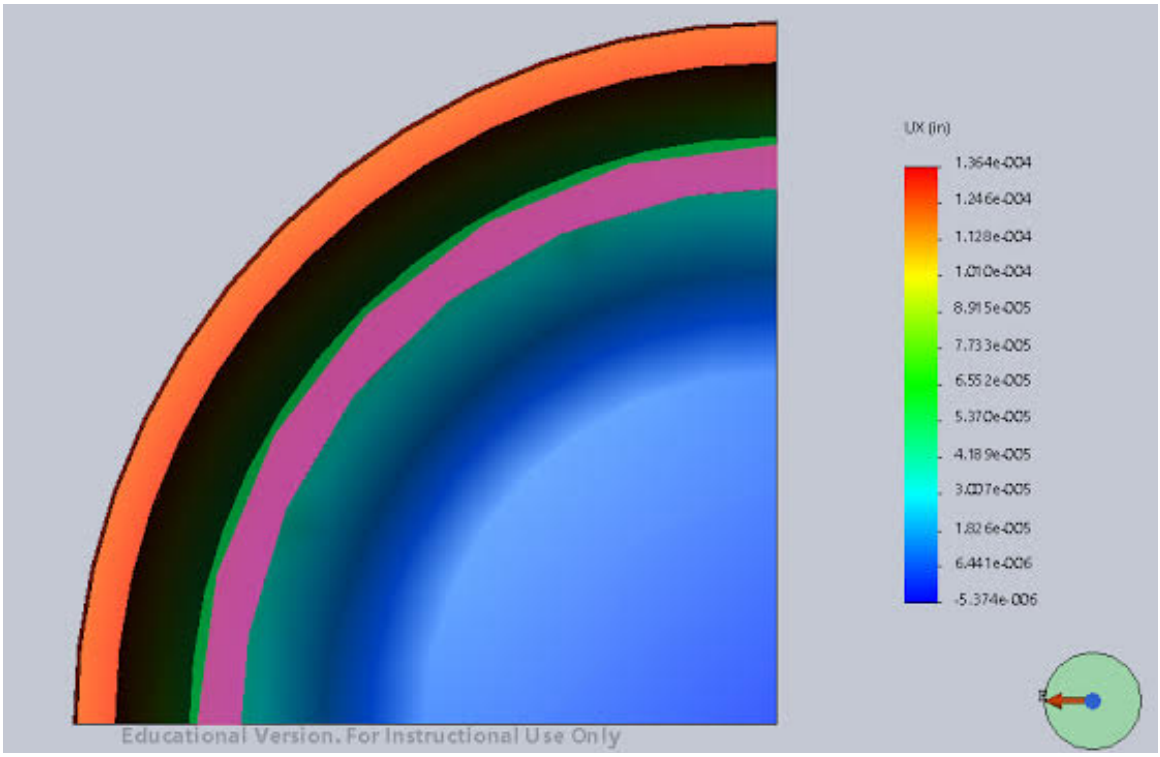

Figure 63. A segment of a model of a catheter was analyzed after simulating an internal pressure.

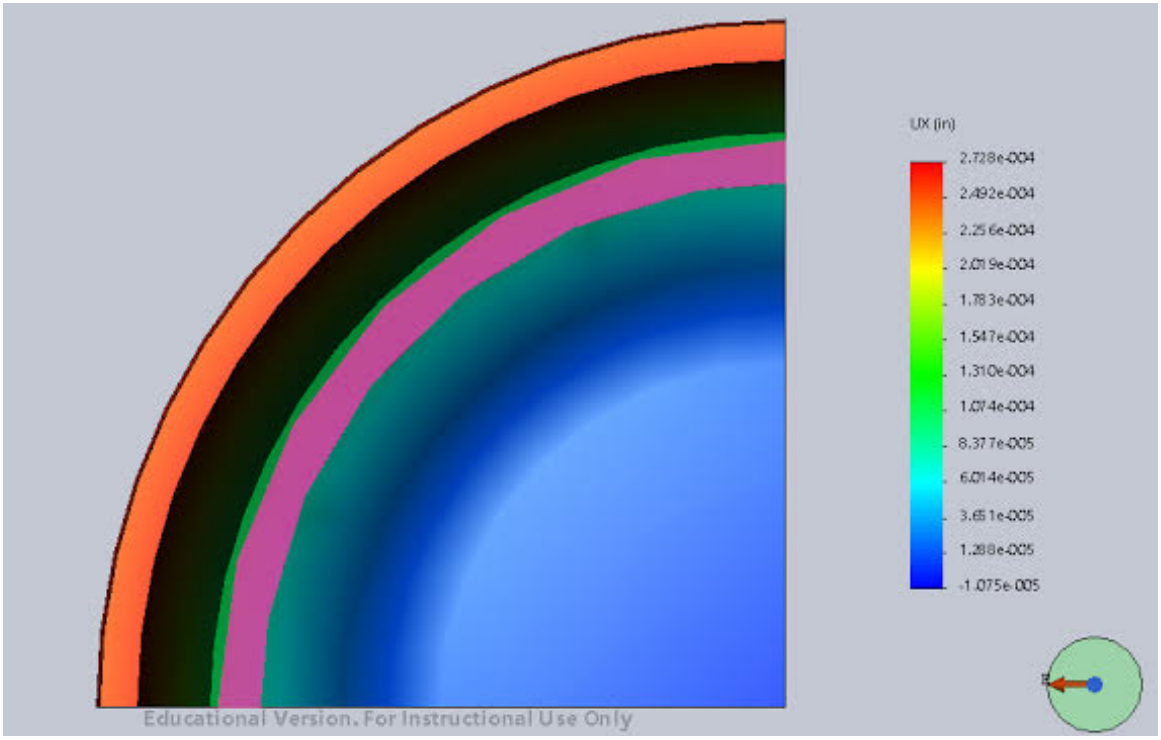

Figure 64. A segment of a model of a catheter was analyzed after simulating an internal pressure.

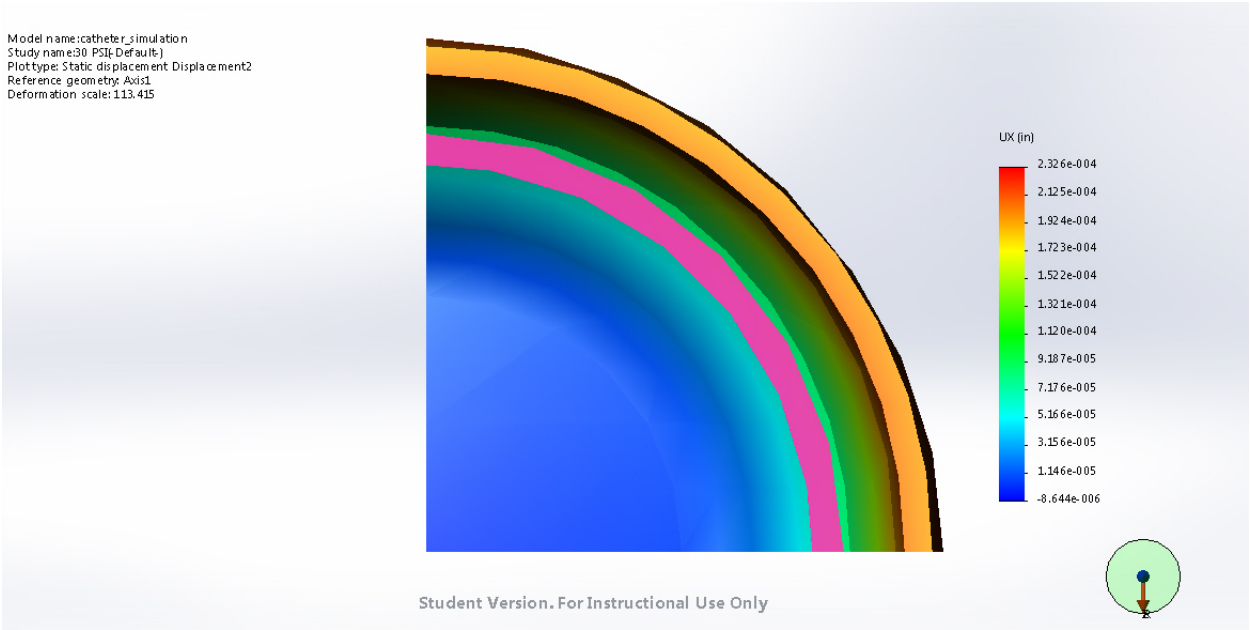

Figure 65. A segment of a model of a catheter was analyzed after simulating an internal pressure for a specific wall thickness.

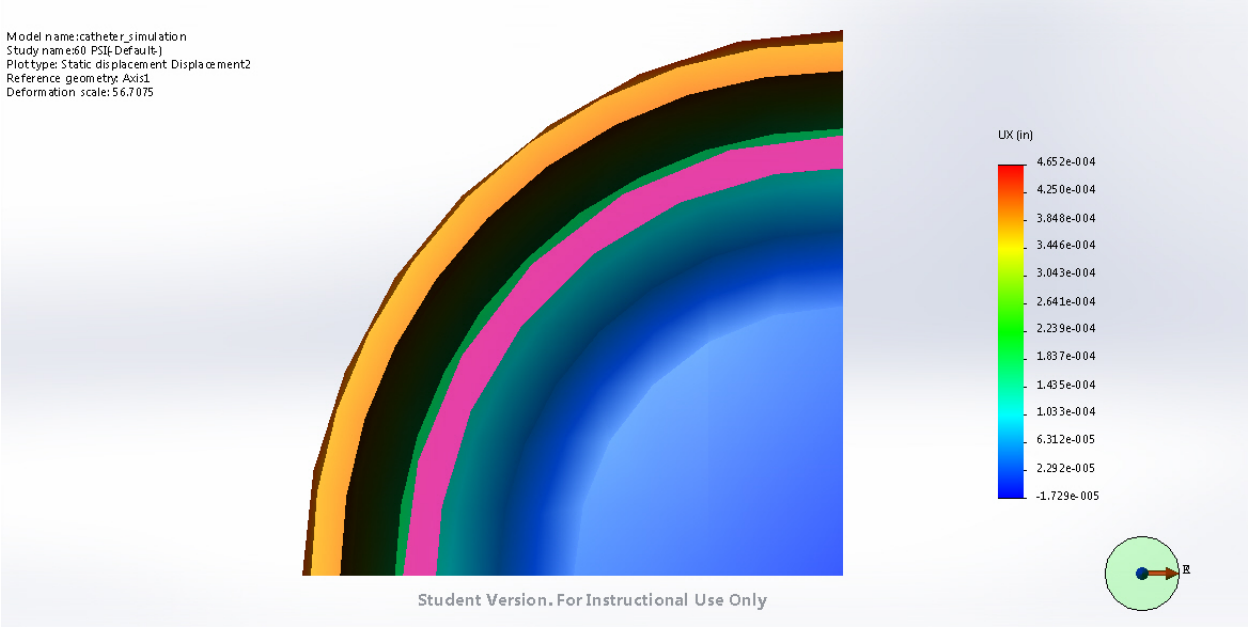

Figure 66. A segment of a model of a catheter was analyzed after simulating an internal pressure for a specific wall thickness.

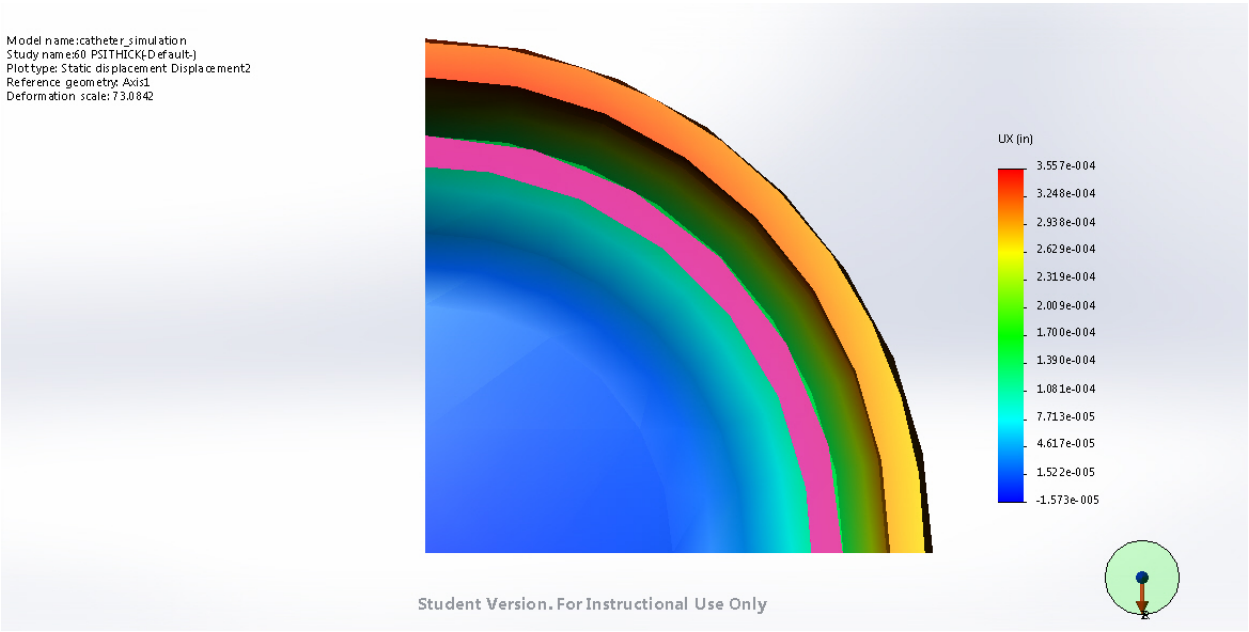

Figure 67. A segment of a model of a catheter was analyzed after simulating an internal pressure for a specific wall thickness.